



# Durham E-Theses

---

## *Vibroseis encoding*

Bernhardt, Thomas

### How to cite:

---

Bernhardt, Thomas (1977) *Vibroseis encoding*, Durham theses, Durham University. Available at Durham E-Theses Online: <http://etheses.dur.ac.uk/8261/>

### Use policy

---

The full-text may be used and/or reproduced, and given to third parties in any format or medium, without prior permission or charge, for personal research or study, educational, or not-for-profit purposes provided that:

- a full bibliographic reference is made to the original source
- a [link](#) is made to the metadata record in Durham E-Theses
- the full-text is not changed in any way

The full-text must not be sold in any format or medium without the formal permission of the copyright holders.

Please consult the [full Durham E-Theses policy](#) for further details.

# VIBROSEIS ENCODING

by

Thomas Bernhardt

A Thesis submitted for the Degree of  
Doctor of Philosophy in the  
University of Durham

The copyright of this thesis rests with the author.  
No quotation from it should be published without  
his prior written consent and information derived  
from it should be acknowledged.

Graduate Society

September 1977



## ABSTRACT

The FM signals, called sweeps, used in the Vibroseis method of seismic exploration show a considerable amount of energy in the sidelobes after correlation detection. These sidelobes represent signal generated noise and if not kept low in amplitude they might mask subsequent reflections, thereby reducing the detection capability of the Vibroseis system.

The purpose of this research has been to investigate new coded signal design techniques for the use with Vibroseis, in order to achieve sidelobe suppression. Some of the codes examined have already been known to radar and communication theory, whilst some codes are original developments of this research exercise.

Binary and quaternary complementary series are found to be especially suitable for a Vibroseis encoding technique. A new and simple algorithm for the generation of quaternary series from known binary complementary sequences is given and the concept of correlation matrices is introduced to complementary series, permitting signal design in the detection window. The encoded Vibroseis input signals were tested on a computer and showed perfect sidelobe suppression a certain distance away from the main compressed pulse, when detected by a matched filter.

Field tests with the coded signals were conducted, taking advantage of a computerized Vibroseis field system. The tests showed promising results. However, it became clear that the vibrator control devices will have to be adjusted to the transmission of such sophisticated signals, in order to allow substantially better results than in the conventional Vibroseis system.

A 'Continuous Vibroseis Transmission System' is suggested, transmitting energy during the normal listening period. Such a system has been developed with the help of so-called 'Mutually-Orthogonal-Complementary Sets of Sequences' and although not yet practically tested its anticipated advantages and disadvantages are described.

Finally, 'Predistortion' as a method of Vibroseis signal design is examined. Providing the correct predistortion parameters are chosen, the signal-to-correlation noise ratio can be increased. A spectrum whitening effect observed on addition of selected pre-distorted sweeps can be of advantage in a quaternary complementary coded Vibroseis system, permitting an optimal wavelet design in the detection window.

## ACKNOWLEDGEMENTS

May I express my sincere thanks to my supervisor Mr. J.H. Peacock who suggested the investigation into coding techniques for the Vibroseis system and encouraged me to undertake this research. His advice and assistance are gratefully acknowledged.

I am also indebted to Professor M.H.P. Bott for giving me the opportunity to study at Durham University.

Grateful thanks are also due to the members of the Department of Computing at Durham University for their help (...and great patience in dealing with my queries) during my period of research.

A special acknowledgement is due to the Science Site Library in Durham whose kind cooperation and excellent service in providing vital papers have been very much appreciated.

The practical tests in the second part of this research have been performed by the PRAKLA - SEISMOS GmbH, Hannover, West Germany. In particular I would like to mention Herrn Dr. H. Edelmann with whom I had many stimulating discussions and whose assistance was invaluable in the field tests of the Vibroseis Encoding Technique. I should also like to thank the employees of PRAKLA - SEISMOS who worked so hard making the transmission of the very sophisticated coded Vibroseis signals possible.

The author received a grant from the DAAD (Deutscher Akademischer Austauschdienst) during the second part of the research and this is gratefully acknowledged.

Finally, I would like to thank my wife, Angela, for being a source of constant encouragement and for helping with the typing and presentation of this thesis.

The presented Ph.D.-Thesis is the continuation of a Thesis entitled 'Coding Techniques for the Vibroseis System' which was submitted in September 1975 in partial fulfillment of the requirements for the degree of Master of Science at the University of Durham.

In the M.Sc. work the chances of the application of a coding technique for the Vibroseis system were assessed after an extensive study of the relevant literature.

CONTENTS

	Page	
CHAPTER 1	INTRODUCTION	
	1.1. Introduction	1
	1.2. A Brief Description of the Vibroseis System of Exploration	2
CHAPTER 2	THE VIBROSEIS PARAMETERS	
	2.1. Introduction	9
	2.2. The Input Signal - The Sweep	11
	2.3. The Amplitude Spectrum of a Sweep	14
	2.4. The Matched Filter Concept in Vibroseis	18
	2.5. The Output Signal - The Klauder Wavelet	22
CHAPTER 3	THE SIGNAL-TO-NOISE PROBLEM IN VIBROSEIS	
	3.1. Introduction	27
	3.2. The Theory of Sidelobe Reduction	28
	3.3. The Practice of Sidelobe Reduction	35
	3.3.1. Introduction	35
	3.3.2. Some Practical Methods of Increasing the Vibroseis Detection Capability	37
	3.3.3. Summary	42
CHAPTER 4	A BRIEF PULSE COMPRESSION REVIEW	
	4.1. Introduction	43
	4.2. Various Methods of Pulse Compression - Pulse Compression Codes	44
CHAPTER 5	THE CODES	
	5.1. Introduction	56
	5.2. Complementary Series	58
	5.3. Complementary Sets of Sequences and Mutually Orthogonal Complementary Sets of Sequences	65
	5.4. Quaternary Complementary Series	74

	Page	
CHAPTER 6	THE APPLICATION OF COMPLEMENTARY CODING IN THE VIBROSEIS SYSTEM OF EXPLORATION	
6.1.	Introduction	81
6.2.	The Choice of Code Members	84
6.3.	Examples of Binary and Quaternary Coded Vibroseis Signals	88
CHAPTER 7	A CONTINUOUS TRANSMISSION SYSTEM	
7.1.	Introduction	108
7.2.	The Complementary Continuous Transmission Code	111
7.3.	Example of a Complementary Coded Continuous Vibroseis System	122
7.4.	Summary	131
CHAPTER 8	FIELD TESTS OF THE ENCODED VIBROSEIS SYSTEM	
8.1.	Introduction	133
8.2.	The Use of Computerized Recording Instruments in the Vibroseis Encoding Technique	134
8.3.	Problems of the Practical Coded Signal Transmission and their Solutions	141
8.4.	Summary	165
CHAPTER 9	PREDISTORTION AND ITS APPLICATION TO VIBROSEIS AND THE VIBROSEIS ENCODING TECHNIQUE	
9.1.	Introduction	166
9.2.	Predistortion	167
9.3.	Combi-Sweep Method	172
9.4.	New 'Predistortion' Analysis	175
9.5.	Predistortion in the Vibroseis Encoding Technique and the Combi Sweep Method	182

	Page
CHAPTER 10    CONCLUSIONS	184
BIBLIOGRAPHY	186
APPENDIX     PAIRED ECHO ANALYSIS IN PULSE COMPRESSION SYSTEMS	193

"The copyright of this thesis rests with the author.  
No quotation from it should be published without his  
prior written consent and information derived from it  
should be acknowledged."



CHAPTER 1

INTRODUCTION

1.1. Introduction

In February 1960 John CRAWFORD, William E.N. DOTY and Milford R. LEE published a paper in "GEOPHYSICS" entitled "Continuous Signal Seismograph" and thereby introduced a totally new system for seismic mapping - the 'Vibroseis'\*) system. The theoretical implications of an entirely controllable surface energy source were very attractive and many geophysicists saw in 'Vibroseis' the seismic tool of the future.

Following almost 10 years of intensive and costly research work carried out by the Continental Oil Company, licensing to industry started in 1961. Since then the continuous signal idea has found widespread application and proved to be very successful as a prospecting technique.

It is not intended to describe the Vibroseis system in detail, but the basic principles are presented. There are, however, a vast number of papers available to the interested reader, and some are contained in the list of references at the end of this thesis:

ANSTEY (1963); BRODING et al (1971); COLE (1967); DAVITT (1976); EDELMANN (1966); ERLINGHAGEN (1975); GEYER (1968); GOUPILLAUD et al (1963); GOUPILLAUD (1976); KREY (1972); LAING (1972); LEE (1968).

\*) Trade and service mark of the Continental Oil Company



## 1.2. A Brief Description of the Vibroseis System of Exploration

In the Vibroseis system the use of very strong impulses, as generated by explosives, is replaced by one or more emissions of energy of lower power extended in time. The signal transmitted is a frequency swept sinusoid which is commonly known as a sweep. The Vibroseis input signal will be discussed in greater detail at a later stage.

The sweep is transmitted into the subsurface by sophisticated hydraulically driven vibrators, which are normally mounted on trucks and are pressed into contact with the ground by transferring the truck's weight onto the vibrator's base plate.

The output of vibrators is quoted in thrust pounds or thrust tons - multiplying piston area by maximum hydraulic pressure. In seismic prospecting, vibrator-truck units between 4.0 and 9.0 thrust tons are most widely used. They are normally designed to transmit sweeps in a frequency band of 10 Hz to 100 Hz and of up to 30 sec. duration. However, vibrators capable of generating frequencies from 2 Hz to 200 Hz and rated at 18 thrust tons have been developed mainly for research purposes.

Just recently, 1972/73, such a vibrator was employed to generate sweeps in a range of 2.0 Hz to 15.0 Hz. J.C. FOWLER and K.H. WATES (1975) describe a project using 'Vibroseis' methods for deep crustal reflection recordings in which this very powerful vibrator found its application.

In the early days of the Vibroseis system the energy source was two contrarotating eccentric masses driven by a petrol engine. By throttle control the sine-wave output signal could be frequency swept. The next step in the development presented an electrically

driven system which provided better frequency control. The first servo-hydraulic signal generator came into service by 1958 and allowed a certain phase control. Some elimination of phase distortions, due to variations in the vibrator-earth coupling, was made possible by the introduction of a feedback system. For higher frequency responses, electrodynamic vibrators have also been developed ("Shakers").

Basically, modern vibrators still employ most of the above mentioned features but are normally computerized. Small digital field computers can calculate the master sweep, control the phase, the amplitude and the feedback system as well as the recording of the reflection data onto a magnetic tape, and produce a field vibrogram.

Transducers are also built for marine Vibroseis operations since 1968 (BRODING et al, 1971). Similar servo-hydraulically driven vibrators produce a sweep signal by the displacement of water at a depth of 30 - 40 feet.

In general, three or four vibrators are working simultaneously in order to increase the overall energy of the input signal and to combat certain noise (e.g. surface waves) detrimental to any geophysical interpretation, by transmitting in specific patterns. Therefore, a highly accurate and reliable synchronization is absolutely essential.

As in explosive reflection seismology, the transmitted sweep will be reflected from each horizon in the subsurface. The geophones receive a superimposition of time delayed replicas of the input signal, thus producing an uninterpretable seismic record as can be seen from Figure 1.

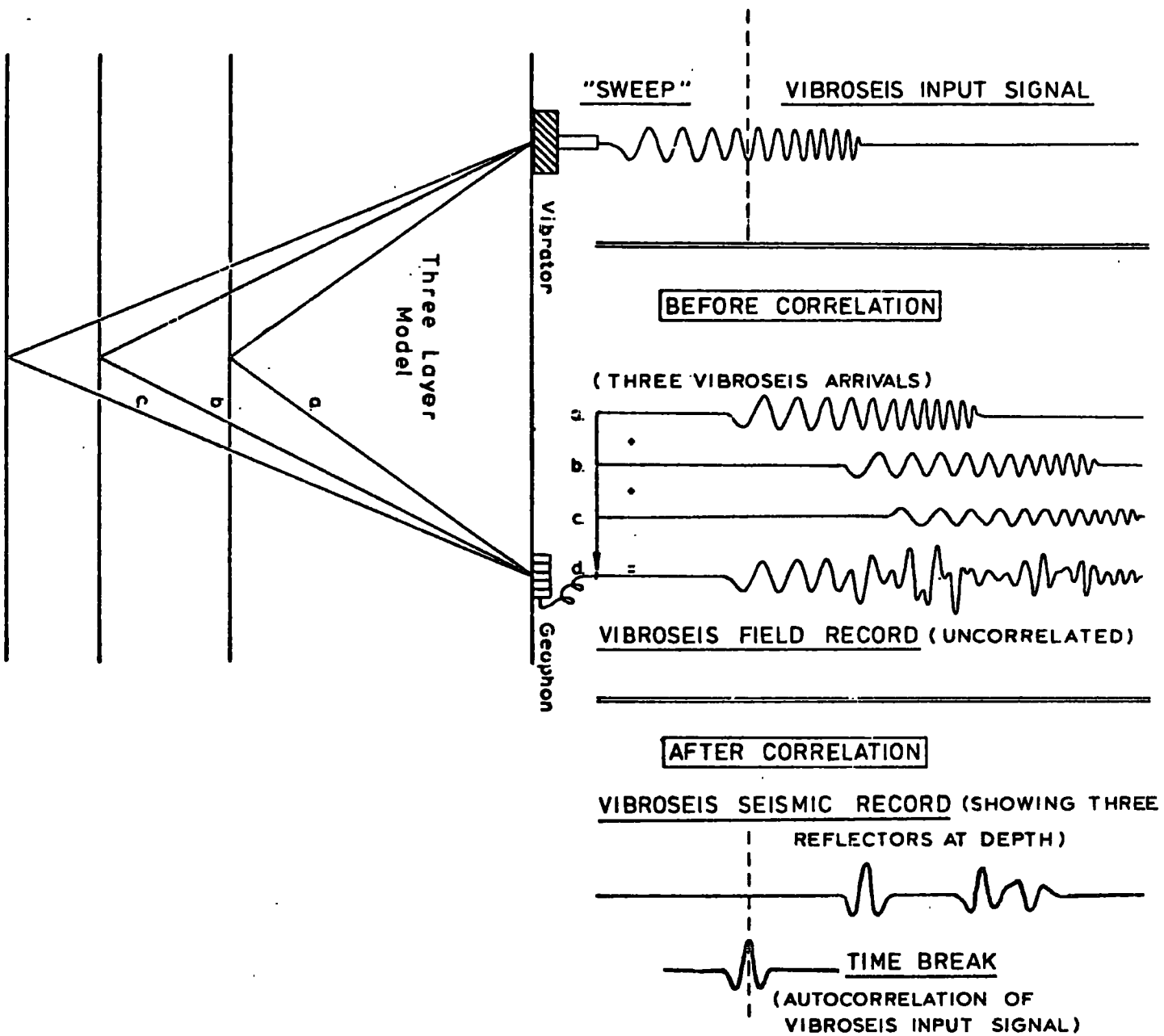


FIG. 1 - THE BASIC PRINCIPLES OF THE VIBROSEIS<sup>®</sup> SYSTEM

® REGISTERED TRADE AND SERVICE MARK OF CONTINENTAL OIL COMPANY

The mathematical technique of correlation enables the Vibroseis record to be transformed into a conventional seismogram. Qualitatively, the correlation process could be described as a method of measuring the similarity between two waveforms.

If the Vibroseis record is crosscorrelated with the master- or pilot signal, maximum correlation values (i.e. maximum similarity) will occur where the master signal 'finds' itself whilst being slid along the unreadable record. In this way the correlation process detects all reflections and indicates them by placing a correlation wavelet in its position. These wavelets will differ in amplitude, polarity and arrival time according to the physical properties of the examined subsurface and can be processed and interpreted by means of the usual methods already developed for impulse reflection records. The time break or zero time is found by autocorrelating the input signal as seen in Figure 1.

The correlation technique could also be described as a filter process and in fact a "Matched Filter" is nothing else than a correlator. The crosscorrelation procedure allows to discriminate against incoherent noise as it basically represents an almost ideal rectangular passband.

A major problem in the Vibroseis technique is the coupling of the vibrator baseplate with the ground. Nonlinear processes due to this imperfection are responsible for the highly undesired transmission of certain harmonics of the sweep, e.g. besides a 10 Hz to 40 Hz sweep a 20 Hz to 80 Hz second harmonic might be generated. During correlation at the processing stage, the original frequency swept signal will not only correlate with itself, but also with certain parts of the harmonic waveform (...in the above example with the 20 Hz to 40 Hz part) allowing for relatively high amplitudes away from the centre peak.

It can easily be seen, that for downsweeps this distortion will appear to the right and for upsweeps to the left of the main autocorrelation wavelet. Figure 2 illustrates the harmonic distortion problem for a downsweep of duration  $T$  and frequency range  $d=f_2-f_1$ . The name harmonic ghosting is sometimes used to describe the same disturbance, referring to the fact that the harmonic crosscorrelation tends to pretend non-existing events. Unfortunately, it might also mask weaker reflections and it is therefore vital to choose appropriate sweep parameters in order to suppress this noise.

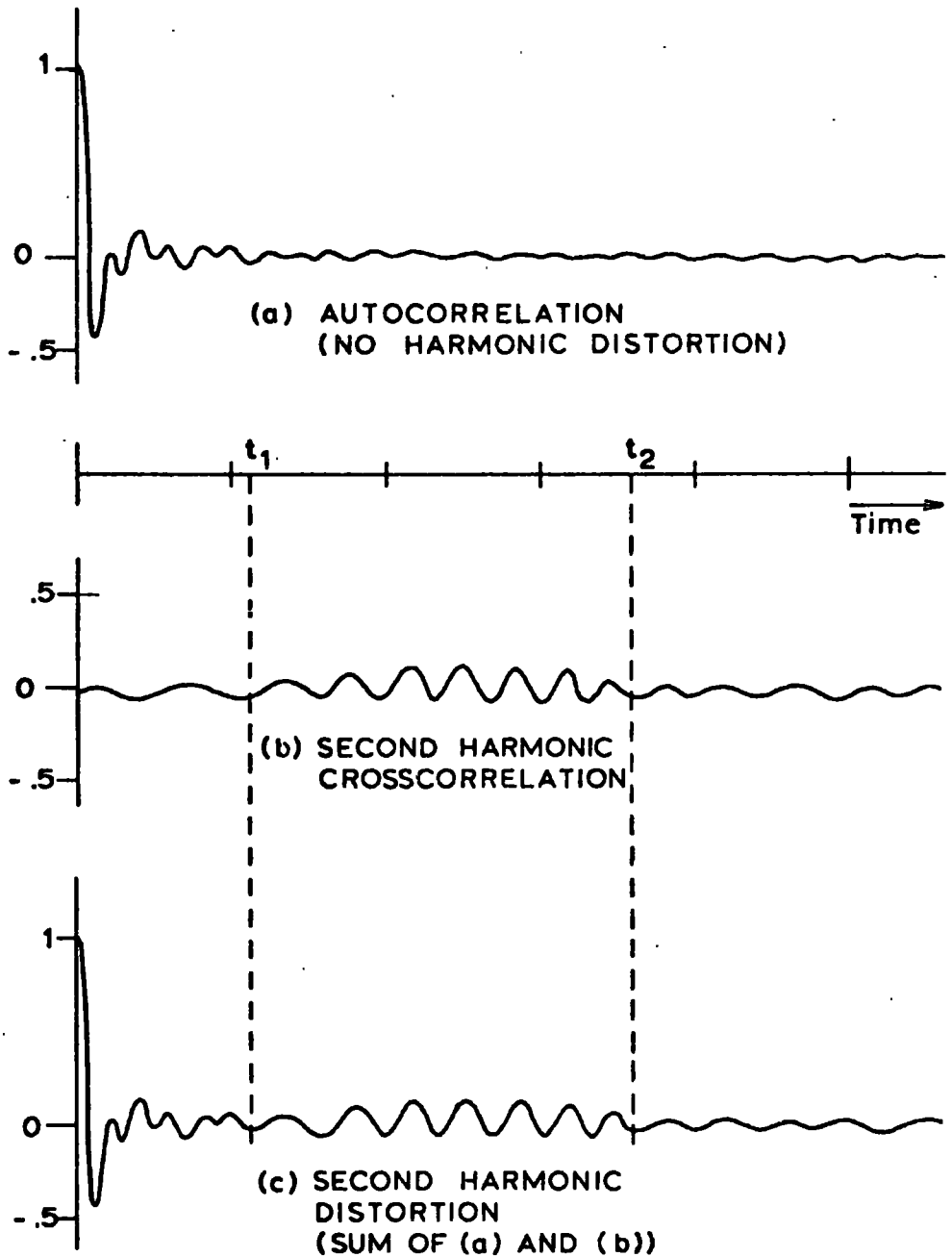
Using the outgoing, i.e. the already distorted sweep signal as the correlator does not yield any improvement. On the contrary, the situation is made worse because the harmonic distortions will now appear as forerunners and tails, independent of the type of sweep used (up- or downsweep). There is, however, a slight increase in the amplitude of the actual correlation peak.

The duration and position of the disturbance can be calculated by means of the two formulae in Figure 2. It follows that the duration of the sweep  $T$  determines the distance  $t_1$  from the main peak. This fact can be exploited in order to push the harmonic distortion beyond the range of interest in a seismogram, by choosing the right downsweep duration  $T$ .

The effect of harmonic distortion and the possible counteractions have been investigated thoroughly by SHERIFF and KIM (1970) and ERLINGHAGEN.

Summarized, the advantages of the Vibroseis system are:

- 1) Elimination of the use of explosives, thereby allowing its use in urban areas and other environmental critical regions.



$$t_1 = \frac{(h-1)T f_1}{\Delta} \quad \text{and} \quad t_2 = \frac{(h-1)T f_2}{h \Delta}$$

$h$  = order of harmonic ;  $\Delta$  =  $f_2 - f_1$  = bandwidth

FIG. 2 - 2<sup>nd</sup> HARMONIC DISTORTION ON  
DOWNSWEEP A/C WAVELET.

- 2) The use of a controllable surface low power long duration signal source, avoids wasting energy crushing rocks or generating frequencies which will be highly attenuated on their way through the earth.
- 3) It is an economical system as costs for explosives and drilling are saved.
- 4) The correlation process in connection with the frequency swept input signal provides a built-in filter.

However, there are some disadvantages, too:

- 1) The increase in surface waves excited by the vibrators.
- 2) Harmonic ghosts can lead to dangerous misinterpretations as they pretend reflections.
- 3) The hydraulic vibrators and the sophisticated control devices are very expensive.
- 4) The apparently inevitable correlation noise introduced through the correlation process.

It will be the main task of this work to show how to reduce the correlation noise and therefore how to improve the signal-to-noise ratio of Vibroseis seismograms.

However, in order to fully appreciate the suggested methods of correlation noise reduction, it is essential to understand the theoretical implications of the Vibroseis wavelet, the matched filter concept and the Vibroseis input signal.

## CHAPTER 2

### THE VIBROSEIS PARAMETERS

#### 2.1. Introduction

Before describing some of the Vibroseis characteristics in more detail, it is worthwhile to trace back the origin of the underlying principles.

Without the outstanding work of SHANNON (1948) and WIENER (1942) in communication and information theory, "Vibroseis" would probably not exist today. Their work helped to set forth the idea of signal detection by means of crosscorrelation and the concept of matched filtering, which was taken over by physicists and network mathematicians towards the end of the Second World War, in an attempt to overcome the radar peak power problems. These early pulse compression developments faced almost identical problems to the ones the Vibroseis system encountered several years later. It should therefore be realised, that the extensive theoretical work on all aspects of pulse compression in radar technology favoured a rapid progress of this technique in reflection seismology.

It is because of the deep relationship of pulse compression radar and Vibroseis, that throughout most of this work the problems of these techniques and their solutions are considered to be equivalent.

There are, however, quite substantial differences between the objectives and application of radar and Vibroseis, not to forget the vastly diverse specifications of the input signals (i.e. chirp / sweep): Whilst 'chirps' have a frequency range comprising several megahertz and a duration of only a few microseconds ( $\mu\text{sec}$ ), the sweep usually does not exceed 100 Hz and rarely starts with less than 5 Hz, but lasts 10 sec. or longer. A chirp radar system also does not need

to handle the complex propagation path inhomogeneities affecting the Vibroseis technique.

These differences have to be kept in mind, when the Vibroseis parameters are explained in the light of a general pulse compression theory.

In this chapter the Vibroseis input signal, as well as the sweep amplitude spectrum and the matched filter concept, will be explained and the Vibroseis wavelet characteristics are discussed in detail. The name "Klauder Wavelet" serves as an equivalent term for the latter, because it was J.R. KLAUDER (1960) who developed the theoretical framework for the chirp radar system and its associated pulse compression wavelet.

## 2.2. The Input Signal - The Sweep

Figure 3 shows the idealized sweep characteristics. If one assumes a small and constant sweep rate  $u$ , which allows for all frequencies to be represented almost equally well, the rectangular amplitude spectrum is a fairly good approximation to reality. In our idealized case let  $w_0$  be the carrier frequency, then

$$w = w_0 + ut \quad \text{for } |t| \leq T/2 \quad (1)$$

(Note:  $t = 0$  is at the centre of the signal). The phase of the transmitted frequencies can be expressed as

$$\phi(t) = \int w dt = w_0 t + ut^2/2 + C \quad (2)$$

where  $u = \text{sweep rate} = d/T$ ;  $d = \text{swept spectrum bandwidth}$ ;

$T = \text{duration of sweep}$ . The square-law term  $ut^2/2$  in equation (2), is responsible for the parabolic phase spectrum in Figure 3.

Finally, the frequency modulation can be understood as the time derivative of the phase modulation yielding the expected linear function.

Unfortunately, the analysis of sweep characteristics, especially the computation of the amplitude and phase spectra, is far more complicated than indicated above. The classical paper on this subject is KLAUDER et al (1960), 'The Theory and Design of Chirp Radars'. Further work was done by CHIN et al (1959), RAMP (1961), COOK (1960), COOK (1958) and COOK (1967). The most important results of the chirp analysis, as far as they are relevant to the Vibroseis system, will be briefly summarised here.

A general formula for pulse compression waveforms could be:

$$s(t) = a(t) \cos(2\pi f_0 t + \phi(t)) \quad (3)$$

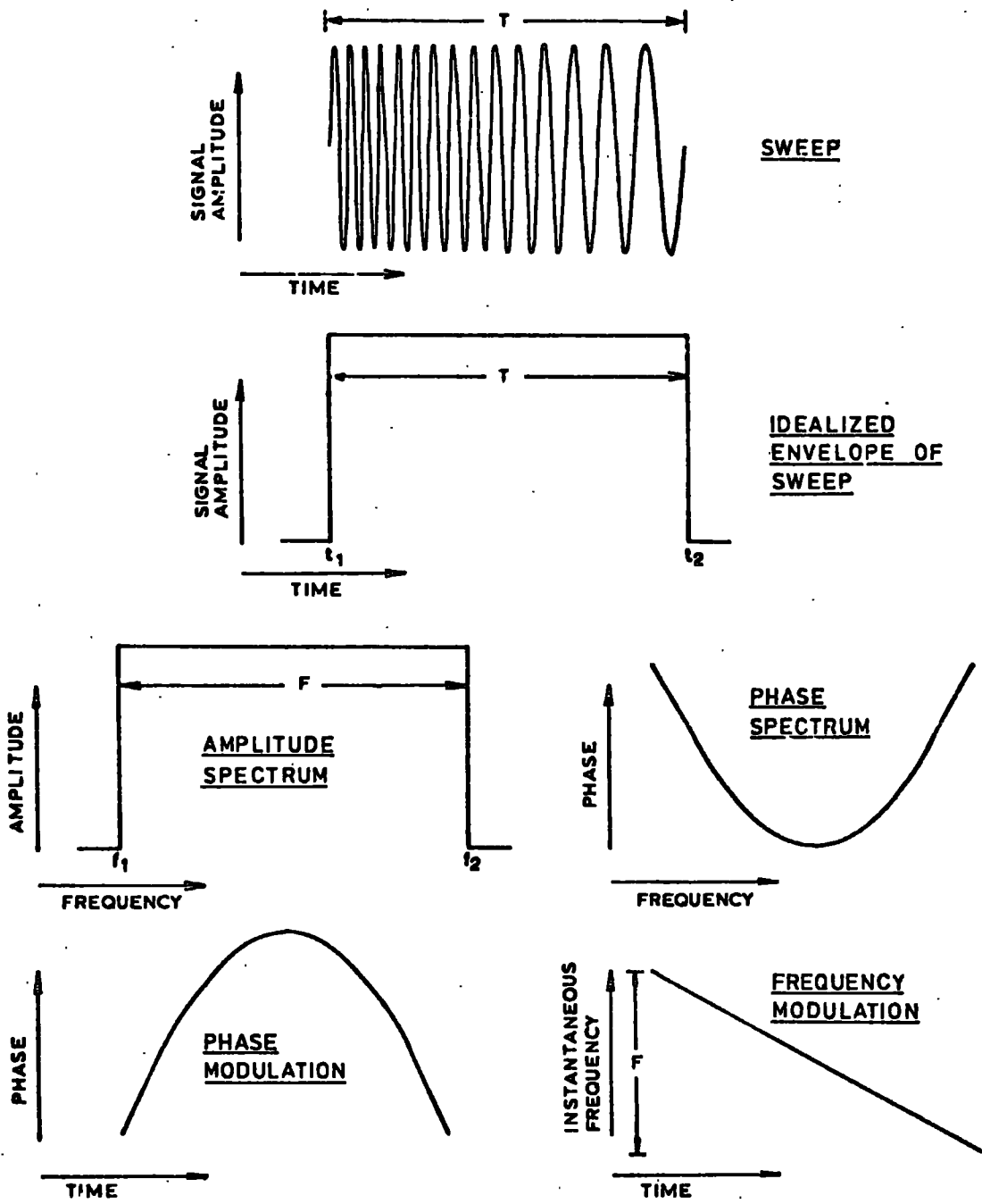


FIG. 3 - IDEALIZED SWEEP CHARACTERISTICS

where  $a(t)$  = amplitude modulation;  $f_0$  = carrier frequency (equivalent to the midfrequency of a sweep);  $\phi(t)$  = phase modulation.

Sweeps and chirps are linear FM modulated signals and they can be defined by:

$$s(t) = a(t) \cdot \cos(2\pi(f_0 \pm \frac{1}{2}(d/T)t)t) \quad (4)$$

for  $-T/2 \leq t \leq +T/2$

where  $T$  = duration of signal and  $d = f_2 - f_1$  = bandwidth. According to the + or - sign the above formula represents an up-sweep or a down-sweep, respectively.

For the calculations of amplitude and phase spectra, however, it is a matter of convenience to use the real part of the following complex waveform to characterize a sweep or chirp.

$$E_1(t) = \text{rect}(t/T) \cdot \exp(2\pi i(f_0 t + ut^2/2)) \quad (5)$$

where  $\text{rect}(z) = 1$  if  $|z| < \frac{1}{2}$   
 $= 0$  if  $|z| > \frac{1}{2}$

The instantaneous frequency  $f_i$  of (5) is defined as

$$f_i = (1/2\pi)(d\phi/dt) = f_0 + ut \quad (6)$$

for  $|t| \leq T/2$

where  $\phi$  = phase =  $2\pi(f_0 t + ut^2/2)$ . The instantaneous frequency changes in a linear fashion from

$$f_0 - uT/2 \quad \text{to} \quad f_0 + uT/2 \quad \text{in } T \text{ seconds.}$$

The frequency range of a sweep is therefore

$$d = (f_0 + uT/2) - (f_0 - uT/2) = uT = f_2 - f_1 \quad (7)$$

By introducing the variables  $y = t \cdot d$  and  $x = f/d$ , equation (5) can be rewritten as

$$E_1(y) = \text{rect}(y/D) \cdot \exp(2\pi i(x_0 y + y^2/2D)) \quad (8)$$

with  $x_0 = f_0/d$  and  $D = T \cdot d$ .

'D' is called the "Time-Bandwidth-Product" or "Dispersion" and is

of great importance in the design of good frequency swept signals.

### 2.3. The Amplitude Spectrum of a Sweep

In calculating the amplitude spectrum of a sweep one has to deal with Fresnel integrals. For a detailed derivation the interested reader is referred to the excellent and rigorous analysis of linear FM pulse compression spectra by CHIN et al (1959).

In general, it can be shown that the amplitude spectrum of a sweep is not perfectly rectangular as in Figure 3. Here, for the first time, the dispersion factor plays an important role, because the spectrum deviates considerably from the ideal rectangular shape for small D's (i.e.  $D < 10$ ) and approaches the ideal case only for very large D's. The spectrum is considered to be rectangular, in practice, when D is greater than 80.

However, KLAUDER (1960) calculated by means of numerical integration, that even for small D's almost 95% of the spectral energy is contained in the frequency range  $d = f_2 - f_1$ , whilst for  $D = 100$  about 99% is contained in this band.

Mathematically it can be shown, that the Fresnel integrals introduce the ripples observed on the spectrum, as they are quasi oscillatory in nature. The spectrum of the linear FM signal  $s(t)$

$$s(t) = A \cos(\omega_0 t + ut^2/2) \quad (9)$$

$$\text{for } |t| \leq T/2$$

where  $u = 2\pi d/T$ , would be  $S(\omega)$  with  $A=1$

$$S(w) = \int_{-T/2}^{+T/2} \cos(w_0 t + ut^2/2) \exp(-iwt) dt \quad (10)$$

The solution to this integral involves Fresnel integrals and after a few suitable algebraic steps the above formula changes into

$$S(w) = \frac{1}{2}(\pi/u)^{\frac{1}{2}} \exp(-i(w_0 - w)^2/2u) \cdot [C(X_1) + iS(X_1) + C(X_2) + iS(X_2)]$$

where  $X_1 = (uT/2 + (w_0 - w))/(\pi u)^{\frac{1}{2}}$

$$X_2 = (uT/2 - (w_0 - w))/(\pi u)^{\frac{1}{2}} \quad (11)$$

C(X) and S(X) are Fresnel integrals and are shown in Figure 4.

(Note the oscillatory nature.)

$$C(X) = \int_0^X \cos \frac{\pi}{2} y^2 dy \quad (12)$$

$$S(X) = \int_0^X \sin \frac{\pi}{2} y^2 dy \quad (13)$$

According to COOK (1960) the linear FM spectrum consists of two components.

1) The spectrum amplitude term:

$$|S(w)| = \frac{1}{2}(\pi/u)^{\frac{1}{2}} \left[ [C(X_1) + C(X_2)]^2 + [S(X_1) + S(X_2)]^2 \right]^{\frac{1}{2}} \quad (14)$$

2) The phase term:

$$\phi(w) = (w_0 - w)^2/2u - \tan^{-1} \left[ (S(X_1) + S(X_2)) / (C(X_1) + C(X_2)) \right] \quad (15)$$

Only the square-law phase term in (15) is of importance

$$\phi_1(w) = (w_0 - w)^2/2u \quad (16)$$

because the remainder, the so-called residual phase term, can be ignored for large D as it only contributes a constant phase angle over the spectrum bandwidth.  $\phi_1(w)$  will be matched in the matched filter design by a conjugate phase term

$$-\phi_1(w) = -(w_0 - w)^2/2u \quad (17)$$

The ripples due to the Fresnel integrals influence become smaller for large D. They have a degenerate effect at the processing stage, as they introduce additional sidelobes. Figure 5b shows the

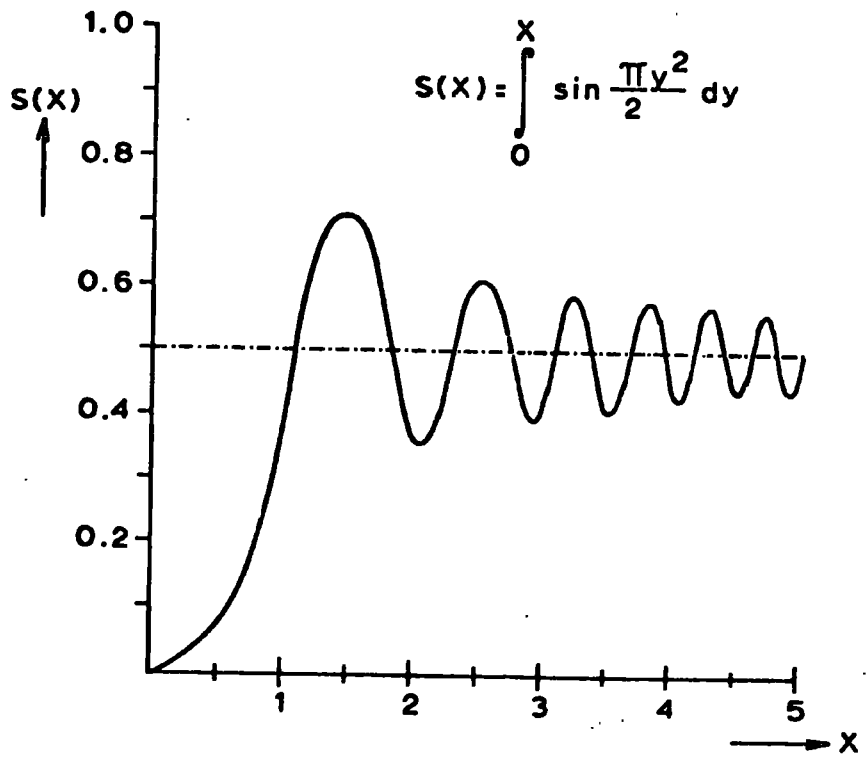
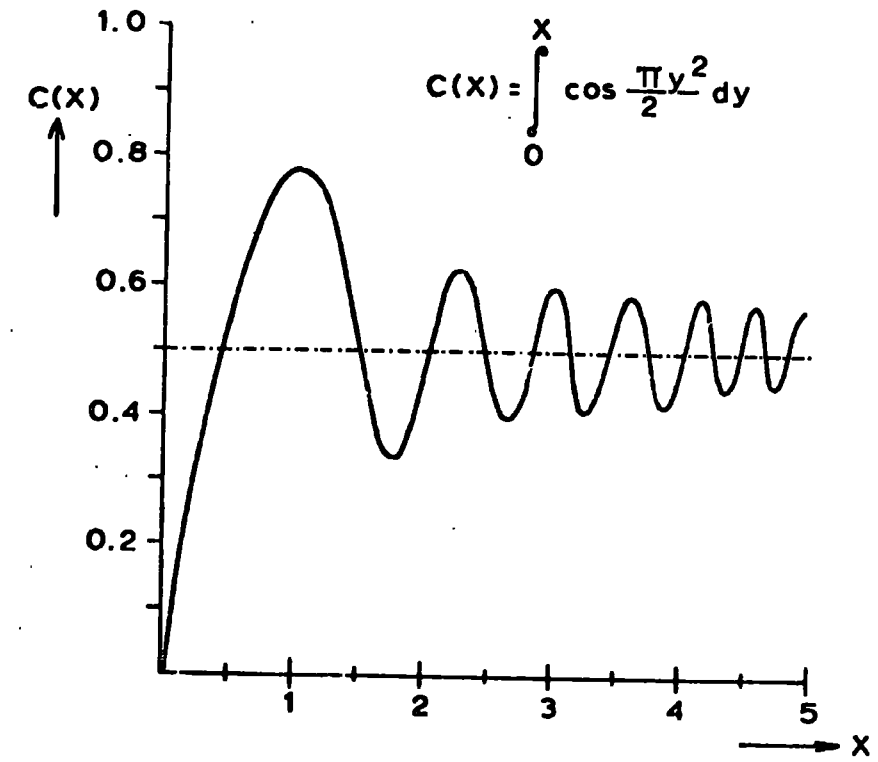


FIG. 4 - FRESNEL INTEGRALS

F(a) REPRESENTS THE FOURIER TRANSFORM OF f(x)  
SHOWING THE CHARACTERISTIC [SIN Z]/Z - SHAPE.

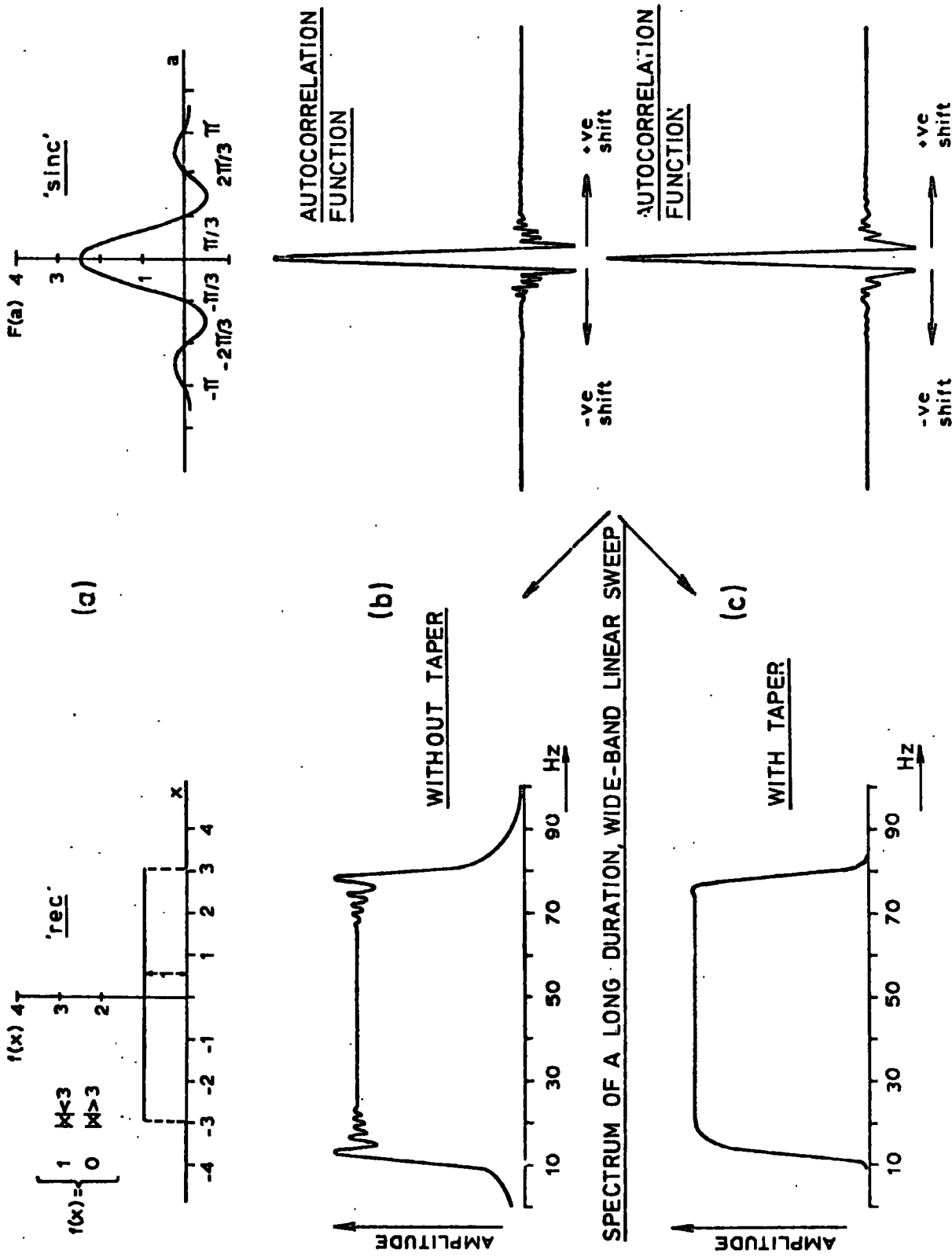


FIG. 5

amplitude spectrum of an untapered sweep, and Figure 5c the spectrum after tapering the same signal. In Figure 5c the Fresnel ripples are greatly suppressed, but both spectra deviate from the ideal rectangular shape in Figure 5a quite distinctly.

#### 2.4. The Matched Filter Concept in Vibroseis

As already outlined the raw Vibroseis data as received by the geophones is uninterpretable unless processed in a suitable manner. The technique of matched filtering transforms the signals received into a form which is useful for interpretation.

A filter which is matched to a physical waveform  $s(t)$  has, by definition, the impulse response

$$h(t) = ks(t_D - t) \quad (18)$$

where  $k$  is a normalising factor and  $t_D$  an arbitrary delay constant, required to make the filter physical realizable.

It is well-known that the transfer function of a linear filter system is the Fourier transform of the impulse response. Therefore:

$$\begin{aligned} H(i\omega) &= \int_{-\infty}^{+\infty} h(t) \exp(-i\omega t) dt \\ &= k \int_{-\infty}^{+\infty} s(t_D - t) \exp(-i\omega t) dt \end{aligned} \quad (19)$$

Substituting  $t' = t_D - t$

$$H(i\omega) = k \cdot \exp(-i\omega t_D) \cdot \int_{-\infty}^{+\infty} s(t') \exp(i\omega t') dt' \quad (20)$$

$$F[s(t)] = S(i\omega) = \int_{-\infty}^{+\infty} s(t) \exp(-i\omega t) dt = \text{spectrum of } s(t) \quad (21)$$

It follows that a comparison of (20) and (21) leads to

$$H(i\omega) = k \cdot S(-i\omega) \cdot \exp(-i\omega t_D) = k \cdot S^*(i\omega) \cdot \exp(-i\omega t_D) \quad (22)$$

In general (22) can be expressed as

$$H(\omega) = S^*(\omega) \quad (23)$$

ignoring the normalization factor  $k$  and the delay constant  $t_D$ .

Therefore, the transfer function of a filter matched to a certain signal is the complex conjugate of the spectrum of that signal. The equivalent time domain function to (23) can be derived from (18).

$$h(t) = k \cdot s(-t) \quad (24)$$

If a real valued signal  $s(t)$  is put through a linear system, such as a matched filter, the output  $y(t)$  can be described either by:

$$y(t) = (1/2\pi) \int_{-\infty}^{+\infty} H(\omega) \cdot S(\omega) \cdot \exp(i\omega t) d\omega \quad (25)$$

which is the reverse Fourier transform of  $H(\omega) \cdot S(\omega)$  or by

$$y(t) = \int_0^{+\infty} h(\tau) \cdot s(t-\tau) d\tau \quad (26)$$

Finally, (25) and (26) can be rewritten as

$$y(t) = (1/2\pi) \int_{-\infty}^{+\infty} |S(\omega)|^2 \cdot \exp(i\omega(t-t_D)) d\omega \quad (27)$$

and

$$y(t) = \int_0^{+\infty} s(t_D-\tau) \cdot s(t-\tau) d\tau \quad (28)$$

respectively, using (23) and (18).

(27) is obviously the inverse Fourier transform of the signal energy spectral density  $|S(\omega)|^2$ . Equation (28) can easily be recognized as the autocorrelation function of the input  $s(t)$ .

Because of (28) a matched filter is sometimes called a correlator, as it performs the correlation process. A matched filter has also been given the name "Conjugate Filter", which is a reasonable description if one recalls equation (23).

To recapitulate:

The correlation of two waveforms can be performed by passing one waveform through a linear system whose impulse response is the time reverse of the other waveform. If both waveforms are identical the linear system is called a matched filter.

In the Vibroseis system the matched filter is almost entirely represented by very fast purpose built digital computers (correlators), which are capable of correlating digital Vibroseis data quickly and accurately. These correlators transform the unprocessed and unreadable Vibroseis record into a normal well-known seismogram.

Over the last 20 years the matched filter process has been investigated intensively as the following list of references might indicate: NORTH (1943); ROCHEFORT (1954); ELSPASS (1955); TURIN (1960); ANSTEY (1964); ROBINSON (1967).

Optimal matching of the receiver is only feasible for sophisticated signals, i.e. signals with a dispersion factor  $D$  exceeding unity. When matched filter processed, there is no noticeable compression for classical radar signals with rectangular or gaussian envelope. The spectrum width for these signals is about  $1/T$ ,  $T$  = pulse duration. As the compression ratio equals  $d \cdot T = (1/T)T = 1$ , there is no pulse shortening.

Besides performing the pulse compression on the reflected sweeps, the correlation process also combats noise and to that end the matched filter is the best among the linear filters. Under the assumption that the noise in the system is gaussian NORTH (1943) determined that the matched filter maximises the signal to noise ratio.

$$S/N\text{-ratio} = 2E/N_0 \quad (N_0 = \text{noise power density}) \quad (29)$$

where  $E$  = energy of the received signal.

It has to be remarked, that (29) implies that as far as the ability of a matched filter to combat noise is concerned, signals with the same energy on interception at the receiver will show the same performance.

The correlation process against a signal with rectangular spectrum works like an ideal bandpass filter which discriminates against all frequencies outside the pass band.

The following set of formulae was given by LANDRUM (1967), describing the signal to noise improvement to be expected in matched filter processing for three noise categories often encountered in the Vibroseis system.

- a) A monofrequency noise (e.g. 50 Hz powerline pick-up) lies within the sweep's bandwidth, i.e.  $f_1 < f_n < f_2$

$$S/N \text{ improvement} \approx 20 \cdot (\log_{10} \sqrt{D}) \text{ db}$$

- b) A monofrequency noise has one of the terminal frequencies of the sweep, i.e.  $f_n = f_1$  or  $f_n = f_2$

$$S/N \text{ improvement} \approx 20 \cdot (\log_{10} 2\sqrt{D}) \text{ db}$$

The S/N improvement will increase drastically for  $f_n < f_1$  or  $f_n > f_2$ .

- c) The noise is random (e.g. environmental noise)

$$S/N \text{ improvement} \approx 20 \cdot (\log_{10} \sqrt{T \cdot d_n}) \text{ db}^*$$

where T = sweep duration and  $d_n$  = bandwidth of noise.

This formula proves, that in the case of random noise, the matched filter works best the longer the input signal.

A detailed study of the signal to noise ratio can be found in Krey's paper entitled: "Remarks on the signal to noise ratio in the Vibroseis system". (KREY (1969))

\*

$d_n = f_{n2} - f_{n1}$  is limited by the specifications of the recording system: e.g.  $f_{n2}$  = cutoff frequency of anti-alias filter in amplifiers, and  $f_{n1}$  = geophone cutoff frequency. The approx. formula c) holds in these limits.

2.5. The Output Wavelet - The Klauder Wavelet

If a signal is passed through a perfect matched filter, the autocorrelation function of that signal will result. In the case of a sweep, the matched filter acts a phase equaliser removing its phase distortion. A linearly frequency swept signal was described by:

$$E_1(t) = \text{rect}(t/T) \exp(2\pi i(f_0 t + ut^2/2))$$

It follows that the ideal matched filter impulse response has to be:

$$y(t) = E_1^*(-t)$$

$$y(t) = \text{rect}(t/T) \cdot \exp(2\pi i(f_0 t - ut^2/2)) \quad (30)$$

The matched filter action amounts to the convolution of  $E_1(t)$  with  $E_1^*(-t)$ , i.e.

$$\text{MFO} = \text{Matched Filter Output} = y(t) * E_1(t) = E_1^*(-t) * E_1(t)$$

or

$$\text{MFO} = \int_{-\infty}^{+\infty} E_1^*(\tau-t) \cdot E_1(\tau) \, d\tau$$

$$= \int_{-\infty}^{+\infty} \text{rect}(\tau-t/T) \cdot \text{rect}(\tau/T) \cdot \exp \left[ 2\pi i \left( f_0 t + \frac{(u/2)\tau^2}{- (u/2) \cdot (\tau-t)^2} \right) \right] \, d\tau \quad (31)$$

The solution to (31) describes the Klauder wavelet:

$$\text{Klauder wavelet} = (1/\pi ut) \exp(2\pi i f_0 t) \cdot \sin \pi (utT - ut^2) \quad (32)$$

The graph in Figure 6 represents the real part of the above complex equation.

The envelope of the Klauder wavelet seems to show quite a striking similarity to the Fourier transform of a rectangular pulse, which is normally referred to as the  $(\sin z)/z$  or sinc  $z$  - function. (See Figure 5a). In fact, KLAUDER (1960) and others proved that the autocorrelation function of a sweep will approach a  $(\sin z)/z$  - shape as the time-bandwidth product increases and the spectrum comes nearer to the rectangular form. There exists a functional Fourier

$f_1$  = BEGINNING FREQUENCY OF SWEEP

$f_2$  = ENDING FREQUENCY OF SWEEP

$$f_0 = (f_1 + f_2) / 2$$

T = DURATION OF SWEEP

$P/S_1$  = FUNCTION OF  $f_1/f_2$

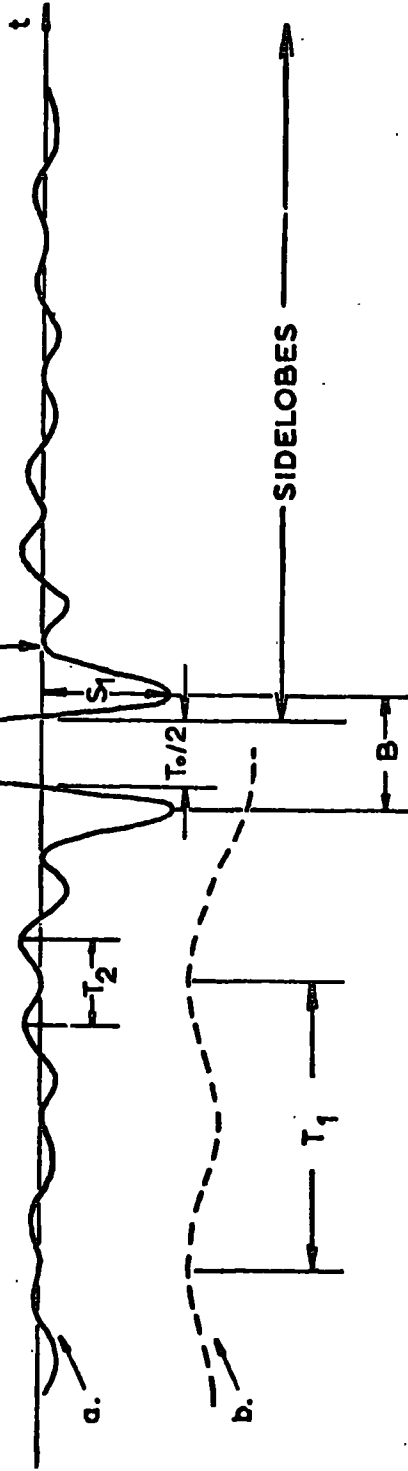
B = BREADTH

CENTRE PEAK

THE GRAPH SHOWS THE REAL PART

OF KLAUDER'S COMPLEX EQUATION:

$$e_{m1}(t) = \frac{1}{\pi ut} e^{2\pi i f_0 t} \sin \pi (u t T - u t^2)$$



$$T_0 = 1/f_0$$

$T_1 = 1/f_1$  = PERIOD OF THE LOW FREQUENCY COMPONENT (b.)

$T_2 = 1/f_2$  = PERIOD OF THE HIGH FREQUENCY COMPONENT (a.)

FIG. 6 - THE KLAUDER WAVELET

transform relationship between matched filter input and output, although both are functions of time. This is always true for matched filter detection and is not only confined to the rect z and sinc z envelopes.

Figure 6 shows the theoretical autocorrelation function of the Vibroseis input signal which has essentially all the characteristics of a true A/C-function and is therefore frequently used to produce synthetic Vibroseis seismograms, by convolving an artificial earth response with this wavelet.

Its purpose here is to highlight the general nature of the Klauder wavelet.

The function shown in Figure 6 is symmetrical about its centre. Quite a few signal parameters should be apparent from the text on the graph.

The frequency band covered by the sweep is of great importance for the basic shape of the wavelet which is determined by the frequency ratio  $f_2/f_1$ , whilst the bandwidth determines the sharpness of the peak.

The interval between the first zero crossings away from the centre is exactly  $T_0/2$ , where  $T_0$  is the period of the average sweep frequency. Sidelobes extend to both sides of the centre peak and it can be seen that they are a composition of high and low frequency components (Figure 6a and 6b). The high frequency part reflects approximately the highest frequency of the signal and superimposes a low frequency component which is essentially equal to the low frequency end of the sweep and  $180^\circ$  out of phase with the centre peak.

In the Vibroseis system the spikeness of the Klauder wavelet is defined by the ratio  $P/S_1$ . If  $f_1$  equals  $f_2$  this ratio would be 1.

In the most commonly used two-octave sweeps,  $P/S_1$  will be about  $\frac{1}{2}$ .

The importance of choosing the right frequency range is underlined in Figure 7. 7a shows the Klauder wavelet of a common Vibroseis sweep - the sidelobes are small and the centre peak is quite spiky.

The wavelet in Figure 7b has the same centre spike (because it has the same centre frequency of 20 Hz), but the sidelobes are of extremely high amplitude, masking the main lobe. The whole signal seems to ring and as it is very important to distinguish between seismic and correlation ringing this wavelet can lead to some confusion. It is therefore not desirable to use narrow bandwidth input signals (i.e. less than 1 octave) in the Vibroseis technique. Common sweeps have ranges of 5 Hz - 20 Hz, 10 Hz - 40 Hz, 16 Hz - 64 Hz, 20 Hz - 80 Hz, which when transmitted over a period of 6 sec. have a time-bandwidth product of 90, 180, 288 and 360 respectively, guaranteeing a good pulse compression.

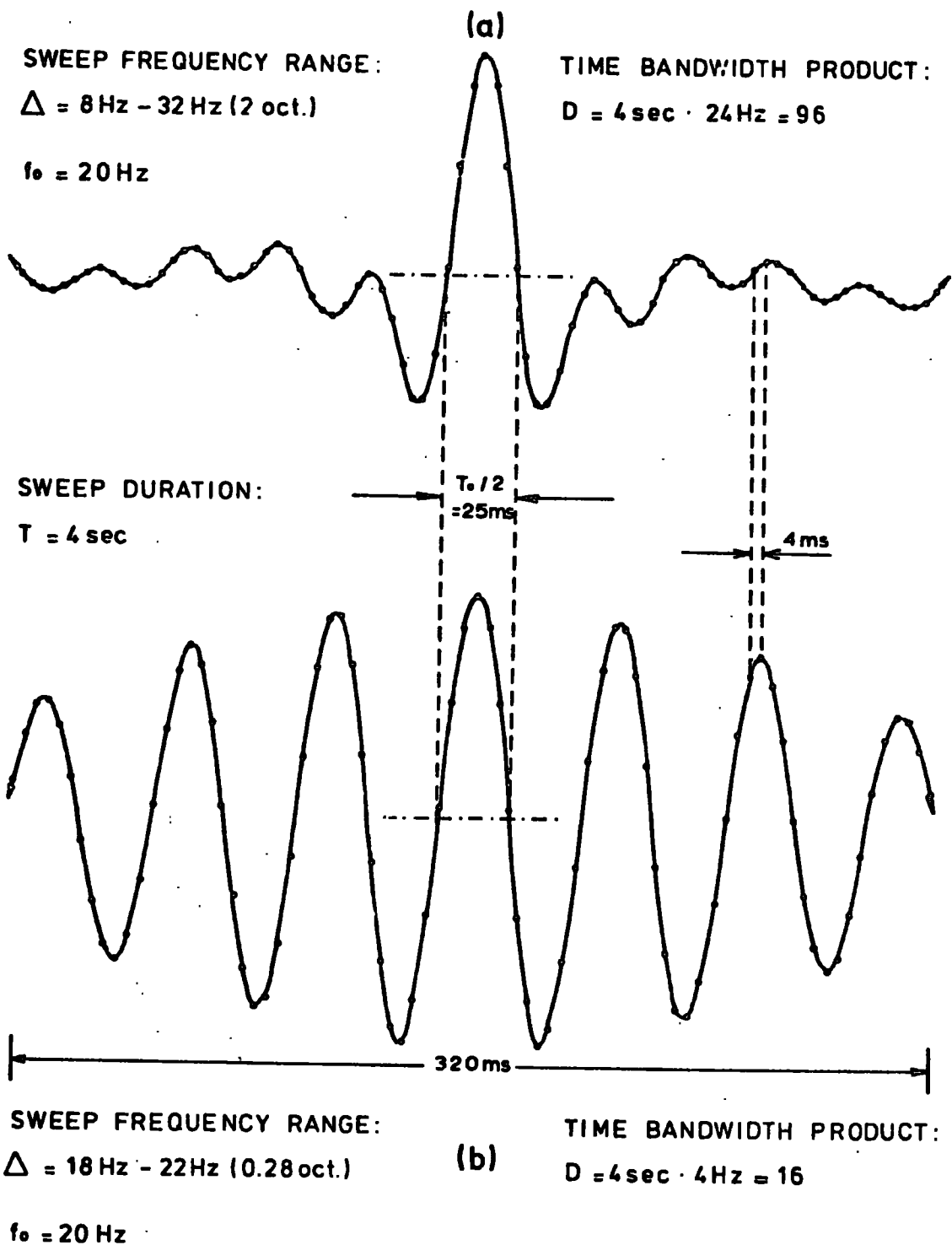


FIG. 7 - A/C-FUNCTION OF TWO DIFFERENT LINEAR SWEEPS

## CHAPTER 3

### THE SIGNAL-TO-NOISE PROBLEM IN VIBROSEIS

#### 3.1. Introduction

In a Vibroseis seismogram the Klauder wavelet's centre peak represents a reflection from the subsurface. Depending on many factors (like reflection coefficient of the reflecting horizon, separation of horizons, seismic velocities etc.) this pseudo spike will have a different amplitude and different spacing in time. Unfortunately, a long sequence of sidelobes is associated with every centre peak. These sidelobes represent signal generated noise and if not kept low in amplitude carefully, they might mask subsequent reflections.

Particularly in radar technology great efforts were made to suppress the disturbing lobes. In Vibroseis, too, various methods are known to lower the correlation noise, in order to increase the detection capability of the system.

Basically, there are four stages of improving the overall signal-to-noise ratio:

- 1) Choose the optimal input signal (i.e. sweep) parameters according to the geological problem encountered and the known ambient noise sources.
- 2) Choose transmitting pattern for vibrators to combat surface waves, for example.
- 3) Take appropriate measures either on the transmitting or receiving/processing side, in order to reduce correlation noise (e.g. taper).
- 4) The use of the matched filter method on processing yields a certain S/N-improvement.

### 3.2. The Theory of Sidelobe Reduction

As outlined previously, the matched filter output waveform will assume the well-known  $(\sin z)/z$ -shape, when the amplitude spectrum of the sweep input signal is rectangular. The sinc-function, however, is characterized by its relatively high intrinsic sidelobes, which are only 13.2 db down with respect to the centre peak. In the Vibroseis system these sidelobes have to be considered to be interfering signals.

The best known method of sidelobe reduction is the introduction of a weighting function  $W(\omega)$ . This function can be designed so that the weighted compressed pulse  $w(t)$  will have lower sidelobes than the sinc-function.

$$w(t) = (1/2\pi) \int_{\omega_0 - \Delta\omega/2}^{\omega_0 + \Delta\omega/2} W(\omega) \cdot \exp(i\omega t) d\omega \quad (33)$$

A time weighted linear FM signal can therefore be represented by

$$s_w(t) = w(t) \cdot \exp(2\pi i(f_0 t + ut^2/2)) \quad \text{for } |t| \leq T/2 \quad (34)$$

Presuming a rectangular spectrum for the linear FM signal and the correct choice of  $w(t)$  as a weighting function for a sweep, the filter output wavelet will show lower sidelobes because of the Fourier transform relationship between input and output signal.

In the radar context the Dolph-Chebyshev (physically unrealizable), the Taylor- and the generalized cosine power weighting functions are familiar terms. A sidelobe reduction of up to 43 db can be achieved in theory by their application. See Table I.

There are basically three methods of correlation noise reduction by means of weighting functions:

- a) The transmitted signal is time shaped by means of  $w(t)$ .

- b) The spectrum of the detection filter is weighted by means of  $W(\omega)$ .
- c) The transmitted envelope and the receiver response are weighted.

COOK and BERNFELD (1967) showed that time weighting of the transmitted signal or frequency weighting of the receiver response function, will yield identical pulse compressed signals.

In the Vibroseis system of exploration only two of the weighting functions in Table I find application - the Hamming function and the cosine-squared function. Both functions are special cases of the set of general cosine weighting functions:

$$w(x) = k + (1-k) \cos^n(\pi x / \Delta x) \quad (35)$$

The Hamming window allows the best sidelobe reduction with almost 43 db. The pedestal height  $k$  has great influence on the final sidelobe suppression (see Figure 8). For  $n=2$  and  $k=0.08$  the Hamming function represents the optimal compromise for sidelobe level and pulse widening if used in method a) or b) which introduce pulse widening and a mismatch loss, because of the divergence from the ideal matched filter concept.

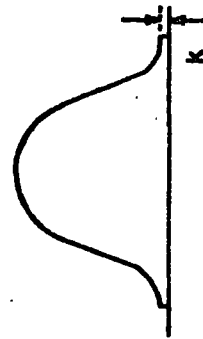
For maximum transmission of energy it is best to taper the filter, but for signal to noise enhancement it is better for the shaping to be shared equally between transmission and detection. However, for the low energy Vibroseis system only time shaping (tapering) of the matched filter time domain function is usual practice.

It must be emphasized at this stage, that for most of the theoretical investigations so far, a perfectly rectangular sweep amplitude spectrum was assumed and the detailed nature of the true spectrum was disregarded. For some of the following discussions this

TABLE I

COSINE WEIGHTING FUNCTIONS AND THEIR EFFECT ON THE KLAUDER WAVELET.

TYPE OF WEIGHTING FUNCTION	LEVEL OF HIGHEST SIDE LOBE IN db	DECREASE FUNCTION OF SIDE LOBES	PULSE WIDENING	MISMATCH LOSS IN db
RECTANGULAR	13.2	1/T	1.0	0.0
HAMMING WINDOW (k=0.08, n=2)	42.8	1/T	1.47	-1.34
COSINE - SQUARED (k=0.0, n=2)	32.0	1/T <sup>3</sup>	1.62	-1.76
COSINE - CUBED (k=0.0, n=3)	39.1	1/T <sup>4</sup>	1.87	-2.38



THE GENERAL COSINE WEIGHTING FUNCTION :  $W(w) = k + (1-k) \cos^n \frac{\pi w}{\Delta w}$

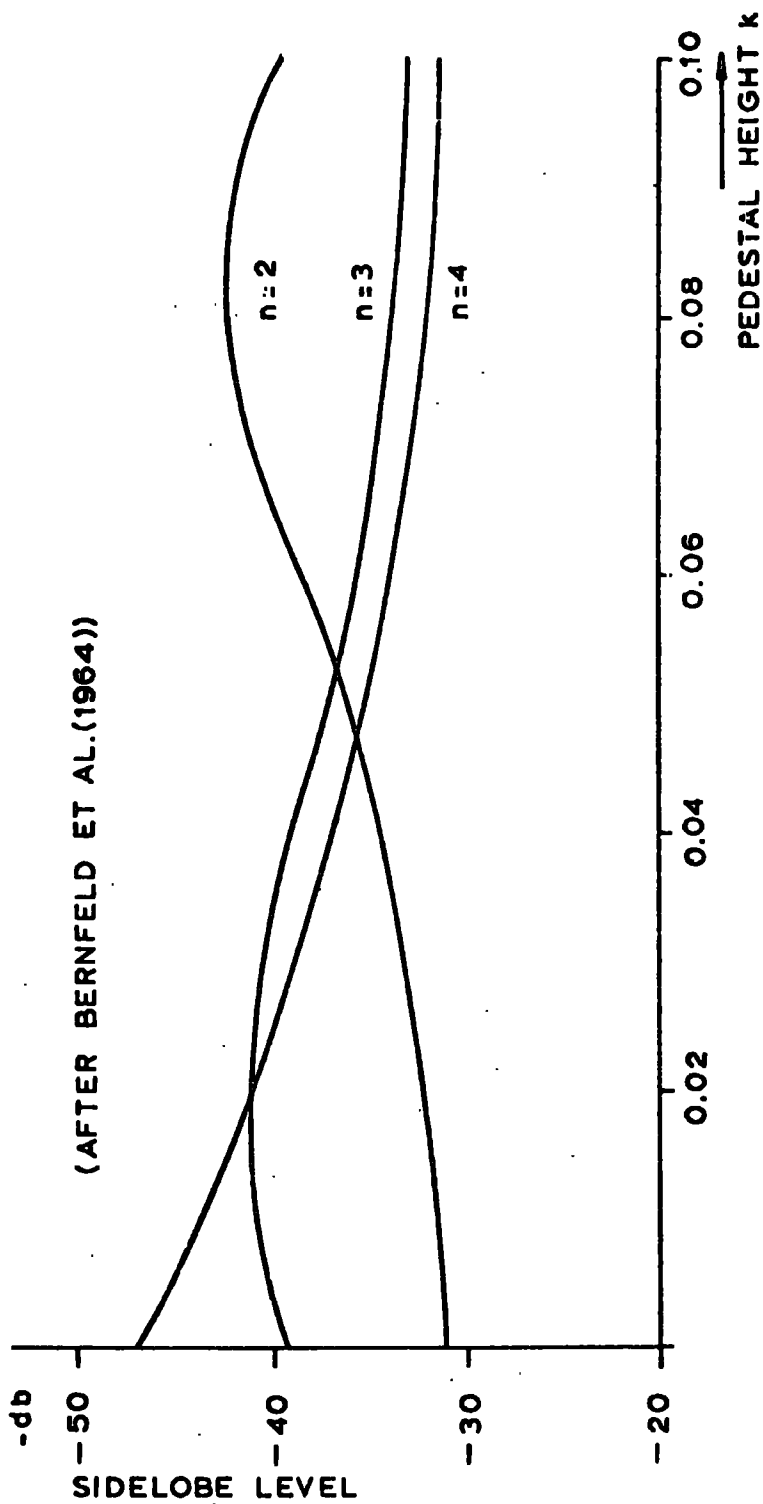


FIG. 8 - EFFECT OF PEDESTAL HEIGHT  $k$  IN COSINE WEIGHTING FUNCTION ON SIDELobe LEVELS.

assumption is no longer sufficient.

With the help of the so-called "Paired Echo" technique (see Appendix) of distortion analysis the effect of the Fresnel ripples in the sweep spectrum has been investigated (BERNFELD et al (1964); COOK et al (1964)).

A combination of simple sinusoidal components approximates the Fresnel amplitude variations. The application of the paired echo theory led to an expression for the compressed pulse which consists of 7 terms. The first term represents the idealized compressed pulse followed by 6 terms of time displaced paired echo distortions.

This specific Fresnel noise is very similar to the sidelobes and superimposes them, but cannot be appreciably reduced by weighting functions.

To summarize: The Fresnel ripples in the amplitude spectrum introduce an additional set of sidelobes of about -30 db.

In order to understand the origin of the Fresnel ripples one has to fall back upon the well-known ripples in the output response of an ideal bandpass filter with unit step cut-off characteristic. The step function response of an ideal filter will have the form of a sine-integral function as shown in Figure 9. The sharp cut-off, or the so-called rise or fall time of the ideal filter amplitude spectrum is responsible for the ripples in the output response (Gibb's phenomenon).

In analogy to the above example it has been argued, that the sharp build-up time of the linear sweep time envelope is causing the Fresnel ripples in the amplitude spectrum. Therefore, slowing down the rise time should result in a reduction of the spectrum distortion

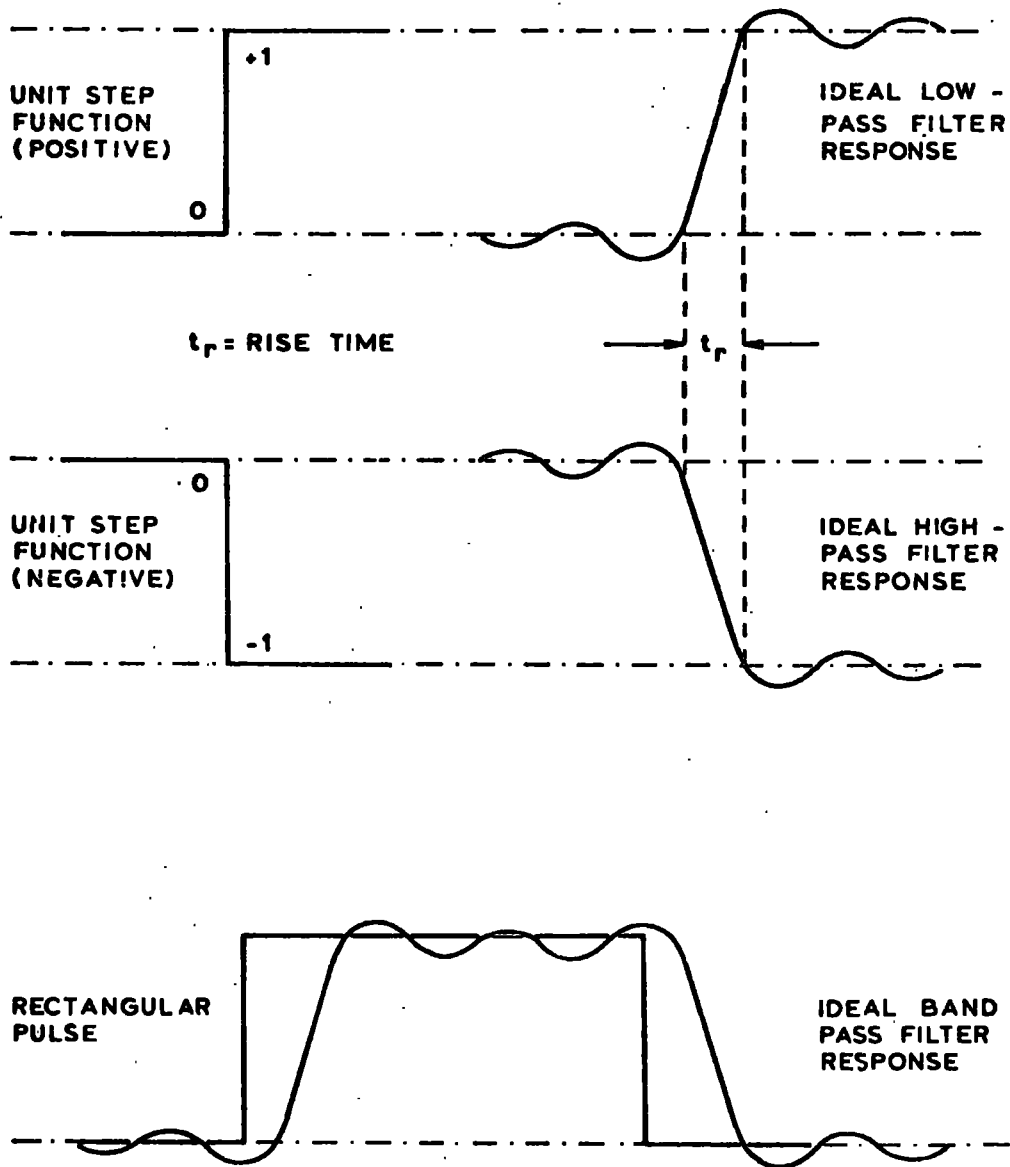


FIG. 9 - RIPPLE DISTORTION DUE TO LIMITED PASSBAND OF IDEAL FILTER.

and the corresponding paired echoes, thereby increasing the S/N-ratio.

Experiments proved the above statement to be correct (COOK (1964)).

### 3.3. The Practice of Sidelobe Reduction

#### 3.3.1. Introduction

So far we have only dealt with idealised characteristics and the idealised performance of the Vibroseis system of exploration. The consideration was purely theoretical.

When discussing harmonic ghosts, warning was given of the difficulties one might encounter in Vibroseis field operations. There the coupling of the vibrator to the ground gave rise to non-linear processes resulting in harmonic correlation wavelets being superimposed on the ideally correlated signal.

As yet the filter effect of the earth has not been mentioned. Normally the transmitted and the received waveform show quite different amplitude spectra, which is due to the fact that higher frequencies are attenuated more strongly than the lower ones on their way through the subsurface. The input waveform amplitude spectrum and a typical spectrum of received Vibroseis data are shown in Figure 10. This attenuation proportional to frequency has been investigated by various geophysicists (ATTEWELL and RAMANA (1966); KNOPOFF (1956)).

From the preceding chapters it becomes clear immediately, that this relative greater loss of the higher frequency components in the amplitude spectrum will have a negative effect on the shape and the frequency content of the corresponding correlation wavelet. In Vibroseis practice the rectangular, or even the Fresnel ripple amplitude spectrum, is no longer of great significance.

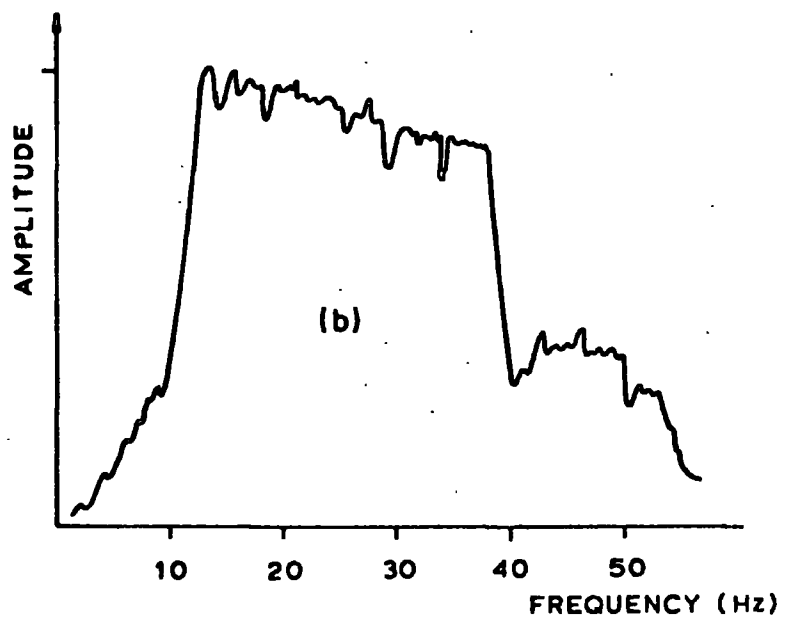
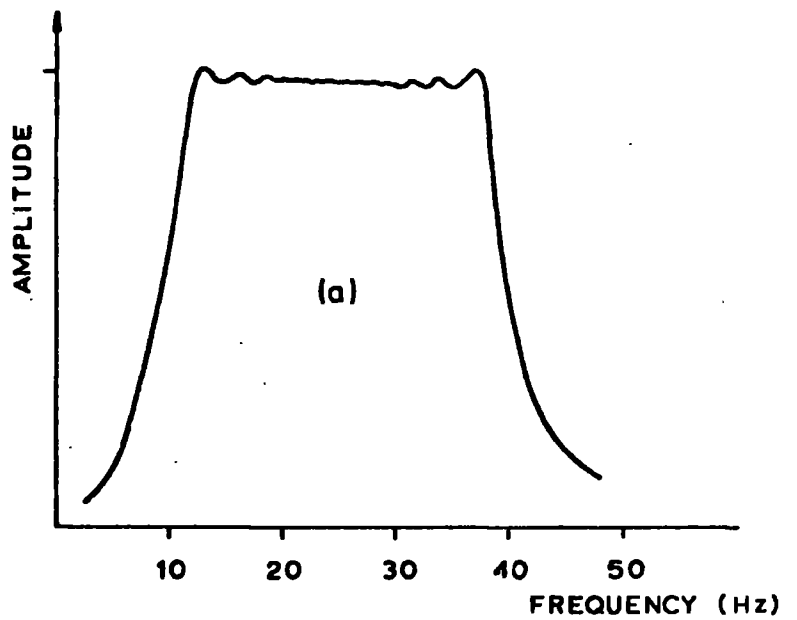


**FIG.10** AMPLITUDE SPECTRA OF  
(a) SWEEP BEFORE TRANSMISSION  
10-40Hz  
(b) VIBROSEIS DATA AS RECEIVED  
AT GEOPHONES.

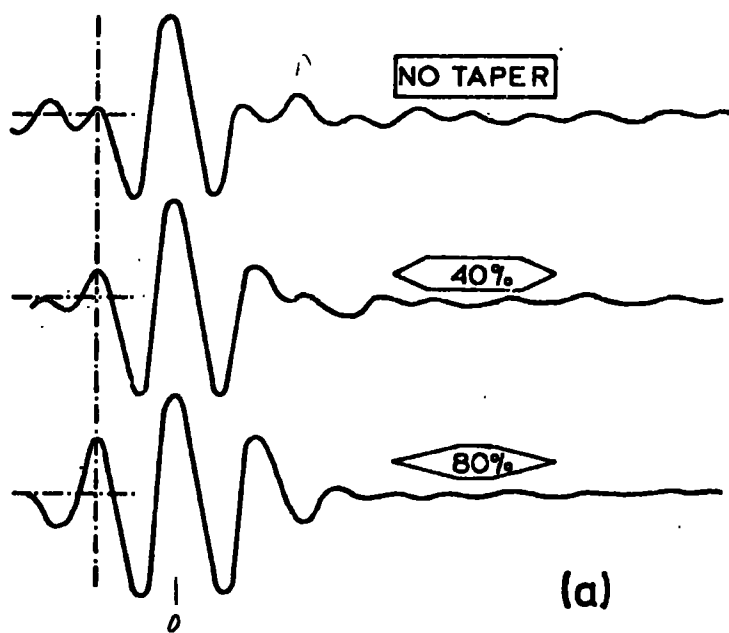
### 3.3.2 Some Practical Methods of Increasing the Vibroseis Detection Capability

On taking the filter effect of the earth into consideration, it seems to be common sense to make an advantage of the natural transmission bandwidth of the subsurface in order to get good quality seismograms. Therefore, the selection of the sweep frequency range is of utmost importance.

Furthermore, before the start of routine field procedures in a survey area, tests to derive, e.g. minimum and maximum offset between source and receiver, pattern configuration, receiver group interval and the number of vibrograms to be stacked, should be performed with great care (EDELMAAN (1966); ERLINGHAGEN).

In theory, tapering of the sweep signal seems to be an effective means of reducing sidelobe levels. But experience has shown, that the combined vibrator-earth coupling and the earth filtering effects introduce such severe distortions, particularly to the amplitude spectrum, that almost all the benefits of tapering the input Vibroseis signal are lost (DAVITT (1976); GURBUZ (1972)).

On the other hand, a sidelobe reduction can be gained when tapering is implemented at the data processing stage. However, the tapering function is never employed over the whole length of the signal, because the first sidelobes to both sides of the centre peak tend to increase to an undesired high amplitude level. This is illustrated in Figure 11a. If tapering is used only on the reception side the inherent mismatch loss has to be taken into consideration as well. As already mentioned in the foregoing theoretical discussion about tapering, slowing down the rise and fall time of a sweep signal



THE EFFECT OF TAPERING

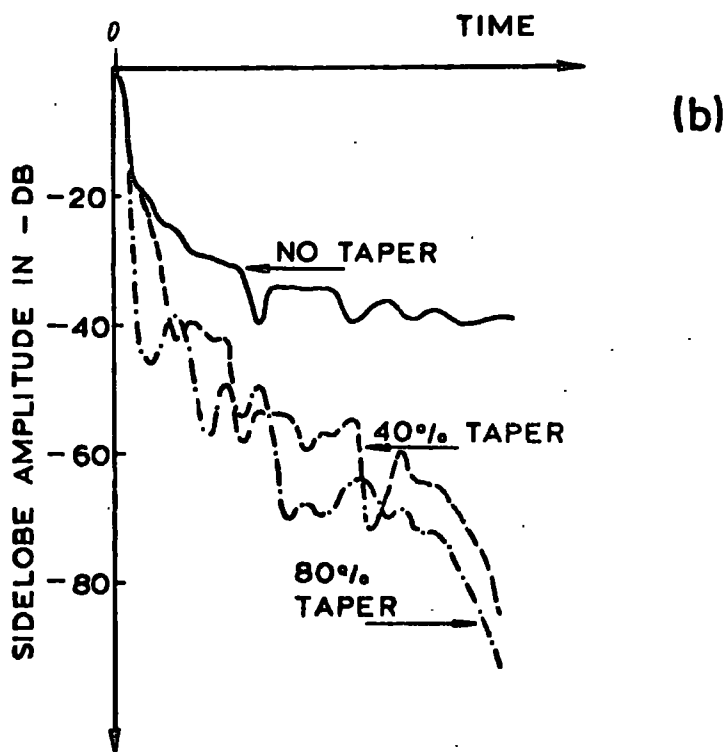


FIG. 11

(After W.E. Davitt (1976))

Note: The time scale of graph a) is different from graph b). In a) only the immediate vicinity of the centre peak is shown.

will have a smoothing effect on the amplitude spectrum as the Fresnel oscillations near the cut off frequencies are greatly suppressed. Gurbuz investigated the use of various taper functions for application on the leading and trailing ends of the reference sweep. He concluded that the cosine squared taper (...already mentioned on page 29) provided the best compromise between low sidelobes and minimum broadening of the centre pulse width, when applied for only 10% of the signal duration. Figure 11b illustrates the fact that there is a considerable reduction of sidelobes if a 40% taper is applied, but the further improvement yielded by 80% tapering is only slight.

When trying to restrict the inherent mismatch loss in a Vibroseis system where only the receiver side has been tapered, one ought not to forget the far more severe mismatch introduced through the earth filtering effect. Depending on the extent of frequency attenuation the shape of the correlation wavelet can differ from the ideal Klauder wavelet quite substantially. There is always a broadening of the centre peak which is also reduced in amplitude. Because the sidelobes do not decrease accordingly their effect is relatively worsened.

Before the input sweep signal arrives at the digital correlator it has normally passed through the sweep generator, the mechanic of the vibrators, the earth, the geophones, amplifiers and some filters, all of which have changed its appearance. In modern Vibroseis processing this is taken into consideration and the reference sweep is also sent through the above chain, except the earth, of course. The rate of attenuation towards the high frequencies of the input signal spectrum, due to the earth filter, will be approximated. The reference or correlation sweep is then modified in the light of this

approximation. This "synthetic" sweep is now used to crosscorrelate with the field data. The above method recovers some of the high frequency attenuation and because the crosspower spectrum has been restored to a nice rectangular shape, a very near ideal correlation wavelet can be achieved when applied very carefully. The principle of this compensation for distortion effects is illustrated in Figure 12.

A final step in improving the general shape of the correlation wavelet in practical Vibroseis is the Vibroseis deconvolution. This processing stage tries to enhance the weaker parts of the distorted amplitude spectrum and therefore has also a great influence on the correlation noise. The Vibroseis deconvolution has been investigated in great detail by RISTOW and JURCZYK (1975) and the interested reader is referred to their paper. It must, however, be mentioned that the conventional deconvolution operator as used in deconvolving impulse reflection seismograms, cannot be used in the Vibroseis system. The Vibroseis wavelet is a mixed delay wavelet contrary to the minimum delay wavelet assumption in the conventional seismic methods.

Just recently the use of non-linear sweeps in the Vibroseis system has been investigated (GOUPILLAUD (1976)). Unfortunately, Goupillaud had to come to the conclusion, that little, if any advantage should be expected from the application of non-linear sweeps.

The linear sweep therefore remains the preferred Vibroseis input signal.

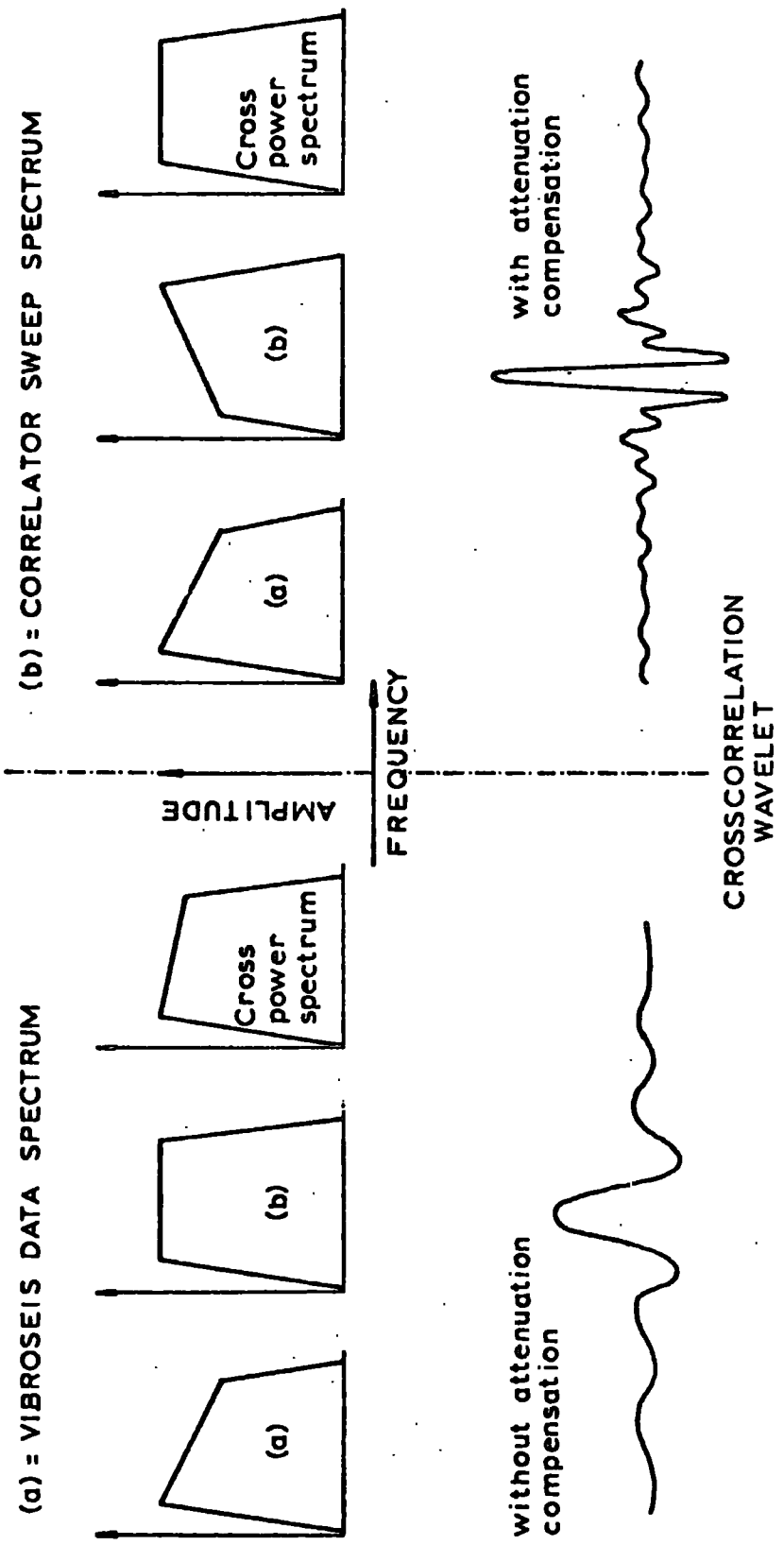


FIG.12 - THE PRINCIPLE OF FREQUENCY ATTENUATION COMPENSATION

### 3.3.3. Summary

Correlation wavelet control in the Vibroseis practice is an extremely difficult problem.

The theoretical dependency of the Klauder wavelet on a smooth and rectangular amplitude spectrum for minimum sidelobes and optimal centre lobe, has directed almost all the efforts of improving the system towards the recovery of such a rectangular spectrum. This has been highlighted on the last few pages.

As yet no attempt has been made to totally eliminate the so very disturbing sidelobes. None of the classical techniques are able to offer such perfect sidelobe reduction. A new method, however, has been found which allows just that: The Vibroseis Encoding Technique.

## CHAPTER 4

### A BRIEF PULSE COMPRESSION REVIEW

#### 4.1. Introduction

The pulse compression technique and the matched filter concept were developed during the Second World War in the early 1940's. It was then realised, that pulse compression could help to overcome the peak power problems which represented a serious impediment in the search for improved radar performance. Therefore, the signal designer strived for a signal with a great bandwidth for good range resolution, and also a long duration for high velocity resolution (...considering Doppler effects of the radar signal) and high transmission energy, yet low peak power.

An early solution was a signal whose frequency, or to be more correct, whose phase derivative is linearly swept with time. Such a signal was named "Chirp" in radar technology, and is commonly known as a "Sweep" in the Vibroseis context. The invention of the chirp considerably improved the detection and moreover the estimation capability of radar. The new signal provided the possibility of increasing average power with no loss in pulse resolution.

The chirp signal is the oldest and best known method of pulse compression in radar technology. The classic paper about "The Theory and Design of Chirp Radars" is by KLAUDER et al (1960).

#### 4.2. Various Methods of Pulse Compression - Pulse Compression Codes.

Another important step forward in the history of pulse compression is Barker's paper on "Group Synchronization of Binary Digital Systems" which was published in 1953 (BARKER (1953)). A suitable pattern of binary digits (+1; -1) was used for synchronization preceding the actual message and thereby helping to pin-point the origin of time. The pattern or "Code" would unambiguously be recognised at the receiver, a matched filter, which then generated a pulse to indicate the beginning of the message.

Barker's code was the first of many pulse compression codes to follow in the last two decades.

The properties of pulse compression sequences are exhibited by one class of Barker codes in particular: the "Ideal Pattern" or "Optimum Codes" as they were named by TURYN (1960). The autocorrelation function of an optimum code has a central spike of amplitude  $n$ , where  $n$  equals the length of the code (i.e. number of entries +1's and -1's) and sidelobes of amplitude -1. See Figure 13.

In general, a pulse compression code would be defined as follows:

A pulse compression code is a sequence (...or function) with a very narrow autocorrelation function. This means, that if the pulse compression code is passed through a corresponding matched filter, the output will be compressed in time, ideally to a single centre spike with very low sidelobes, or none at all.

As the first sidelobe of an autocorrelation of a sequence, with entries +1 and -1 only, must have an amplitude of at least  $\pm C/n$  (where  $C$  = centre

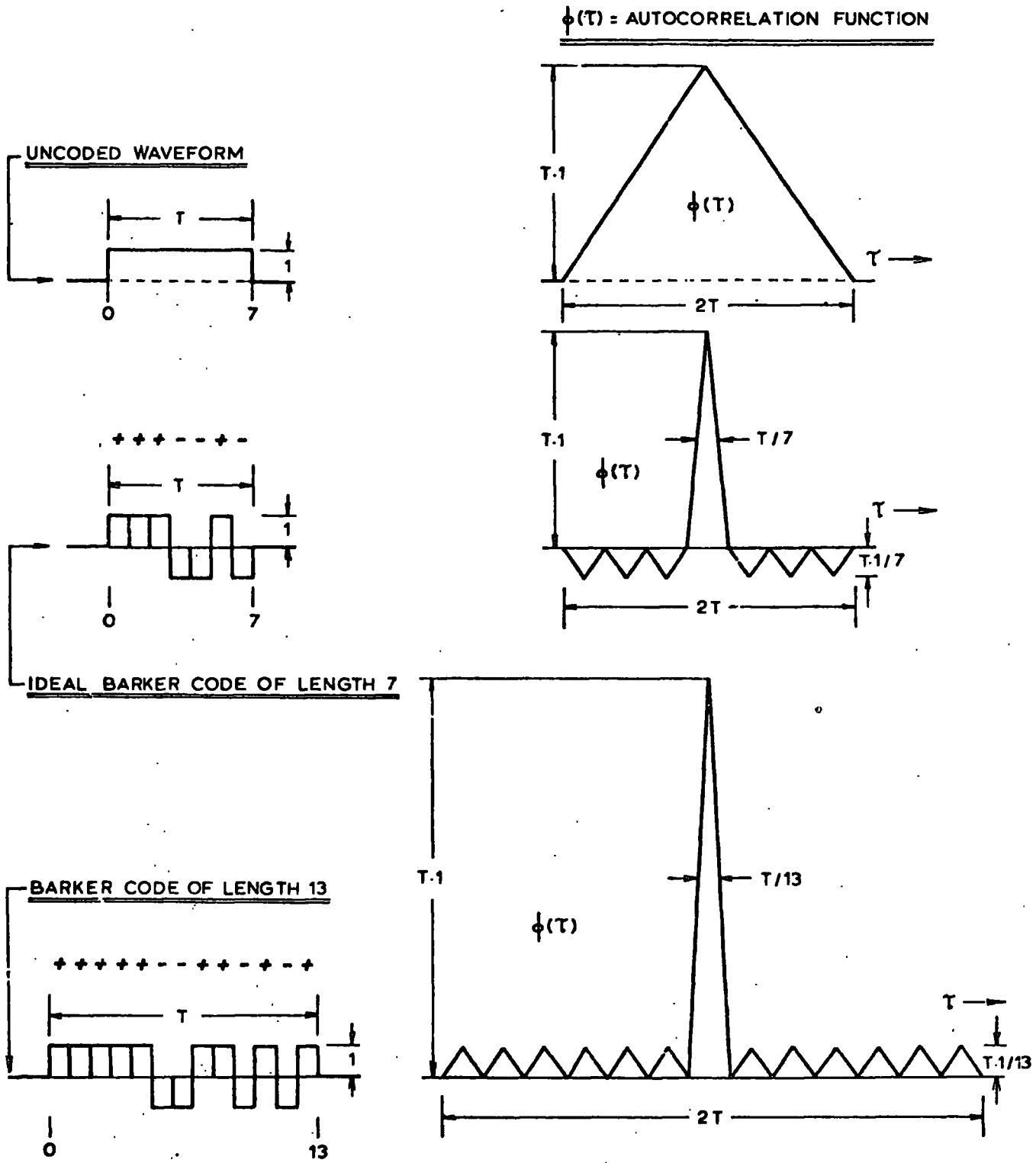


FIG.13 - THE BARKER PULSE COMPRESSION CODE

peak of A/C-function), the Barker codes achieve the optimal centre peak-to-sidelobe ratio for a binary code and that is why they are called "Optimum Codes".

Barker sequences up to length 13 have been found and it was shown by TURYN (1960) that odd length codes of n more than 13 do not exist. LUENBERGER (1963) proved that Barker codes of even length must be of length n, which is a perfect square, the exception being the code of length 2. He also verified the non-existence of even length Barker codes of length 16. Turyn came to the conclusion that only very few, if any, such sequences for  $n > 4$  exist. As a matter of fact, it is believed that Barker codes do not exist at all for lengths greater than 13. The known sequences are:

n = 2    + +  
       2    - +  
       3    + + -    (ideal optimum code)  
       4    + + - +  
       4    + + + -  
       5    + + + - +  
       7    + + + - - + -    (ideal optimum code)  
      11    + + + - - - + - - + -    (ideal optimum code)  
      13    + + + + + - - + + - + - +

and they all fulfil the following condition:

Let  $a_i = \pm 1$  and  $i=1, \dots, n$  and let

$$c_j = \sum_{i=1}^{n-j} a_i \cdot a_{i+j}$$

then  $|c_j| \leq 1$  for  $0 < j < n$  and  $c_0 = n$ .

In an interesting paper about "Binary Pulse Compression Codes",

Ann M. BOEHMER (1967) describes an analytical technique for finding a class of good (...but not necessarily optimum) pulse compression codes of prime length.

A pulse compression code, which is repeated over and over and shows periodic pulse compression properties (e.g. large spikes surrounded by small sidelobes) is called a periodic code. A binary pulse compression code will only achieve low autocorrelation sidelobes, if its periodic correlation sidelobes are low (...necessary, but not sufficient condition). Therefore, Boehmer's paper examined good periodic codes in detail before deriving the binary pulse compression codes. Her analytical method helped to compile a suite of binary codes of lengths longer than  $n = 13$  with lowest possible sidelobes, since in radar practice pulse compression ratios much greater than 13 are often required.

Where very long binary sequences are needed, as for example in space craft ranging, pseudorandomly arranged binary sequences have been used. For a perfectly matched filter the centre peak will always be of amplitude  $n$ , whilst the sidelobes of a pseudorandom code are small, as there should be no similarity between the correlating sequences once the centre position is passed in the autocorrelation process. In general, codes of great length are required in order to achieve satisfactory pulse compression properties.

Besides Barker's classical binary codes there are many non-binary pulse compression codes. GOLOMB and SCHOLTZ (1965), for example, further developed the Barker sequences into so-called generalized codes. These sequences are not confined to a two member alphabet and still show the above stated Barker properties. The authors investigated

codes for different alphabet lengths and code sizes. A six element alphabet appeared to be particularly interesting, because Barker sequences were found for every length up to  $n=12$  and there seems to be no theoretical constraint which would not allow for longer codes. An  $m$  element alphabet consists of  $u^0, u^1 = \exp(2\pi fi/m), u^2, u^3, \dots, u^{m-1}$ . A large number of generalized Barker sequences are tabulated in Golomb's and Scholtz's paper.

In order to implement binary codes on radar systems a phase reversal mode is used almost exclusively. Pulses of equal duration and frequency are phase modulated according to the code considered; i.e. the code determines which of the pulses in the sequence are  $180^\circ$  phase inverted and which will keep their initial phase. Therefore, the original Barker code is sometimes referred to as a two phase code. For example:

- 1 (or -) corresponds to  $0^\circ$  phase and
- +1 (or +) corresponds to  $180^\circ$  phase, or vice versa.

Long before Golomb and Scholtz generalized the idea of Barker- or optimum codes, DELONG Jr. (1959) described so-called "Optimum Three Phase Codes" and defined them to be finite sequences of symbols  $\omega_1; \omega_2; \omega_3$  (representing the cube roots of unity). It was hoped, that it would be easier to find long optimum three phase codes than optimum two phase codes which proved to require extremely expensive trial and error runs on computers as no analytical method was known. As it turned out, optimum three phase codes were even harder to find than two phase Barker codes. The following sequence is one example of a Delong code:

$$\omega_1, \omega_2, \omega_2, \omega_3, \omega_2, \omega_3, \omega_2, \omega_2, \omega_1$$

In his paper "The generation of Impulse-Equivalent Pulse Trains", HUFFMAN (1962) discusses a non-binary pulse compression code which has to be heavily weighted in order to achieve large peak to correlation noise ratios. Since the Huffman pulse trains are very close to having the same autocorrelation function that a single high energy pulse would have, the name impulse-equivalent pulse trains has been chosen. See Figure 14. The pulse trains can be of arbitrary length and the amplitudes of the pulses are not confined to some specific values, as for example, +1 or -1. Each pulse, however, is of the same duration. The aim is to produce zero sidelobes away from the centre spike, but it has to be realized that all pulse trains of finite length will have non-zero sidelobes for shift positions corresponding to one less than  $n$ , where  $n$  is the number of pulses in the code. Figure 14 shows a Huffman code of length 14 and its autocorrelation function with all but the first and last sidelobe vanishing. The heavy weighting of the code members is shown quite clearly.

Contrary to the amplitude modulation in Huffman's impulse-equivalent pulse trains, FRANK (1963) preferred phase modulation to derive his "Polyphase Codes with Good Non-periodic Correlation Properties". The word 'Good' refers to the fact that the sidelobes are being kept relatively low compared with the zero-shift amplitude in the autocorrelation function.

For a code of length  $n$ ,  $\sqrt{n}$  different phases are required. The difference between the phase angles is  $2\pi/\sqrt{n}$ . Basically, Frank's polyphase codes represent an advancement of Delong's three phase codes.

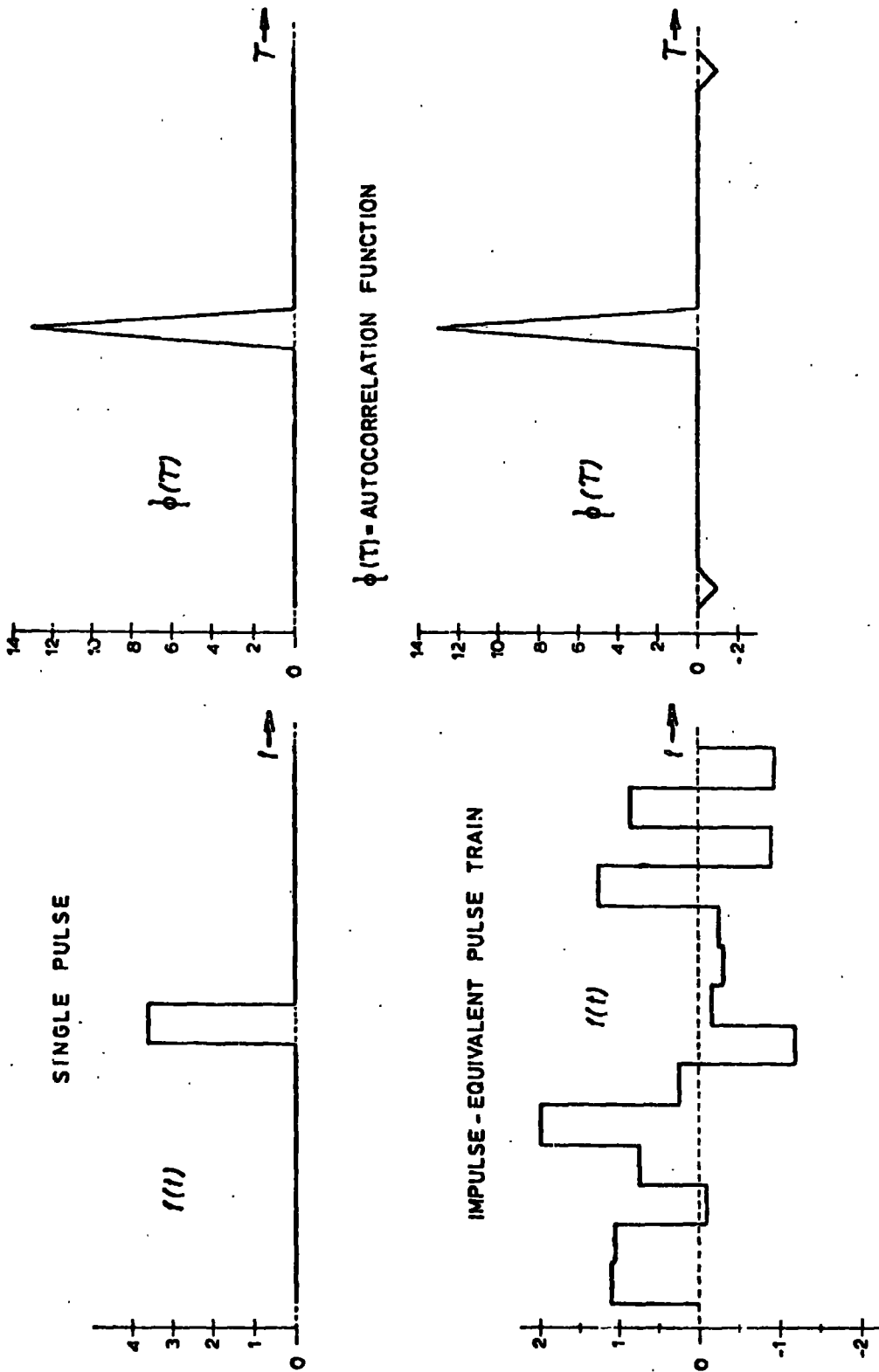


FIG.14 - SINGLE PULSE — IMPULSE-EQUIVALENT PULSE TRAIN  
COMPARISON.

Two polyphase sequences and their corresponding autocorrelation functions are shown in Figure 15. Some properties of these codes can readily be verified in Figure 15.

- a) The autocorrelation function is zero for multiples of the shift position  $\sqrt{n}$  and
- b) for shift positions of  $a\sqrt{n} - 1$  and  $a\sqrt{n} + 1$ , where  $a = 1, 2, 3, \dots, \sqrt{n}$  the autocorrelation function equals +1.
- c) The sidelobes have a symmetric appearance.

The polyphase codes proved to be very much better in the sidelobe suppression than binary codes of similar length. Figure 16 shows the improvement of the centre peak-to-sidelobe ratio as compared with the best binary codes. It also underlines the fact, that only very long code sequences result in relatively low side peak levels and for total sidelobe suppression infinitely long codes are needed. This is true for all the codes mentioned above.

The codes considered so far are time discrete, i.e. the amplitude or phase only changes at certain points in time. If in Frank's polyphase codes one allows the difference between the time points to go to zero, and the corresponding phases being chosen from a continuum of values, the chirp signal, which has been mentioned in the introduction to this chapter, will result.

It is therefore possible to refer to the chirp or sweep as a continuous pulse compression code.

At this stage it is important to realize, that however hard the signal designers tried to eliminate the disturbing sidelobes (or correlation noise) in their pulse compression codes, they did not succeed. The binary codes, which are of special interest because of

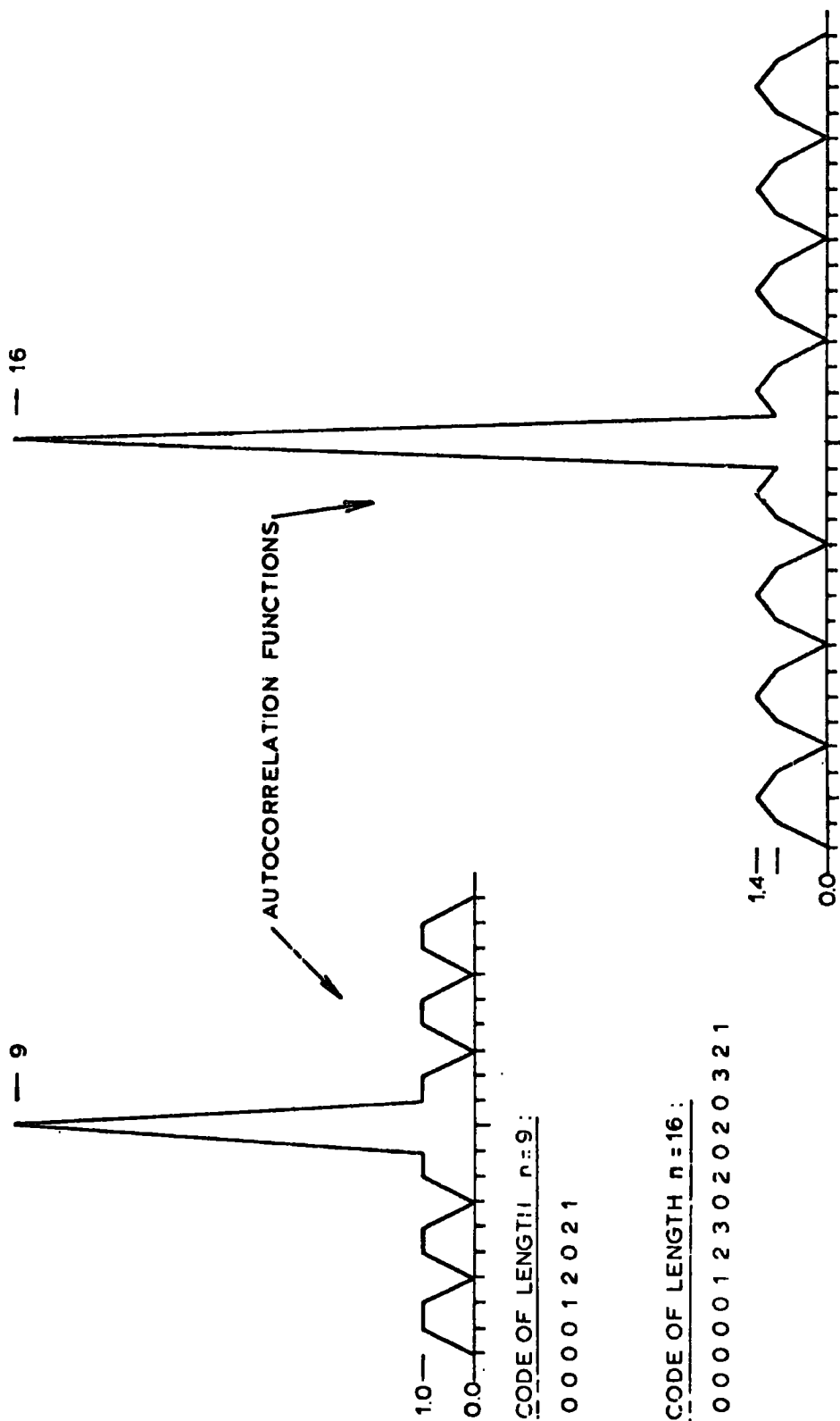


FIG.15 - FRANK'S POLYPHASE CODES OF LENGTH  $n=9$  AND  $n=16$

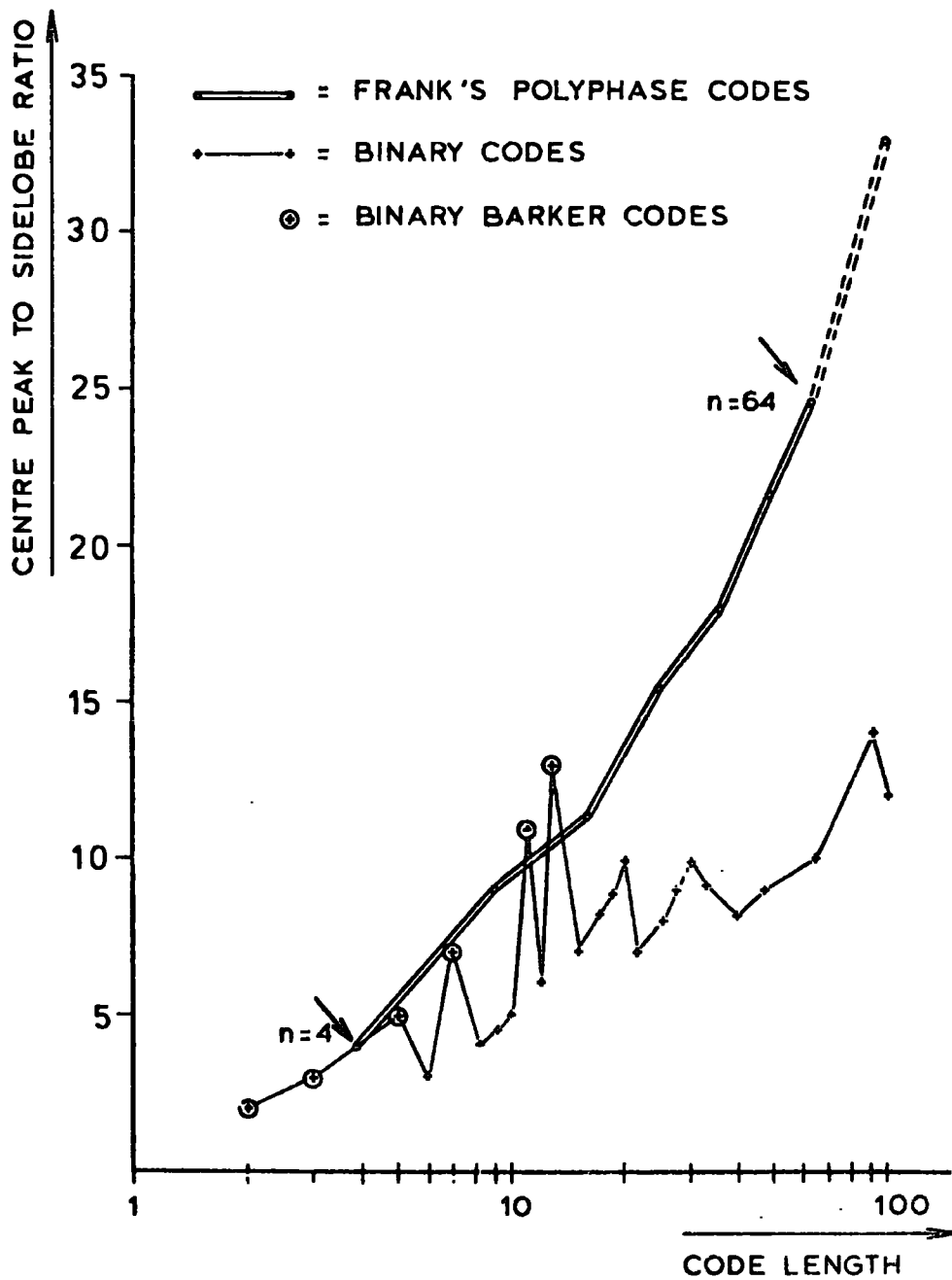


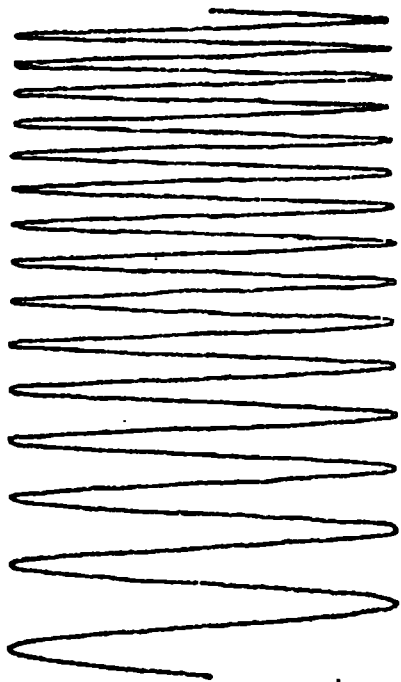
FIG.16- COMPARISON BETWEEN  
POLYPHASE }  
and BINARY } PULSE COMPRESSION CODES

(AFTER FRANK(1963))

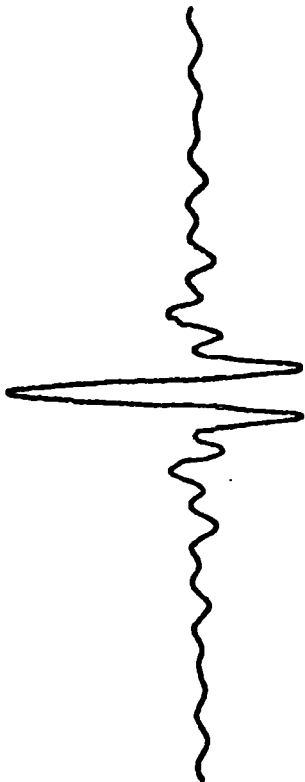
the ease of their implementation, demand very long sequences in order to show a reasonable side peak level. To achieve zero sidelobes for binary coded sequences is definitely not possible as pointed out in the above discussion of the two phase Barker codes.

Non-binary codes show, theoretically at least, a much better performance. In practice, however, they add substantial complexity to the generation and the processing of signals.

The linear chirp signal has found widespread applications, mainly because it represents something of a compromise: it is relatively easy to implement and process and it shows a high centre peak-to-sidelobe ratio if properly designed and detected by a carefully adapted matched filter. Figure 17, for example, shows the influence on the autocorrelation function when tapering the sweep (or chirp) signal, in the case of a perfectly matched receiver.



SWEEP SIGNAL  
3 - 12 HZ



AUTOCORRELATION  
FUNCTION

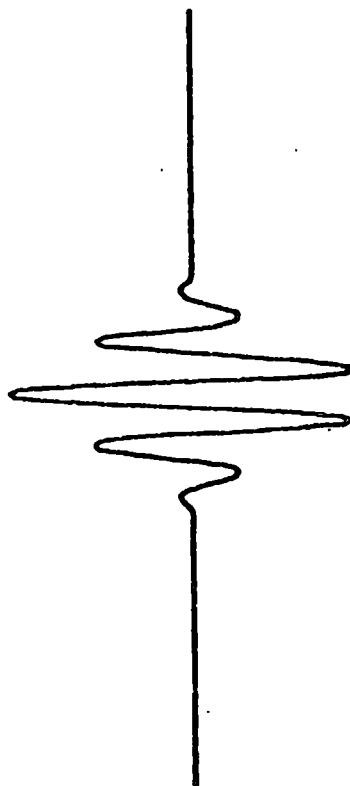


FIG. 17 - THE 'CHIRP' OR 'SWEEP' SIGNAL AND ITS AUTOCORRELATION  
FUNCTION

## CHAPTER 5

### THE CODES

#### 5.1. Introduction

Our first aim in reflection seismology is to extract as much information as possible from the received seismograms. The number of reflections and their exact arrival times are of particular interest.

The earth mainly represents, what the radar engineer would call a 'dense target environment', because the targets, i.e. the horizons to be detected, might only be separated by a relatively small distance. Therefore, if with the Vibroseis system one wants to detect reflections with confidence, the system resolution has to be optimized. The frequency band and the duration of the transmitted sweep impose a natural limit on the resolution and detection capability as they determine the basic shape of the correlation wavelet, - our reflection indicator.

Extremely high amplitude ratios have to be expected in practice and that is why the signal induced noise, the sidelobes, are especially detrimental. Towards the end of a vibrogram, the correlation noise originating from a strong, early reflection may well reach the amplitude of a weaker, later event. For that reason sidelobe reduction has for a long time been the criterion of interest for many geophysicists working with the Vibroseis system of exploration.

As outlined in the preceding chapters considerable progress has been done in the signal design and the processing of Vibroseis data, but as yet sidelobes remain a serious problem in high resolution continuous signal work.

The "Vibroseis Encoding Technique" represents a new approach to the solution of this correlation noise problem. The use of ordinary pulse compression codes proved to be of no advantage, as their own inherent signal-to-noise ratios were too small for practical code lengths (BERNHARDT (1975)).

However, the investigation of so-called "Complementary Series", a special class of pulse compression codes, promised a successful application in the Vibroseis system as a means of (...theoretically) perfect sidelobe reduction, exploiting their useful property, that the sum of the autocorrelation functions of its sequences is zero, except for the zero shift term.

Particularly in the Vibroseis system with its low power input signal it would be highly desirable to use the listening time of its acquisition period for transmission of energy, whilst recording events. Such a continuous transmission mode might become feasible with the help of "Mutually Orthogonal Complementary Sets of Sequences".

The practical application of both encoding techniques will be discussed in the following two chapters. The complementary sequences, some generation algorithms and some of their important and interesting mathematical properties will now be presented.

## 5.2. Complementary Series

The concept of complementary series as a means of coding has been developed in connection with an optical problem in infra-red multislit spectrometry. In 1949 M. Golay published a paper in the "Journal of the Optical Society of America", presenting the principles of this new coding technique (GOLAY (1949)). A later paper again concentrated on the multislit problem (GOLAY (1951)). Golay devoted his classical 1961 paper entirely to the theoretical aspects of the complementary series itself and indicated their possible application in communication engineering (GOLAY (1961)).

SCHWEITZER (1971) and TSENG et al (1972) generalized Golay's idea of complementary sequences and also introduced the new concept of the so-called mutually orthogonal or non-interacting complementary sets of sequences.

Originally, Golay designed his codes as pairs of binary sequences, but Schweitzer's generalization showed that complementary code sets with more than two series per set and whose sequence members were chosen from the alphabet of real numbers can also be found. However, only complementary sets of binary sequences and a quaternary code are of interest in the Vibroseis encoding technique.

Before a detailed description of the complementary code properties and some of the generation algorithms, Golay's definition of complementary series will be quoted here:

"A set of complementary series is defined as a pair of equally long, finite sequences of two kinds of elements which have the property that the number of pairs of like elements with any one given

separation in one series is equal to the number of pairs of unlike elements with the same given separation in the other series".

(GOLAY (1961))

An equivalent definition could be given as follows, already stating the most important property of complementary series:

- Complementary series are defined as sequences, e.g.

$$A = (a_1, a_2, \dots, a_n) \text{ and } B = (b_1, b_2, \dots, b_n)$$

whose elements  $a_i$  and  $b_i$ ,  $i = 1, 2, \dots, n$  are either +1 or -1

and whose autocorrelation functions

$$\phi_{aa}(j) = \sum_{i=1}^{i=n-j} a_i a_{i+j} \quad \text{and}$$

$$\phi_{bb}(j) = \sum_{i=1}^{i=n-j} b_i b_{i+j}$$

will add up to zero except for the zero shift position, i.e.

$$\phi_{aa}(j) + \phi_{bb}(j) = 0 \quad \text{if } j \neq 0$$

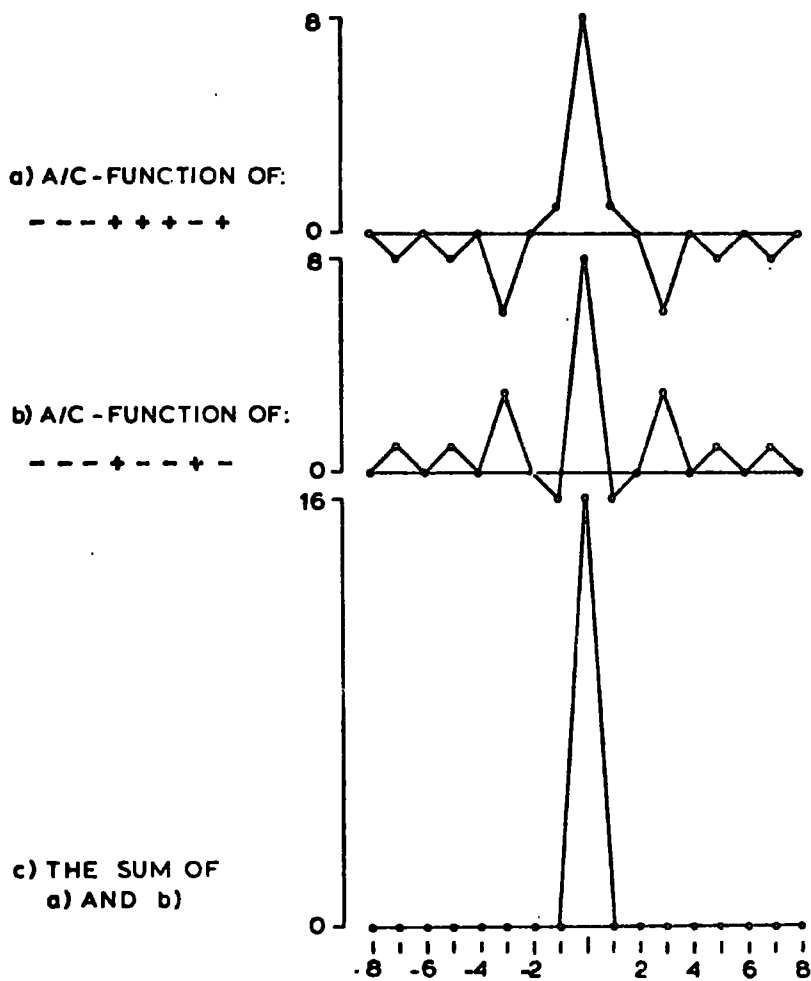
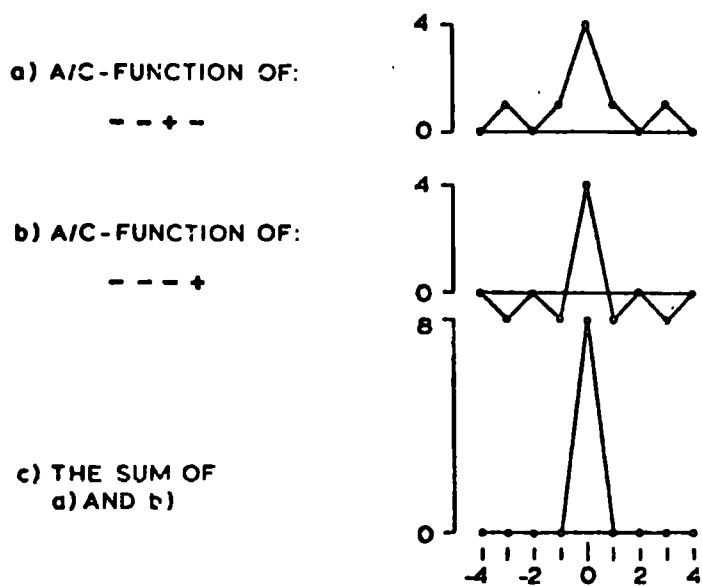
$$\phi_{aa}(j) + \phi_{bb}(j) = 2n \quad \text{if } j = 0$$

Three examples of Golay's binary complementary series can be seen in Figures 18 and 19. It should be noted that the binary code members in these series obey the following multiplication table\* :

$$\begin{vmatrix} aa & ab \\ ba & bb \end{vmatrix} = \begin{vmatrix} 1 & -1 \\ -1 & 1 \end{vmatrix} \quad \text{(A.)}$$

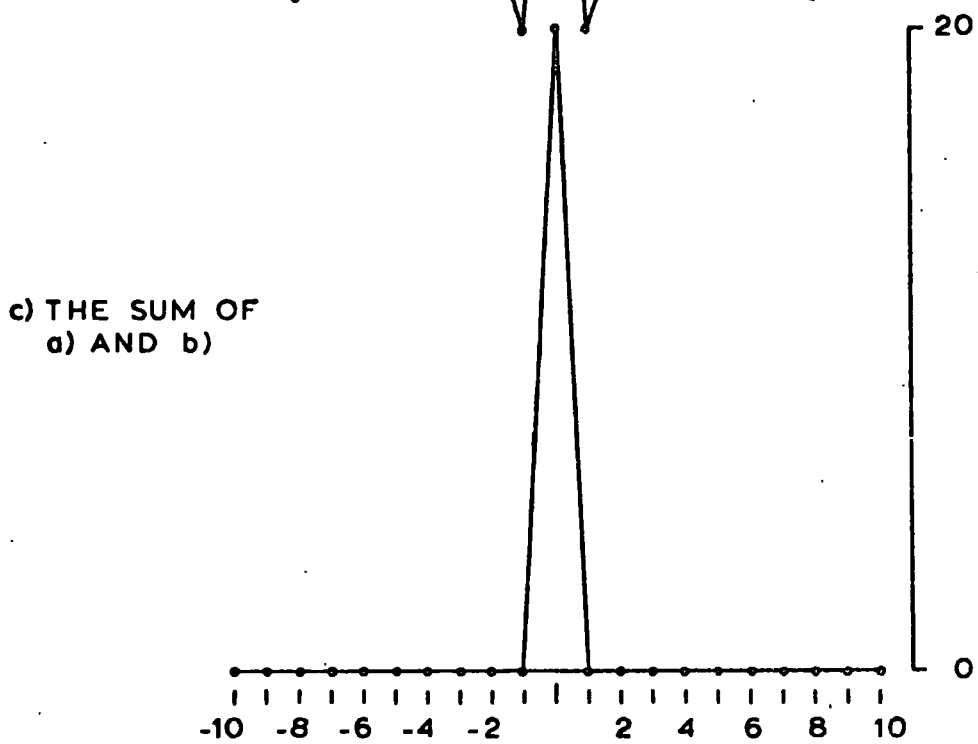
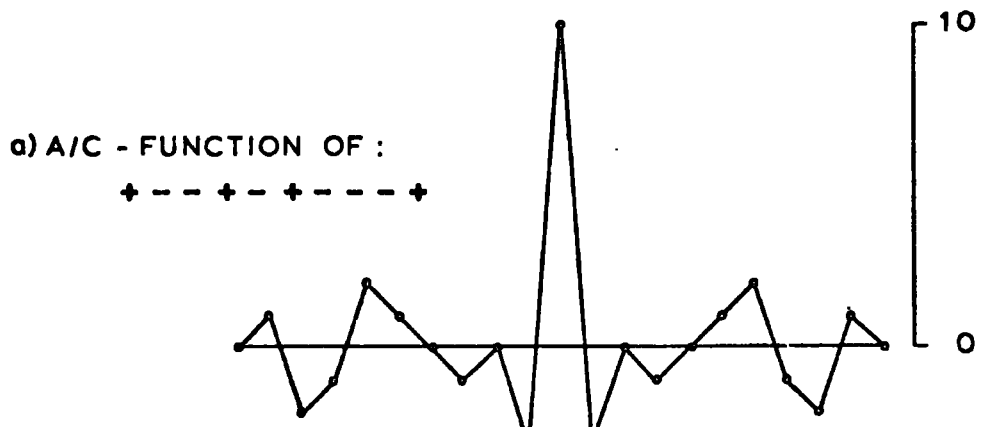
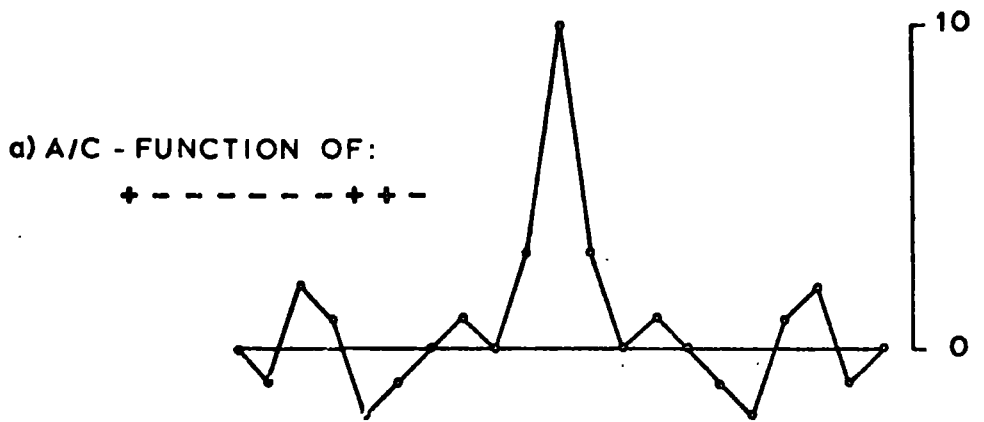
In his paper Golay gave an algorithm for generating complementary series. The given method, however, only works for series whose length  $n$  is a power of 2. Where  $n$  is not a power of 2 complicated 'longhand' searches mainly with computers have revealed only series of length  $n = 10$  and  $n = 26$  (JAUREGUI (1962); GOLAY (1962)). It has been proved

\* Multiplication table, product table, correlation matrix and identity matrix are used as equivalent terms throughout this work.



NOTE: All A/C-Functions show the "Even-Shift-Orthogonal" property.

FIG.18 - GOLAY'S COMPLEMENTARY SERIES OF LENGTH  $n=4$  AND  $n=8$ .



NOTE: NO "EVEN-SHIFT-ORTHOGONAL" PROPERTY !

FIG.19 - GOLAY'S COMPLEMENTARY SERIES OF LENGTH  $n=10$ .

that complementary series do not exist for  $n=18$  (KRUSKAL (1961)).

Golay's codes possess a great number of properties. The most important ones will be listed below. In particular it should be noted that many properties of the complementary series enable us to construct new and/or longer codes from one given set of complementary sequences.

- a) The number of elements in complementary series has to be even.
- b) The number of elements in both sequences of a complementary series has to be equal.
- c) The two sequences are interchangeable.
- d) Either or both of the two sequences may be reversed. (\*)
- e) Either or both of the two sequences may be altered, i.e. each element in a sequence is replaced by an element of the other kind, e.g.  $-1$  by  $+1$ . (\*)
- f) In both sequences elements of even order may be altered. (\*)
- g) Let  $A = (a_1, a_2, \dots, a_n)$  and  $B = (b_1, b_2, \dots, b_n)$  be the two sequences of a complementary series (length =  $n$ ) and  $B' = (b'_1, b'_2, \dots, b'_n)$  the sequence  $B$ , but altered, then the two sequences

$$Y = A \oplus B = (a_1, a_2, \dots, a_n, b_1, b_2, \dots, b_n) \text{ and}$$

$$Z = A \oplus B' = (a_1, a_2, \dots, a_n, b'_1, b'_2, \dots, b'_n)$$

form another complementary series of length  $2n$  by simply concatenating ( $\oplus$ ) the sequences  $A$  and  $B$ , as well as  $A$  and  $B'$ . (\*)

- h) Let  $A = (a_1, a_2, \dots, a_n)$  and  $B = (b_1, b_2, \dots, b_n)$  be the two sequences of a complementary series and  $B' = (b'_1, b'_2, \dots, b'_n)$  the sequence  $B$ , but altered, then the two sequences

$$V = A \boxtimes B = (a_1, b_1, a_2, b_2, \dots, a_n, b_n) \quad \text{and}$$

$$W = A \boxtimes B' = (a_1, b'_1, a_2, b'_2, \dots, a_n, b'_n)$$

form another complementary series of length  $2n$  by interleaving ( $\boxtimes$ ) the sequences  $A$  and  $B$ , as well as  $A$  and  $B'$ . (\*)

- i) Let  $A = (a_1, a_2, \dots, a_n)$ ,  $B = (b_1, b_2, \dots, b_n)$  and  $C = (c_1, c_2, \dots, c_m)$ ,  $D = (d_1, d_2, \dots, d_m)$  be two complementary series of length  $n$  and  $m$ , respectively, then the two sequences

$$R = A^{c_1} \oplus A^{c_2} \dots \oplus A^{c_m} \oplus B^{d_1} \oplus B^{d_2} \dots \oplus B^{d_m} \quad \text{and}$$

$$S = A^{d_m} \oplus \dots \oplus A^{d_2} \oplus A^{d_1} \oplus B^{c'_m} \oplus \dots \oplus B^{c'_2} \oplus B^{c'_1}$$

form another complementary series of length  $2nm$ . (\*)

(The series  $A$  and  $B$  are altered depending on the parity of the exponents  $c_1, c_2, \dots, c_m$  and  $c'_1, c'_2, \dots, c'_m$  and  $d_1, d_2, \dots, d_m$ .

If the binary elements used are  $\{1\}$  and  $\{0\}$  the exponent's parity is either odd or even, respectively, and alteration takes place only when the exponent is odd.

Example:

$$A = (0,0) = (a_1, a_2) \quad ; \quad B = (0,1) = (b_1, b_2)$$

$$C = (1,0) = (c_1, c_2) \quad ; \quad D = (1,1) = (d_1, d_2)$$

$$\text{and } C' = (0,1) = (c'_1, c'_2) \quad (n=m=2)$$

Then the two sequences

$$R = (1,1,0,0,1,0,1,0) \quad \text{and} \quad S = (1,1,1,1,1,0,0,1)$$

form a new complementary series of length  $2nm=8$ . )

- j) Following the same logic as outlined in i), but interleaving sequences yields the following complementary series:

$$M = (A^{c_1} \oplus A^{c_2} \dots \oplus A^{c_m}) \boxtimes (B^{d_1} \oplus B^{d_2} \dots \oplus B^{d_m})$$

$$= A^{c_1} \oplus B^{d_1} \oplus A^{c_2} \oplus B^{d_2} \dots \oplus A^{c_m} \oplus B^{d_m} \quad \text{and}$$

$$\begin{aligned} N &= (A^{\overset{d}{m}} \oplus \dots \oplus A^{\overset{d}{2}} \oplus A^{\overset{d}{1}}) \otimes (B^{\overset{c'}{m}} \oplus \dots \oplus B^{\overset{c'}{2}} \oplus B^{\overset{c'}{1}}) \\ &= A^{\overset{d}{m}} \oplus B^{\overset{c'}{m}} \oplus \dots \oplus A^{\overset{d}{2}} \oplus B^{\overset{c'}{2}} \oplus A^{\overset{d}{1}} \oplus B^{\overset{c'}{1}} \end{aligned} \quad (*)$$

It is obvious from the above listed properties, that once a complementary series has been derived a great number of codes are at hand by applying one or more of the operations described and marked with an asterisk (\*).

### 5.3. Complementary Sets of Sequences and Mutually Orthogonal

#### Complementary Sets of Sequences

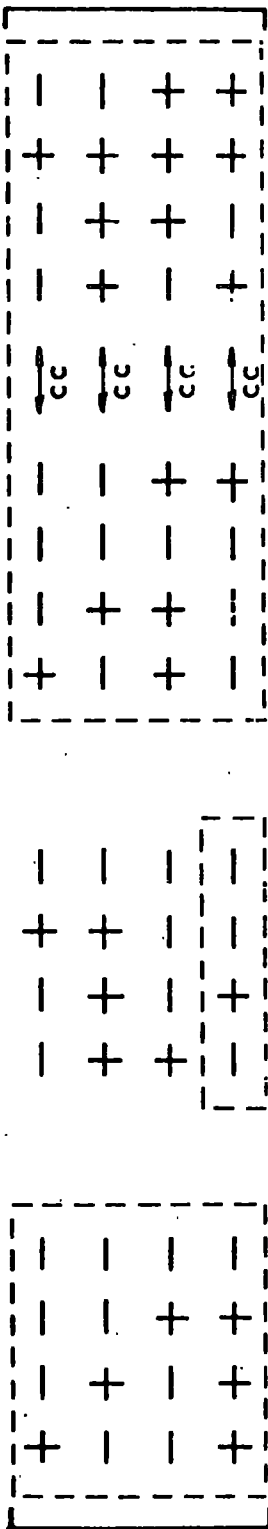
The concept of complementary sets of sequences will now be introduced. It became possible to derive a "Continuous Transmission System" with the help of these sets, taking advantage of their special properties.

TSENG et al (1972) and SCHWEITZER (1971) were able to lift Golay's original restriction of two binary sequences and investigated the possibility of so-called non-interacting or mutually orthogonal complementary sets. Schweitzer also presented the concept of generalized complementary sets allowing the sequence entries not only to be the binary digits +1 and -1 but any real number. The implementation of such an alphabet extended complementary code, however, introduces additional complexity in code generation and transmission and for practical reasons the study of binary or quaternary codes is preferred.

A 'Set of Complementary Sequences' (henceforth abbreviated as SCS) consists of an arbitrary number of equally long, finite sequences, whose autocorrelation functions add up to zero except for the zero shift position. To each set of complementary sequences it is possible to find at least one SCS containing the same number of binary sequences, but with the property that the sum of the cross-correlation functions of corresponding sequences is zero everywhere. One normally refers to such a set as the "Mate" of another SCS.

If any two sets of sequences of a number of complementary sets are mates to each other, then these sets are said to be mutually orthogonal or non-interacting. Such sets are frequently presented

A 4 x 4 M.O.C. - MATRIX



A COLUMN IN A M.O.C.-MATRIX REPRESENTS A SET OF COMPLEMENTARY SEQUENCES.

AN ELEMENT OF A M.O.C.-MATRIX REPRESENTS ONE BINARY SEQUENCE OF A COMPLEMENTARY SET.

ANY TWO SETS OF COMPLEMENTARY SEQUENCES IN A M.O.C.-MATRIX ARE "MATES" TO EACH OTHER, I.E. THE SUM OF THE CROSSCORRELATIONS (CC) OF CORRESPONDING SEQUENCES IS ZERO EVERYWHERE.

FIG. 20 - THE MUTUALLY-ORTHOGONAL-COMPLEMENTARY-SETS (M.O.C.)-MATRIX.

in a matrix form, each column is a complementary set and any two columns possess the non-interactive property. The elements of the matrix are the binary sequences. Such a matrix (M.O.C.-Matrix) is shown in Figure 20.

It has been proved by TSENG et al (1972) that SCS have to contain an even number of sequences of the same length. Similar to Golay's series in a SCS any number of sequences can be reversed, altered or interchanged, and alternate elements in all sequences may be altered without affecting their complementary property.

It is also possible to generate new sets of complementary series from a known SCS or mutually orthogonal complementary sets already existing. A few useful generating algorithms are given:

a) Let  $A_i = (a_{i1}, a_{i2}, \dots, a_{in})$   $i=1, p$  and  $n=\text{length of binary sequences}$ ,  
be a SCS.

$A_i^e = (a_{i2}, a_{i4}, \dots, a_{in})$  are the sequences with the even placed elements  
of the  $A_i$ 's only.

$A_i^o = (a_{i1}, a_{i3}, \dots, a_{i(n-1)})$  are the sequences with the odd placed  
elements of the  $A_i$ 's only.

Then all the  $A_i^e$  and  $A_i^o$  sequences constitute a new complementary  
set of sequence-length  $n/2$ . An example can be seen in Figure 21.

b) Let  $A_i = (a_{i1}, a_{i2}, \dots, a_{in})$   $i=1, p$  be a SCS and

$B_i = (b_{i1}, b_{i2}, \dots, b_{in})$   $i=1, p$  is one of its mates.

Then

$C_i = A_i \otimes B_i = (a_{i1}, b_{i1}, a_{i2}, b_{i2}, \dots, a_{in}, b_{in})$

is another set of complementary sequences.

Example:

Consider the following M.O.C.-Matrix

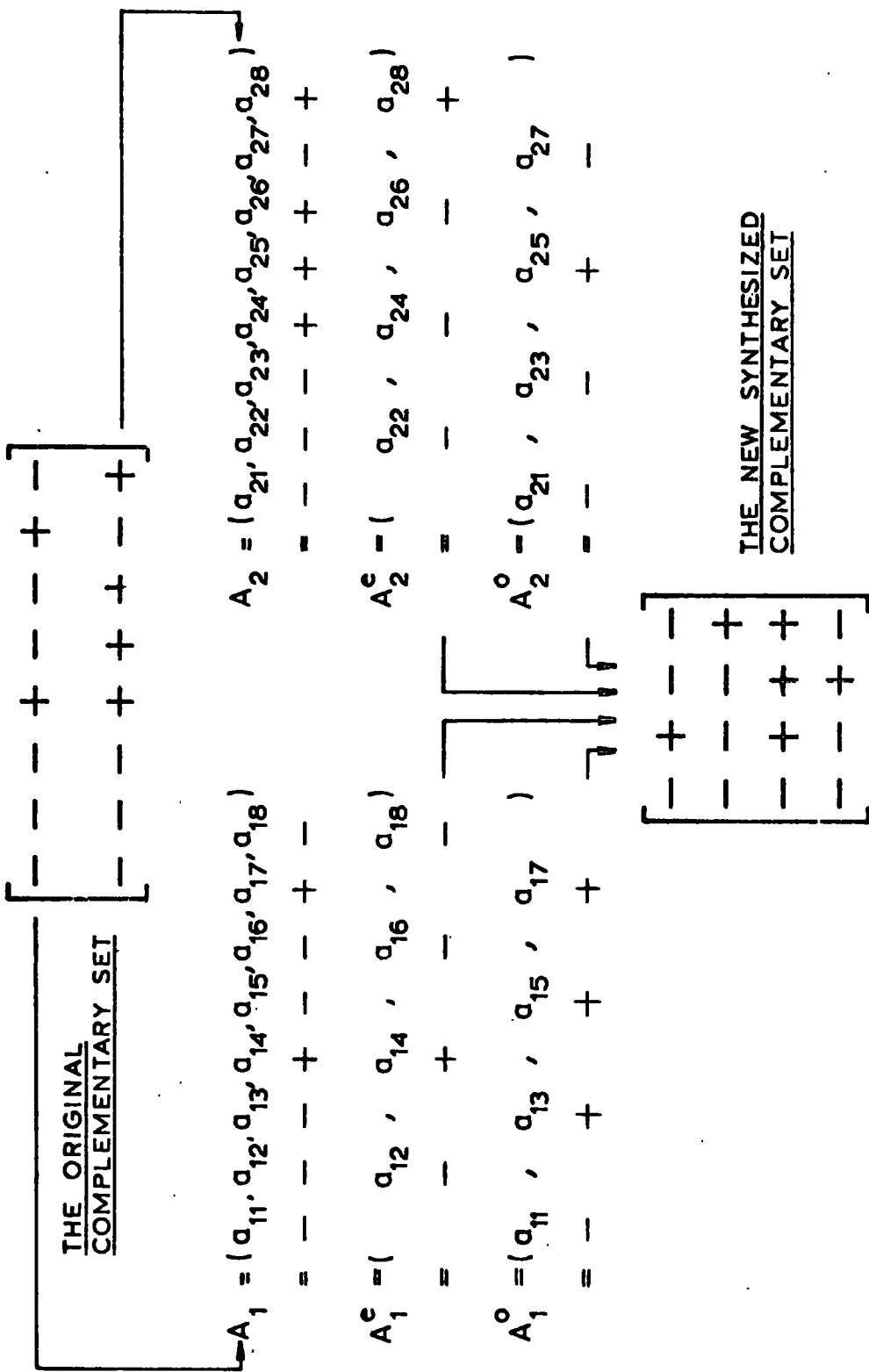


FIG.21 - SYNTHESIS OF COMPLEMENTARY SETS OF BINARY SEQUENCES (I)

$$\begin{vmatrix} + & - & - & - & & - & - & + & - \\ - & + & - & - & & + & + & + & - \end{vmatrix}$$

Here + - - - , - + - - is a complementary binary set (n=4)  
and - - + - , + + + - is one of its mates.

Interleaving results in the two sequences

$$\begin{matrix} + & - & - & - & - & + & - & - \\ - & + & + & + & - & + & - & - \end{matrix}$$

which is another complementary set of length n=8.

- c) Let  $\underline{H}$  be an orthogonal square matrix whose elements are +1 and -1.  
Let  $h_{ij}$  denote the +1 or -1 entry in the i-th row and j-th column.

Note: An m by m matrix all of whose entries are +1 and -1 and which satisfies  $\underline{H} \underline{H}^T = m\underline{I}$ , where  $\underline{H}^T$  is the transpose of  $\underline{H}$  and  $\underline{I}$  is the identity matrix of order m, is called an "Hadamard Matrix". Except for order 1 and 2, the order of such a matrix has to be divisible by 4. Hadamard matrices up to order 200 (except m=188) are known (BAUMERT et al (1962), PALEY (1933), SPENSE (1967)). An example of an Hadamard matrix can be seen in Figure 22.

If  $\underline{H}$  is a m x m orthogonal matrix and

$$A_k = (a_{k1}, a_{k2}, \dots, a_{km}) \quad k=1, m \text{ is a SCS,}$$

then

$$B_1 = \begin{matrix} h_{11} & h_{12} & \dots & h_{1m} \\ A_1 & \oplus A_2 & \dots & \oplus A_m \end{matrix} \quad \text{and}$$

$$B_2 = \begin{matrix} h_{21} & h_{22} & \dots & h_{2m} \\ A_1 & \oplus A_2 & \dots & \oplus A_m \end{matrix} \quad \text{and}$$

$$\vdots$$

$$B_m = \begin{matrix} h_{m1} & h_{m2} & \dots & h_{mm} \\ A_1 & \oplus A_2 & \dots & \oplus A_m \end{matrix}$$

is a complementary set of m sequences, if

H = HADAMARD MATRIX

$$\underline{H} = \begin{bmatrix} h_{11} & h_{12} \\ h_{21} & h_{22} \end{bmatrix} = \begin{bmatrix} +1 & +1 \\ +1 & -1 \end{bmatrix}$$

LET  $(A_1, A_2)$  BE A COMPLEMENTARY SET OF BINARY SEQUENCES.

FOR EXAMPLE:

$A_1 =$	+	+
$A_2 =$	+	-

THEN

$(B_1 = A_1^{h_{11}} \oplus A_2^{h_{12}}, B_2 = A_1^{h_{21}} \oplus A_2^{h_{22}})$  OR  
 $(B_1 = A_1 \oplus A_2, B_2 = A_1 \oplus A_2')$  OR  
 $(B_1 = , + + + - , B_2 = + + - + )$  OR

$B_1 =$	+	+	+	-
$B_2 =$	+	+	-	+

IS A NEW, SYNTHESIZED COMPLEMENTARY SET.

FIG.22 - SYNTHESIS OF COMPLEMENTARY SETS OF BINARY SEQUENCES (II)

$$A^{h_{ij}} = A \text{ if } h_{ij}=+1 \text{ and } A^{h_{ij}} = A' \text{ if } h_{ij}=-1$$

where A' represents the altered sequence A. This method of synthesizing sets of complementary binary sequences is illustrated by means of an example in Figure 22.

The last of the above examples already indicated the use of Hadamard matrices ( $\underline{H}$ ) as a tool for generating new sets of complementary sequences. They also play an important role in the derivation of mutually orthogonal complementary sets as so-called "Initializing" sets. Only the basic principle will be outlined here and for a detailed description and proof the reader is referred to SCHWEITZER (1971).

"Schweitzer's Theorem" states, that if  $\underline{A}(z)$  is a M.O.C.-Matrix (Note: Sequences are now written in the z-transform notation), then

$$\hat{\underline{A}}(z) = \underline{H} \underline{D}_N(z) \underline{A}(z)$$

is also a matrix containing sets of mutually orthogonal complementary sequences.  $\underline{H}$  is again an Hadamard matrix.  $\underline{H}$  itself represents a M.O.C.-Matrix whose sequences are of length  $N=1$ . Here compression is only achieved trivially, but any two complementary sets (or columns) in  $\underline{H}$  are orthogonal. We therefore set

$$\underline{A}(z) = \underline{H} .$$

In the generation of mutually non-interacting complementary sets the Hadamard matrix acts as an "Initializing" set.

$\underline{D}_N(z)$  is the so-called "Shifting" matrix, with diagonal elements  $1, z^N, \dots, z^{(J-1)N}$  where J is the order of  $\underline{H}$  used in the generation process. All off-diagonal elements in  $\underline{D}_N(z)$  are zero.

Figure 23 illustrates the application of "Schweitzer's Theorem".  $\underline{A}(z)$  has + and - signs as entries to distinguish it from the initialization matrix  $\underline{H}$  which has +1 and -1 as elements.  $\underline{H}$  is of order 2. A matrix  $\hat{\underline{A}}(z)$  whose elements are mutually orthogonal complementary sets of binary sequences written in z-transform notation, is the result.

Schweitzer's theorem is of particular importance as it takes advantage of Hadamard matrices, which are known to exist for a great number of orders, as already mentioned.

IF  $\underline{A}(z)$  IS A COMPLEMENTARY SET OF BINARY SEQUENCES OF LENGTH N, THEN

$$\hat{\underline{A}}(z) = \underline{H} \cdot \underline{D}_N(z) \cdot \underline{A}(z)$$

IS A M.O.C. - SET.

EXAMPLE:

$\underline{H}$  = HADAMARD MATRIX OF ORDER  $J = 2$ .

$$\underline{H} = \begin{bmatrix} +1 & +1 \\ +1 & -1 \end{bmatrix}$$

SET  $\underline{A}(z) = \underline{H}$  = INITIALIZING SET OF ORDER  $J = 2$  AND SEQUENCE LENGTH  $N = 1$ , I.E.

$$\underline{A}(z) = \begin{bmatrix} + & + \\ + & - \end{bmatrix}$$

NEXT MULTIPLY  $\underline{D}_1(z)$  AND  $\underline{A}(z)$

$$\begin{bmatrix} 1 & 0 \\ 0 & z^1 \end{bmatrix} \cdot \begin{bmatrix} + & + \\ + & - \end{bmatrix} = \begin{bmatrix} 1 & 1 \\ 1z^1 & -1z^1 \end{bmatrix} \quad (1.)$$

FINALLY MULTIPLY (1.) WITH  $\underline{H}$

$$\hat{\underline{A}}(z) = \begin{bmatrix} +1 & +1 \\ +1 & -1 \end{bmatrix} \cdot \begin{bmatrix} 1 & 1 \\ 1z^1 & -1z^1 \end{bmatrix} = \begin{bmatrix} 1 + 1z^1 & 1 - 1z^1 \\ 1 - 1z^1 & 1 + 1z^1 \end{bmatrix}$$

$\hat{\underline{A}}(z)$  IS EQUIVALENT TO THE BINARY M.O.C. - MATRIX :

$$\begin{bmatrix} + & + & + & - \\ + & - & + & + \end{bmatrix}$$

FIG.23 - SCHWEITZER'S THEOREM AND ITS APPLICATION.

5.4. Quaternary Complementary Series

During the time of the "Vibroseis Encoding" field tests, it became apparent that a quaternary complementary code would offer certain advantages. Such a quaternary pair of sequences was not readily available in the literature.

In 1959 WELTI derived quaternary pulse compression codes for radar, originally not intended to be a complementary series. As it turned out, however, only minor changes were needed to convert these quaternary sequences into the desired Golay type of code.

In his paper, Welti defines a class of binary codes, the D-codes. These codes are defined synthetically to yield the Welti quaternary sequences (E-codes) when the even placed a's and b's in the D-code are replaced by c's and d's, respectively.

Example:

D-code n=16    a a a b b b a b b b b a b b a b  
 E-code n=16    a c a d b d a d b d b c b d a d

The resulting E-code is a pulse code, i.e. a  $\delta$ -function if quaternary code members a,b,c and d can be found that fulfil the following product table:

$$\begin{vmatrix} aa & ab & ac & ad \\ ba & bb & bc & bd \\ ca & cb & cc & cd \\ da & db & dc & dd \end{vmatrix} = \begin{vmatrix} 1 & -1 & 0 & 0 \\ -1 & 1 & 0 & 0 \\ 0 & 0 & 1 & -1 \\ 0 & 0 & -1 & 1 \end{vmatrix} \tag{B.}$$

Welti also introduced the concept of a "Mate" of a quaternary code. An E-code and a mate are said to be mutually exclusive or orthogonal if their crosscorrelation function is zero everywhere.

However, the quaternary code as defined in Welti's paper is not applicable to the Vibroseis system as will be shown at a later stage.

In the course of this research it became clear that Welti's D-codes belong to a subclass of complementary binary series. To each binary D-sequence it was possible to find a second binary sequence by altering the last  $n/2$  (where  $n =$  length of code) elements of the code. These two sequences then showed complementary behaviour on autocorrelation.

The so derived complementary sequences of Welti's D-code are the binary equivalent to the previously mentioned mates of the E-codes.

Contrary to Golay's complementary series, D-codes only exist for length  $n=2^i$  where  $i$  is an integer. There is therefore no D-code of length 10 or 26.

Welti's quaternary E-codes and mates exhibit the complementary property when the product table (B.) is changed to:

$$\begin{array}{c}
 \left| \begin{array}{cccc}
 aa & ab & ac & ad \\
 ba & bb & bc & bd \\
 ca & cb & cc & cd \\
 da & db & dc & dd
 \end{array} \right| = \begin{array}{c}
 \left| \begin{array}{cc|cc}
 1 & -1 & i & -i \\
 -1 & 1 & -i & i \\
 \hline
 j & -j & 1 & -1 \\
 -j & j & -1 & 1
 \end{array} \right|
 \end{array} \quad (C.)
 \end{array}$$

It can be seen that the  $2 \times 2$  submatrices in (C.) are either identical or very similar (except for the two different characters  $i$  and  $j$ ) to the product table given for Golay's complementary codes on page 59.

Figure 24 illustrates the use of the multiplication table (C.) in a quaternary complementary series of length  $n=8$ . It also shows a property common to both, E-codes and D-codes. For all even shift



positions the autocorrelation values are zero. This, as a matter of fact, is the characteristic property of a special subclass of complementary series, the so-called "Even-Shift-Orthogonal" or "E-Sequences", -...not to be confused with E-codes (TAKI et al (1969)). Among the examples of complementary series in Figures 18 and 19, the codes of length  $n=4$  and  $n=8$  also showed this interesting behaviour. In general, E-sequences exist only for  $n=4 \cdot i$  where  $i$  is an integer.

During intensive studies of the various complementary codes, their generation and special properties, the author became aware of the deep relationship between Golay's series and the quaternary complementary series initially derived from E-codes and their mates. It turned out to be possible to derive quaternary complementary codes from the already known Golay codes without having to generate the D-codes by means of the cumbersome algorithm given in Welty's paper (WELTY (1960)).

Golay's sequences obey the 2 submatrices in the upper left and the lower right of the quaternary product table (C.). If one can find two more code members so that the product table can be totally obeyed, then those two digits can replace the even spaced + and - signs (or a's and b's) in the Golay codes.

Example:

The following two binary sequences are Golay's complementary series of length  $n=16$  (...different from Welty's D-code of the same length).

a b b b a a b a a b b b b b a b (1.)

and

b a b b b b b a b a b b a a a b (2.)

Let a,b,c and d fulfil the product table (C.), then

a d b d a c b c a d b d b d a d (3.)

and

b c b d b d b c b c b d a c a d (4.)

are quaternary complementary sequences.

It is very interesting to note that the two sequences (1.) and (2.) in our above example are not even-shift orthogonal sequences, as are the D-codes. The quaternary codes (3.) and (4.) are quaternary complementary series, but they do not constitute a Welti pair of E-code and mate. If, however, we perform this algorithm on Golay sequences, which are also even-shift orthogonal, we will produce two quaternary sequences which are:

- a) quaternary complementary series if product table (C.) is employed and
- b) a pair of quaternary Welti sequences, i.e. an E-code and its mate, producing a  $\delta$ -function on autocorrelation and crosscorrelating to zero, if correlation matrix (B.) is applied.

Example:

The Golay series of length n=8 are:

- - - + + + - + and - - - + - - + -

These sequences are even-shift orthogonal (see Figure 18). After - and + signs are replaced by a's and b's, respectively, we have

a a a b b b a b and a a a b a a b a

Let a,b,c and d be a suitable set of quaternary code members, i.e. a,b,c and d fulfil (C.), then we arrive at

a c a d b d a d and a c a d a c b c

after we have replaced even placed a's and b's with c's and d's, respectively. These two sequences are a Welti pair of quaternary sequences (use (B.)) and are also quaternary complementary series

(use (C.)) as illustrated in Figure 24.

This new algorithm works for all complementary series of length  $n=2^i$ , where  $i$  is an integer; i.e. it is not possible to convert a Golay code of length  $n=10$  into a quaternary complementary code by means of the above method, and this can be checked quite readily.

Finally, a comment on the "Partially Inversed Codes" introduced by PEACOCK and BERNHARDT (to be published soon) and BERNHARDT (1975).

By interchanging of only two code members (a and b, or c and d) of the quaternary Welts code (E-code) and applying the identity matrix (C.), the original Welts code and the sequence derived therefrom by interchanging the two code members ( $E_i$ ) constitute a pair of complementary quaternary sequences. It was also shown that if E and M represent the E-code and its mate and  $E_i$  and  $M_i$  represent the respective partial inverses, then the following pairs are also complementary :

E is complementary to  $E_i$

M is complementary to  $M_i$

$E_i$  is complementary to  $M_i$

A closer inspection of pairs like E and  $E_i$  revealed the origin of their complementary property.

Consider the 8 bit quaternary Welts code:

a c a d b d a d      = E-code  
( - - - + + + - + )   = binary equivalent; i.e. D-code

Interchanging e.g. the code members a and b results in

$$\begin{aligned} b c b d a d b d &= E_1\text{-code} \\ (+ - + + - + + +) &= \text{binary equivalent} \end{aligned}$$

Both sequences show the expected complementary property. However, if one inspects the equivalent binary sequences, it becomes clear that interchanging 2 elements of the quaternary alphabet amounts to reversing and/or negating one of the original binary complementary codes.

In our example the original binary sequences are

a) - - - + + + - and b) - - - + - - + -. Now take the negative of b) i.e

$$+ + + - + + - +$$

and reverse it, i.e.

$$+ - + + - + + + .$$

This is the binary equivalent of the quaternary interchange code  $E_1$ .

Negation and reversion of complementary sequences are legitimate operations which preserve the complementary property of the series. This example again emphasizes the close relationship between Welty codes and Golay's series.

## CHAPTER 6

### THE APPLICATION OF COMPLEMENTARY CODING IN THE VIBROSEIS SYSTEM OF EXPLORATION

#### 6.1. Introduction

Before a detailed description of the "Vibroseis Encoding Technique" employing complementary coding, let us briefly recall, that the use of "Codes" in reflection seismology is not an entirely new concept.

BARBIER and VIALIX (1973) introduced the 'Sosie' (offshore) and 'Seiscode' (onshore) seismic prospecting systems, which work by means of a specially designed time code:  $y(t)$ . A sequence of seismic pulses, fired according to this time code, is transmitted into the subsurface:  $s(t) * y(t)$ , where  $s(t)$  is the seismic signal used. The interval between successive pulses is very much shorter than the desired listening period and the received signal is a convolution of the earth filter, the seismic pulse and the time code:

$s(t) * y(t) * \text{R.C.-Log}$  where R.C.-Log = Reflection Coefficient Log. The record is uninterpretable as successive reflections are superimposing each other. By crosscorrelating the received signal with the known 'Sosie' or 'Seiscode' - code a conventional seismogram results.

Strictly, this is only true when the autocorrelation function of the used code (ACF  $y(t)$ ) is an impulse as indicated in Figure 25. As with all correlation techniques, Barbier and Viallix had to fight against the unavoidable correlation noise generated during data processing. In an attempt to keep this correlation noise below the ambient noise, the codes are carefully constructed to yield only unity height sidelobes. In the land system a number of crosscorrelated records

(After BARBIER et al (1974))

## PULSE-CODING TECHNIQUE — CONVENTIONAL METHOD

	SOSIE - SEISCODE	CONVENTIONAL
SIGNAL TRANSMITTED	$S(t) * Y(t)$	$S'(t)$
SIGNAL RECORDED	$S(t) * Y(t) * R.C. \log$	$S'(t) * R.C. \log$
DECODING	$S(t) * R.C. \log * ACF Y(t)$	_____
FINAL OUTPUT	$S(t) * R.C. \log$ if ACF $y(t)$ is equivalent to impulse of amplitude $n$	$S'(t) * R.C. \log$

$S(t)$  = seismic signal     $y(t)$  = time function    R.C.log = reflection coefficient log

$ACF(y(t))$  = autocorrelation function of  $y(t)$

FIG. 25

based on different, painstakingly adjusted codes, have to be stacked in order to achieve a reasonable dynamic range. For more detailed discussions and practical examples the reader is referred to VIALIX's and BARBIER's papers (1973), (1974), (1976).

The advantage of 'Sosie' and 'Seiscode', according to their inventors, is the greater volume of data acquired in a given time through repeated transmission during the normal listening period. This is particularly the case in the 'Sosie' system which implements a continuous transmission of coded pulses.

6.2. The Choice of Code Members

The binary complementary codes, as introduced in chapter 5, consisted of two or more sequences with a + or - sign (or +1 and -1, or 'a' and 'b') used as the pair of binary code members. For the quaternary complementary codes the letters a,b,c and d provided the four code members needed. It was emphasized that the elements of Golay's original codes obey the identity matrix (A.), page 59, whilst for the quaternary codes product table (C.), page 75, would be relevant.

The choice of practical seismic signals, equivalent to the binary or quaternary code members, is obviously governed by those product tables. It follows, therefore, that the two signals chosen to replace the a's and b's in the original Golay series must have the same autocorrelation functions (i.e. aa = bb) and all possible crosscorrelation functions (i.e. ab and ba) have to be the exact inverse or mirror image of the autocorrelation functions (i.e. ab = ba = (-1)aa = (-1)bb).

The quaternary product table is more complicated and is again shown below:

$$\begin{array}{c}
 \begin{array}{cc} \text{I} & \text{II} \end{array} \\
 \left| \begin{array}{cc|cc} \text{aa} & \text{ab} & \text{ac} & \text{ad} \\ \text{ba} & \text{bb} & \text{bc} & \text{bd} \\ \text{ca} & \text{cb} & \text{cc} & \text{cd} \\ \text{da} & \text{db} & \text{dc} & \text{dd} \end{array} \right| = \left| \begin{array}{cccc} k & -k & i & -i \\ -k & k & -i & i \\ j & -j & k & -k \\ -j & j & -k & k \end{array} \right| \quad i+j+k \\
 \begin{array}{cc} \text{IV} & \text{III} \end{array}
 \end{array}$$

It can be seen that the four seismic signals needed for the practical implementation of a quaternary complementary code have to have the

following properties:

- a) All possible autocorrelation functions are identical.  
( $aa = bb = cc = dd$ )
- b) Five different crosscorrelation functions must be possible.  
(e.g.  $ab \neq cb \neq ad \neq ac \neq ca$ )
- c) The crosscorrelation functions in the submatrices I and III are the inverse functions of the possible autocorrelations.  
(e.g.  $aa = (-1)ab$ )
- d) In the submatrices II and IV pairs of crosscorrelation functions are complementary to each other, i.e. they compensate on addition.  
( $ac + ad = 0$  and  $ca + cb = 0$ )

It also becomes clear now, that only accurately reproducible seismic signals can be employed satisfactorily for coding. Ordinary explosives, as widely used in today's onshore reflection seismology are obviously not suitable, because they are unable to supply the suite of signals necessary to this encoding technique. An exact repetition of the signal is impossible, as shape and size, as well as the location of the explosives, will influence the form of the transmitted signal.

The only seismic system that allows a good reproduction of signals and a certain degree of freedom in signal design, is the Vibroseis system of exploration.

When using the Vibroseis system, the code members themselves have to show a good autocorrelative property in order to render possible a reasonable pulse compression. Nowadays a linear sweep, the standard signal in the Vibroseis technique, is considered to be the best waveform for this geophysical pulse compression system (GOUPILLAUD (1975)). In fact, the sweep can be defined as a "Continuous

Code". This was explained in chapter 4. Indeed, the linear sweep presents itself as a basic code member, being extensively studied over the years and very well understood.

Two or four correlatable signals, obeying the product tables (A.) and (C.), had to be found for the binary and quaternary codes, respectively. In general, for the realization of such a suite of signals we have three degrees of freedom, namely amplitude, frequency and phase. However, seismic signals suffer heavy losses of energy on transmission. We can expect an attenuation of -1 db per wavelength. For a normal Vibroseis transmission over the seismic frequency range this could yield a differential attenuation of about -120 db and therefore amplitude modulation as a degree of freedom is not available to us. Complicated frequency and phase variations, as for example in stepped frequency functions and pseudorandom signals are not easily implemented on a vibrator, whereas simple phase encoding (e.g. phase reversal mode) has always been a degree of freedom for signal designers. In fact, for the binary complementary code an upsweep and its phase inverted version or a downsweep and its phase inverted version proved to be successful, i.e. the correlations showed the desired complementary signals fulfilling product table (A.).

Crosscorrelating an up- and downsweep results in a new linearly swept waveform with the same frequency range, but very nearly twice the duration. The crosscorrelations of an upsweep with a downsweep and the phase inverted version of an upsweep with a downsweep are complementary, i.e. they add up to identically zero. Furthermore, the correlation functions of up- with downsweep and down- with upsweep are different.

Empirical analysis indicated that upsweep, downsweep and their phase inverted versions represent a set of practical code members which can be employed in quaternary complementary Vibroseis encoding, as they possess all the properties listed above.

The choice of practical code members for binary and quaternary codes is as follows:

Binary code members

a = upsweep (or downsweep)

b = phase inverted upsweep (or phase inverted downsweep)

Quaternary code members

a = upsweep (or downsweep)

b = phase inverted upsweep (or phase inverted downsweep)

c = downsweep (or upsweep)

d = phase inverted downsweep (or phase inverted upsweep)

6.3. Examples of Binary and Quaternary Coded Vibroseis Signals

In order to test if the choice of code members was correct for a binary and quaternary Vibroseis encoding, advantage was taken of the IBM 370/360-computer in Newcastle to which the University of Durham has access.

Synthetic coded Vibroseis signals were calculated, auto-correlated and then stacked. Throughout the computer evaluations it was tried to use code members which are commonly employed in Vibroseis practice. It had therefore been decided to compromise on sweeps having a frequency range of about 2 octaves with the lowest frequencies not below 2 Hz and the highest frequencies not exceeding 100 Hz. For illustrative purposes only, low frequency code members are used in this thesis. Obviously, sweeps of greater bandwidth and longer duration would unquestionably render better results than the one presented.

Let us examine a pair of binary complementary coded Vibroseis signals first. The complementary series of length  $n=8$

```
  a a a b b b a b
(- - - + + + - +)

  a a a b a a b a
(- - - + - - + -)
```

are used (see also Figure 18). Therefore, the encoded Vibroseis signals consist of a sequence of eight sweeps which are phase inverted in accordance with the codes above. The first of the encoded sweep sequences will contain, for example, four upsweeps (-) and four phase inverted upsweeps (+), and the second signal comprises of six upsweeps and two phase inverted upsweeps.

The code members used in the examples are all of the

frequency range 4 Hz to 12 Hz. The duration of transmission is assumed to be 2 x 8 sec. per complementary coded set of sweep sequences, allowing each bit to be 1 sec. long in this eight code member signal. Figure 26 shows the autocorrelation function of a conventional sweep having the same frequency range and a duration of 16 sec. The relatively high sidelobes adjacent to both sides of the centre peak can clearly be seen, with a finite amount of sidelobe energy existing for the full duration of the detected signal.

In the encoded Vibroseis system, the first processing step is to autocorrelate the two coded signals. As can be seen in Figure 27 a and b, each sequence in the complementary series acts as a pulse compression code, producing a relatively large central wavelet and four smaller wavelets which represent disturbing sidelobes. These sidelobes, however, are  $180^\circ$  out of phase and will cancel when the second processing step of adding the autocorrelation functions has been performed. In graph c of Figure 27 only a high amplitude Klauder wavelet is left and correlation noise disappears a certain distance away from the zero shift position, this distance being defined by the original bit length.

The remaining wavelet has exactly the shape of the code members' autocorrelation function, but is 16 times amplified. One can therefore conclude, that the technique of encoding provides an output waveform, which is a vertical stack of the autocorrelation functions of the individual bit members.

However, it can be argued, that in practice the same effect could be achieved by stacking a sequence of short duration sweeps.

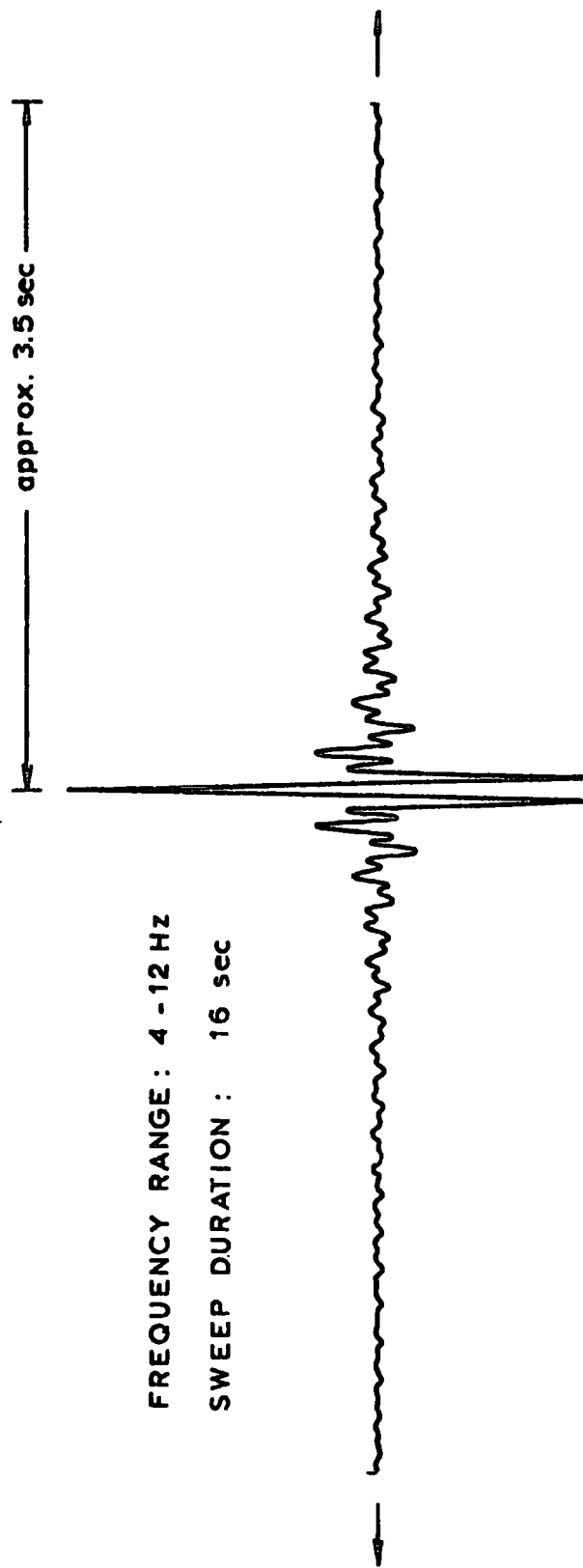
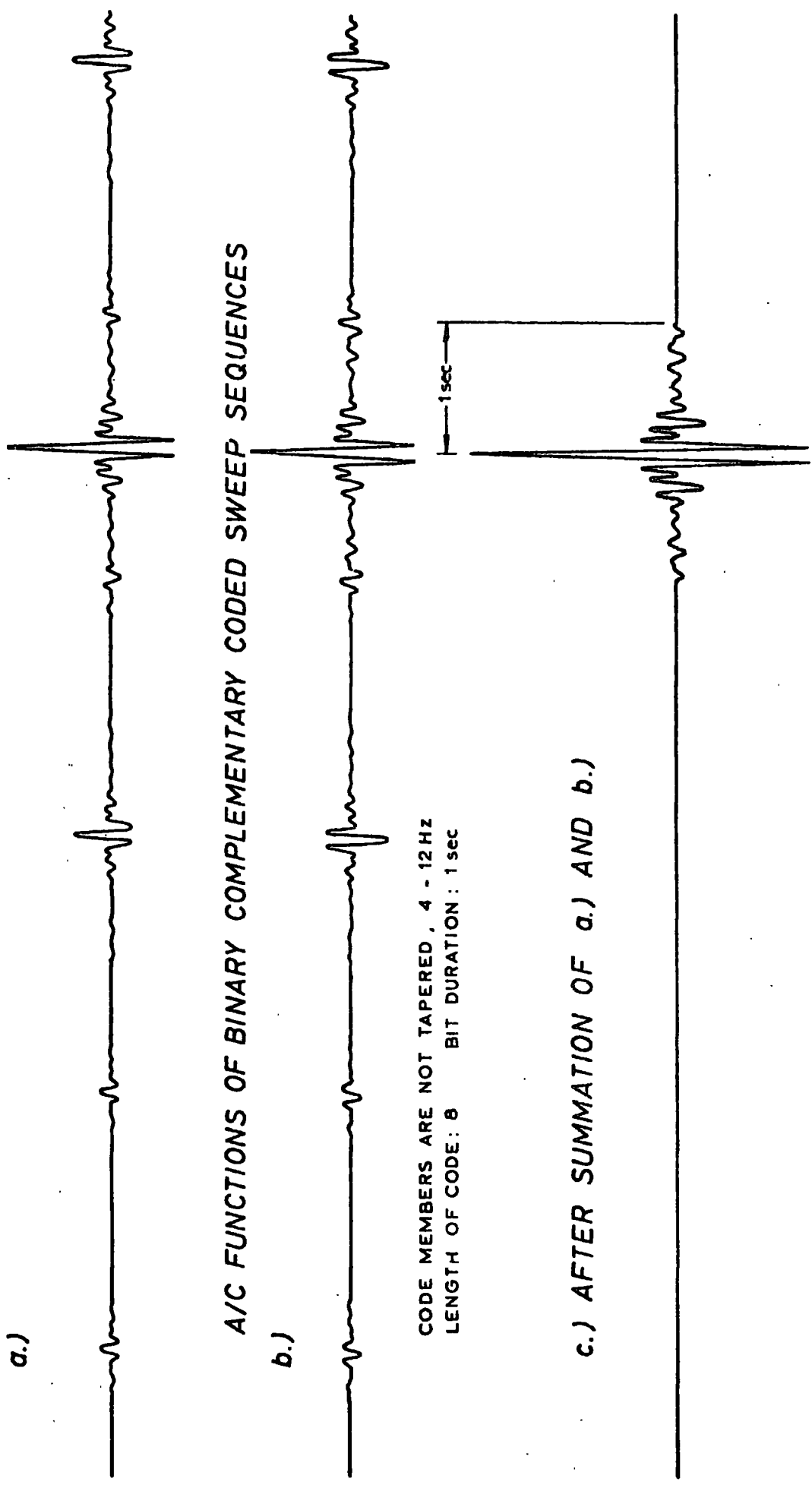


FIG. 26 - A/C-FUNCTION OF CONVENTIONAL VIBROSEIS SIGNAL



a.)

A/C FUNCTIONS OF BINARY COMPLEMENTARY CODED SWEEP SEQUENCES

b.)

CODE MEMBERS ARE NOT TAPERED, 4 - 12 HZ  
LENGTH OF CODE: 8 BIT DURATION: 1 sec

c.) AFTER SUMMATION OF a.) AND b.)

FIG. 27 - VIBROSEIS ENCODING TECHNIQUE I

This, only to a point, may be possible in land systems, because a very much prolonged acquisition period might, for economic reasons, be impractical. The stacking of individual autocorrelation functions is clearly impossible offshore,\* where the encoding technique could be used to its best advantage.

An encoded Vibroseis signal shows exactly the same compressibility as a conventional sweep of equivalent duration and frequency range. This must be so, because the compression ratio only depends on the time-bandwidth product  $D$  of the waveform to be processed by a matched filter.

A similarity between the 'Sosie-Seiscode' system, mentioned in the introduction to this chapter, and the Vibroseis encoding system may be pointed out now. Both techniques take advantage of codes, a time code and a signal code respectively, in order to transmit energy several times during the normal recording time, thereby gaining additional information and reducing acquisition costs as a shorter time may be needed for recording a profile.

In the design of complementary coded sweep sequences utmost attention has to be given to one basic rule which will be called "The Rule of Bit Equivalence".

- The signals replacing the code members in the sequences of a complementary series are not allowed to change their character in any way, but have to stay equivalent throughout the whole of the transmission. -

It follows that tapering of the coded waveform is strictly prohibited, because the equivalence of corresponding code members will be removed.

In our binary example under consideration, the result would be two

...because the movement of the energy source can mean that one uses information from different depth points in the stack.

autocorrelation functions with Klauder wavelets away from the centre wavelet appearing in wrong positions, decreasing in amplitude towards the end of the sidelobes, and the desired property of sidelobe compensation on summation is lost. Tapering, when applied to all code members in like manner, will preserve the complementary property and only affects the actual shape of the processed wavelet.

Studies of the conventional sweep signal indicated that the output autocorrelation is very sensitive to imperfections in the transmitted signal, normally resulting in the production of increased sidelobes. The encoded Vibroseis system is found to be quite inert to variations in the signal envelope or other distortions, providing that any perturbation to a given code member is repeated throughout the entire code, i.e. the rule of bit equivalence is obeyed. It is obvious that all deviations from the ideal sweep characteristics will have some effect on the centre wavelet and therefore input signal distortions should still be kept to a minimum.

Next, a set of quaternary complementary coded sweep sequences will be examined. The complementary series of length  $n=8$  used in the example of binary sweep sequences are also even-shift-orthogonal sequences, as can be seen by inspection of Figure 18. An equivalent quaternary code can be found by means of the algorithm given in chapter 5. The two equivalent quaternary complementary sequences are:

a c a d b d a d  
(- - - + + + - +)

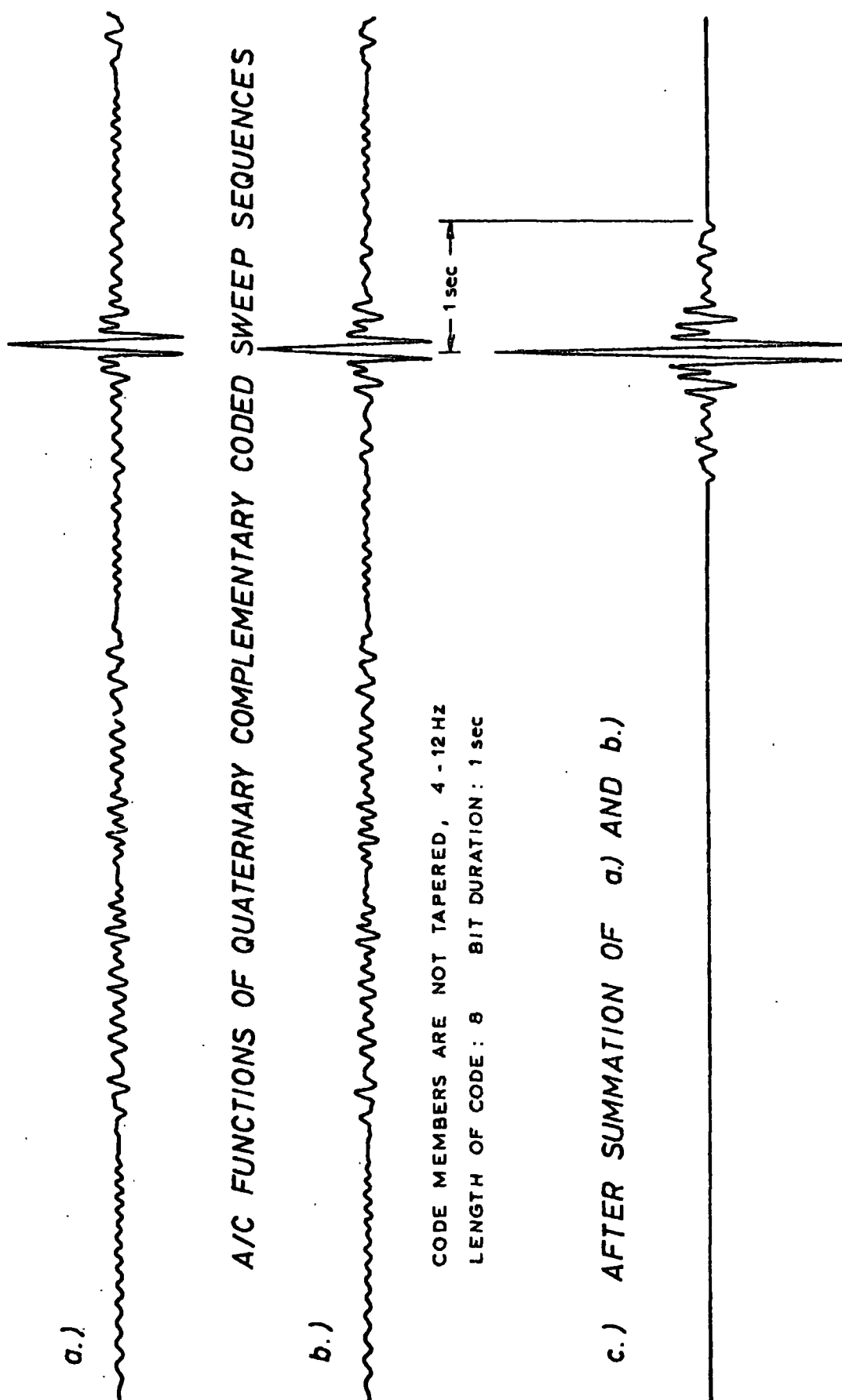
a c a d a c b c  
(- - - + - - + -)

In the quaternary coded Vibroseis signal up- and downsweeps alternate. Generally, both sequences have to start with the same type of sweep, and the complementary coded signals in our example both start with an up-sweep. The sweeps are phase inverted according to the binary code shown in brackets underneath the quaternary codes actually used in this case.

The processing steps are identical to those described for the binary coded signal. Again the frequency range of the code members is 4 Hz - 12 Hz and their duration is 1 sec. The two auto-correlation functions needed for summation can be seen in Figure 28 a and b. System induced noise, which was represented by small Klauder wavelets in the binary example, has now changed its character. The wavelets have disappeared and are replaced by a number of frequency swept signals of low but different amplitude.

The designed quaternary sweep sequences are even-shift-orthogonal, i.e. for even shift positions the autocorrelation function will be zero, except for the centre shift position. In all other shift positions crosscorrelation functions of the four different code members will partially compensate each other (... as already indicated in Figure 24). These crosscorrelations are frequency swept signals of almost twice the duration of the correlated bits. This then explains why the sidelobes in the quaternary examples partly resemble sweeps themselves. It should be noted, that the central wavelet in Figure 28 c is identical to the output waveform in the binary technique.

In Figure 29 a quaternary complementary series of length  $n=16$  was used to implement the Vibroseis encoding method. The



A/C FUNCTIONS OF QUATERNARY COMPLEMENTARY CODED SWEEP SEQUENCES

CODE MEMBERS ARE NOT TAPERED, 4 - 12 HZ  
LENGTH OF CODE : 8 BIT DURATION : 1 sec

FIG. 28 - VIBROSEIS ENCODING TECHNIQUE II

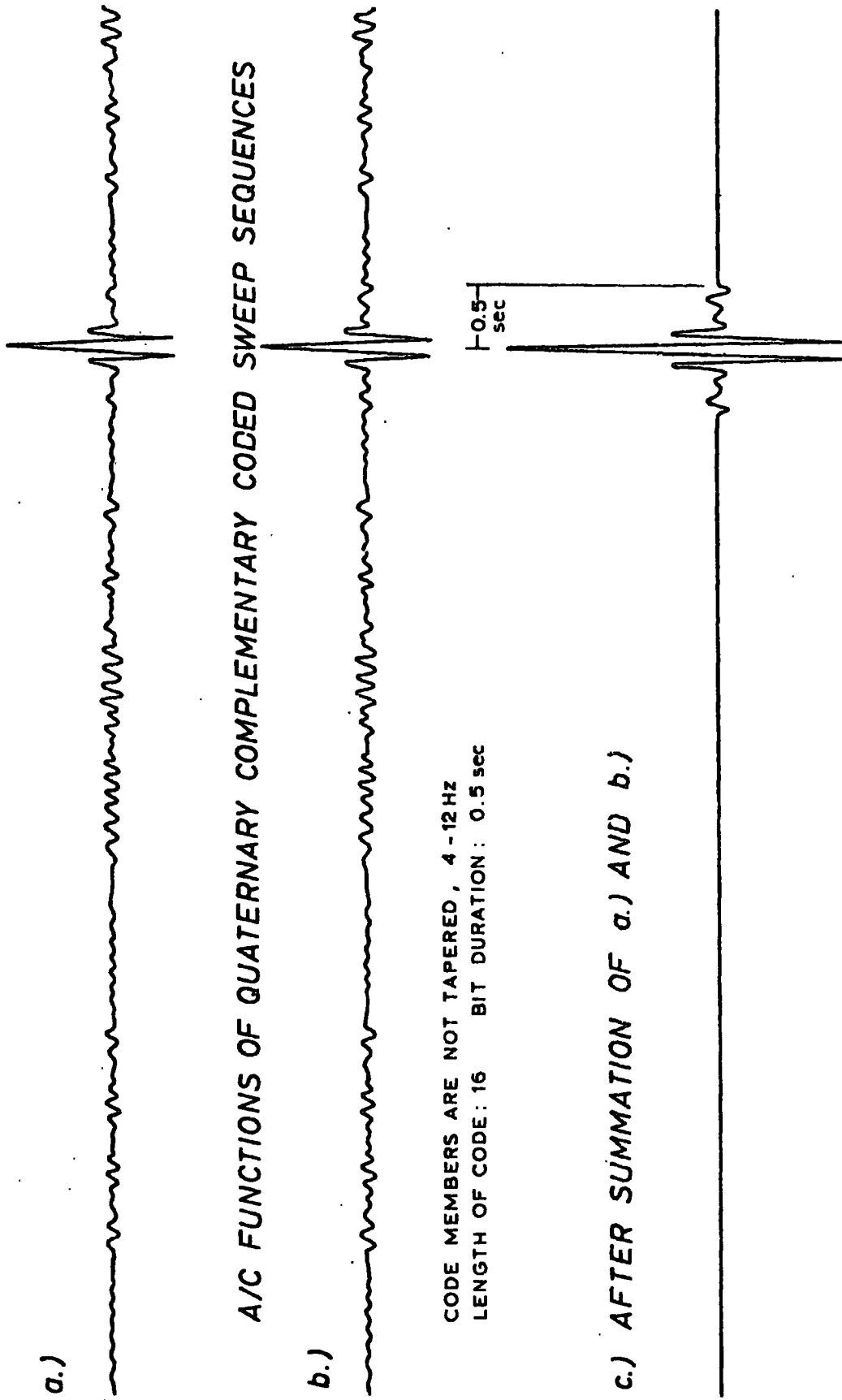


FIG. 29 - VIBROSEIS ENCODING TECHNIQUE III

sequences are E and  $E_i$  as defined in chapter 5.

$$E = a c a d b d a d b d b c b d a d$$

$$E_i = b c b d a d b d a d a c a d b d$$

The code members a,b,c and d are replaced by different sweeps, as above, and the autocorrelation functions show a similar pattern of crosscorrelation functions in the sidelobes. In this example each code member is only 0.5 sec. long, allowing the total transmission time to be kept the same as in the preceding cases.

On comparison of Figures 28 and 29 the processed output wavelet of the 16 bit long signal is distinctly shorter, i.e. more undesired correlation noise has been suppressed. In general, the position of the start of perfect sidelobe compensation is governed by the length of the code members.\* In our last example sidelobes disappeared after 0.5 sec., taking the centre peak as point of reference. It therefore follows, that the greater the length n of the code, the better the compensation of correlation noise for a given time.

Translated into practice this means that it is advantageous to use as short code members as possible in order to transmit a great number of them in a given time. Unfortunately, there are limits to the shortening of sweeps as generated by vibrators, and signal durations of less than 0.5 sec. are considered to be impractical for the frequency ranges most commonly used.

...which becomes clear if we recall that the coded Vibroseis system is essentially performing a stacking process on its code members.

To recapitulate:

The choice of practical code members for a Vibroseis encoding technique, as deduced from the correlation matrices introduced in chapter 5, has been proved to be correct by means of computer modelling. Binary and quaternary complementary series showed their power to rigorously suppress correlation noise at a pre-determined distance away from the centre Klauder wavelet. The greater the length of the code, the better the compensation of sidelobes for a given total transmission time. Imperfections in the transmitted signal which can produce considerable reduction in the performance of the conventional Vibroseis signal by introducing high sidelobe levels, are found to have relatively little or no effect in the encoded system.

Figures 30 and 32 illustrate the Vibroseis encoding effect in greater detail by means of an adjusted amplitude scale applied to the output functions of an uncoded and a Golay ( $n=8$ ) coded waveform, respectively. Both signals have the same total transmission time of 23.808 sec. and a common frequency range of 16 Hz to 48 Hz. The one-sided autocorrelation functions are shown for only four specially selected time intervals, taking the zero shift positions as time origin. Figures 31 and 33 are the corresponding 'Sidelobe Suppression versus Time' - graphs covering 4 sec. of the correlogram. As clearly indicated in Figures 32 / 33, the complementary coded signal will achieve infinite sidelobe suppression after 1.488 sec., which proves that, -at least in theory-, encoding is a method of substantially increasing the signal-to-noise ratio and the detection capability of the Vibroseis system.

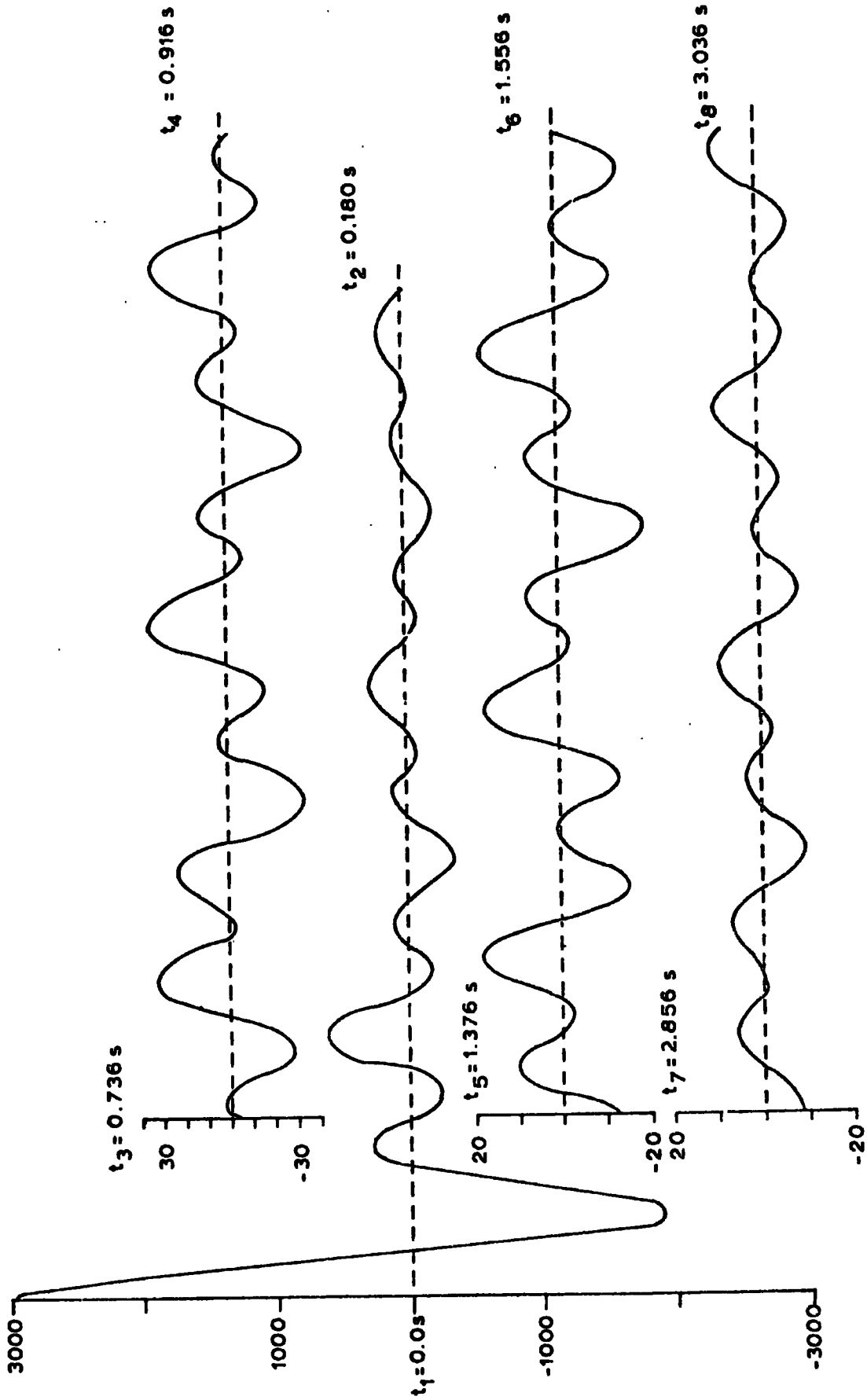


FIG. 30 - A/C FUNCTION OF CONVENTIONAL VIBROSEIS SIGNAL

(FREQUENCY RANGE: 16 - 48 HZ, DURATION: 23.808 sec.)

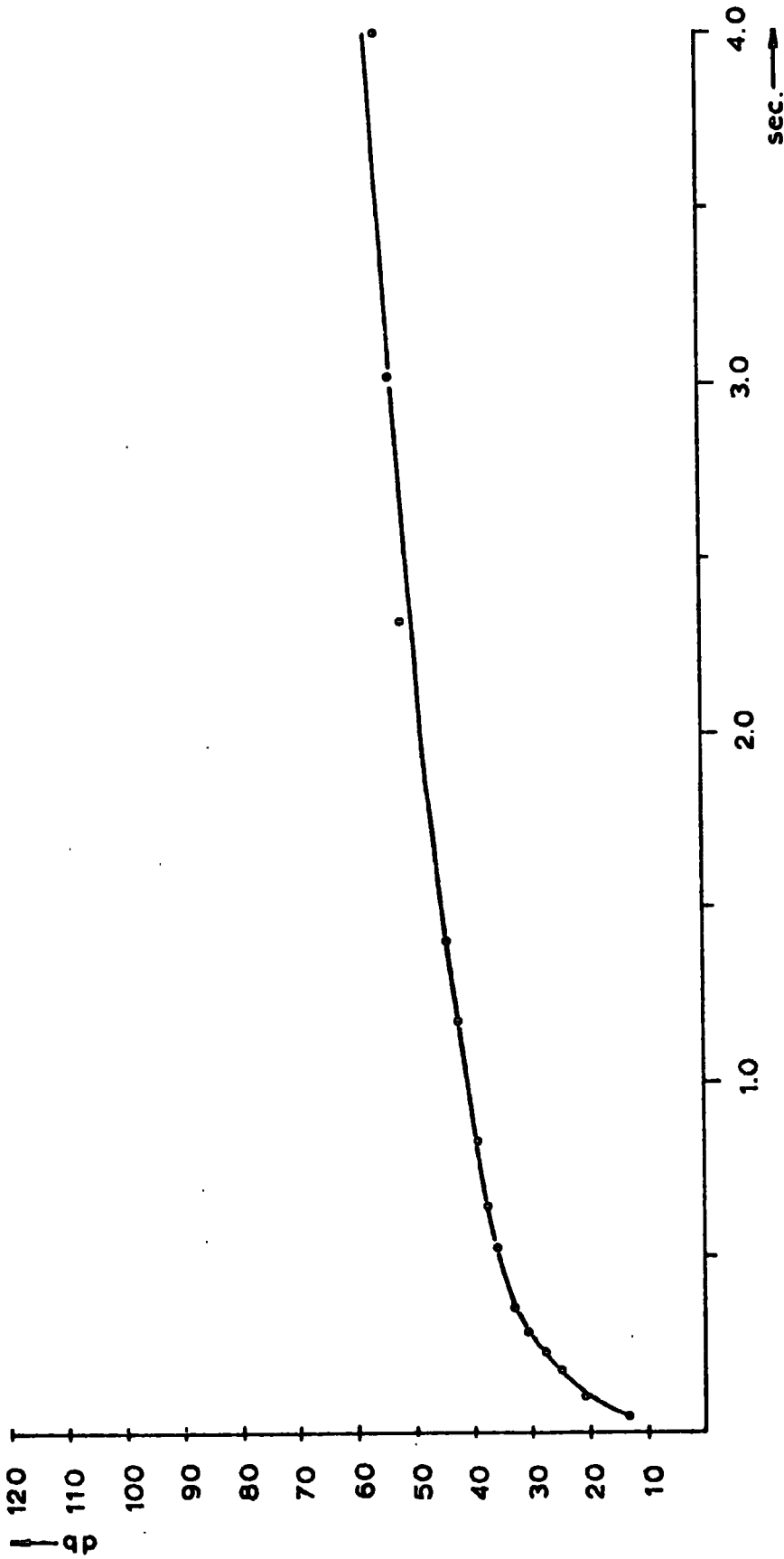


FIG. 31 - "SIDELOBE SUPPRESSION versus TIME" - GRAPH  
(... for the autocorrelation function shown in Figure 30)

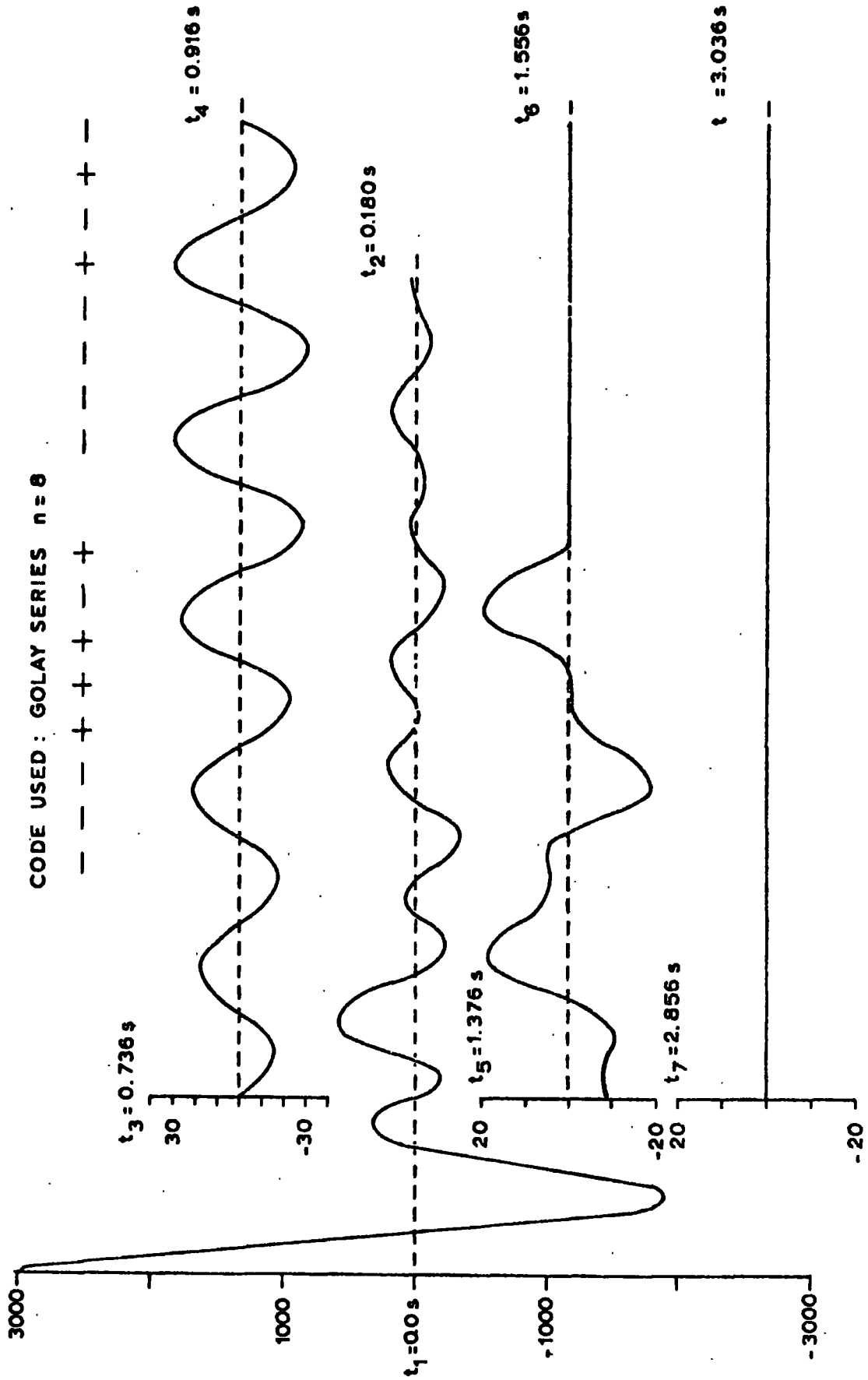


FIG. 32 - OUTPUT FUNCTION OF COMPLEMENTARY CODED VIBROSEIS SIGNALS  
(FREQUENCY RANGE: 16-48 Hz, SIGNAL DURATION:  $2 \times 11.904 \text{ sec.}$ )



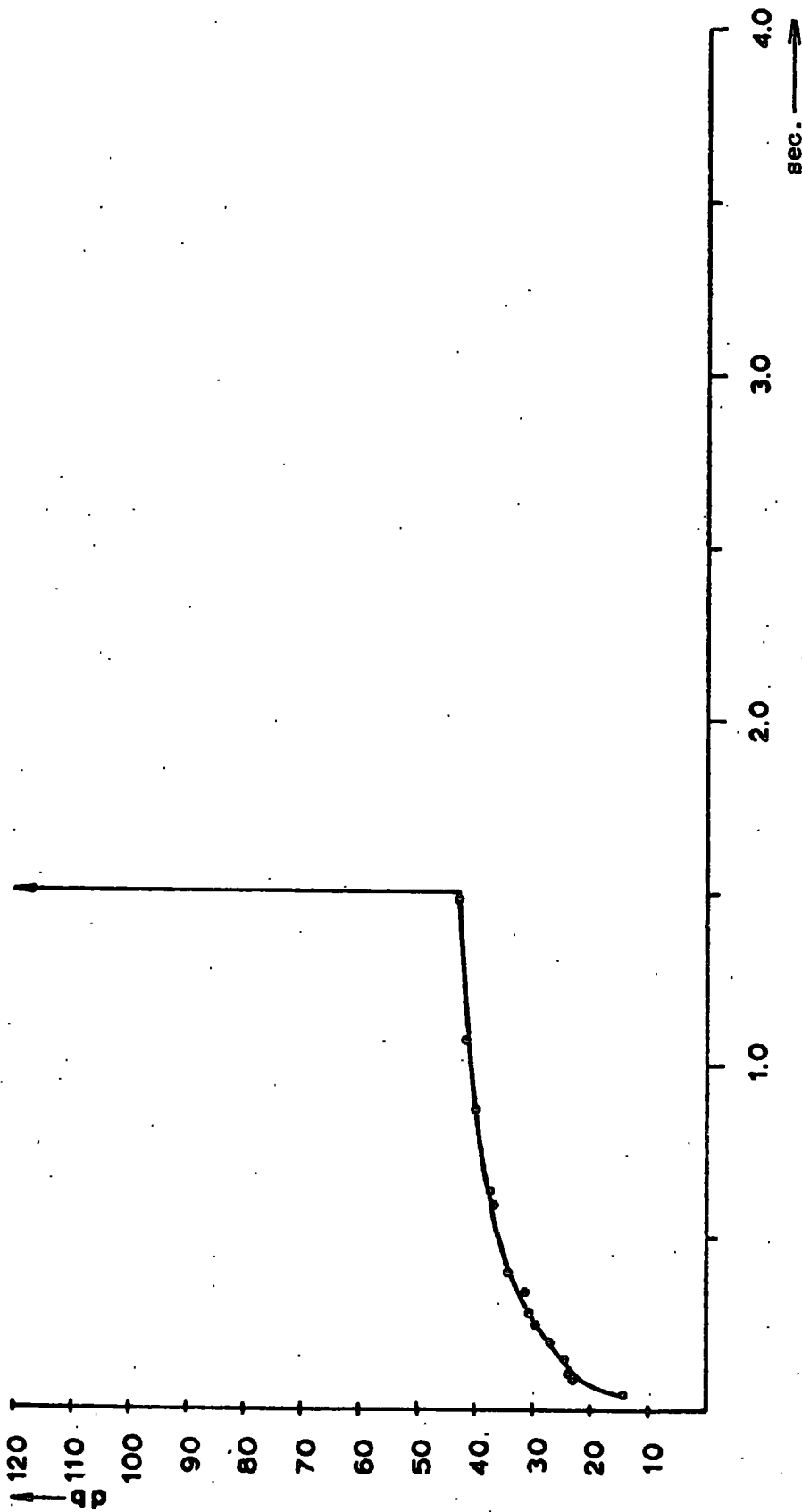


FIG. 33 - "SIDELOBE SUPPRESSION VERSUS TIME" - GRAPH  
( ... for the output function shown in Figure 32 )

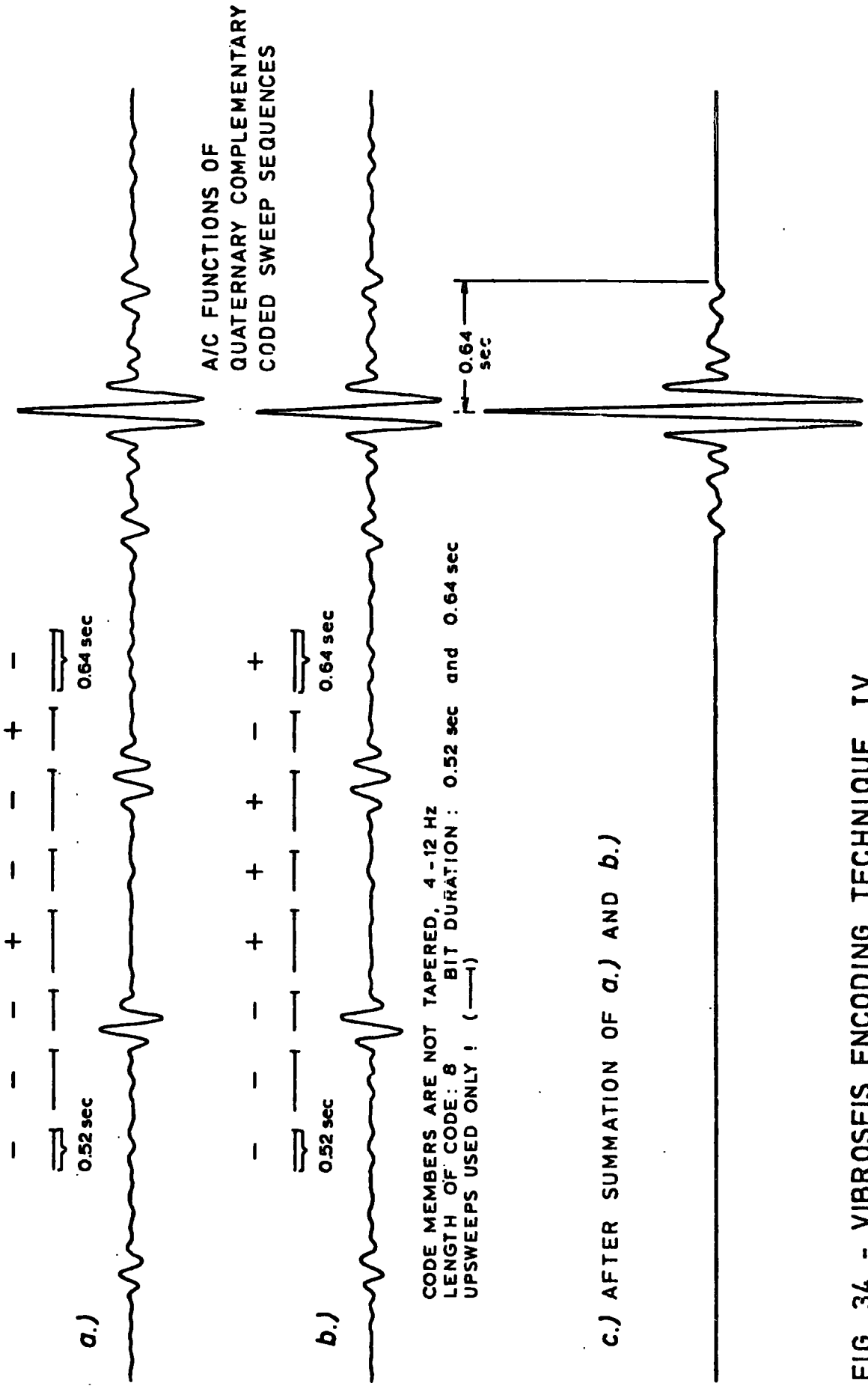
So far, the suites of code members used in the Vibroseis implementation of the binary and quaternary complementary series, consisted of two or four sweeps respectively, which showed identical Klauder wavelets on autocorrelation. The sweeps were chosen so as to comply with the binary and quaternary correlation matrices (A.) and (C.). It can be seen, that the main or principle diagonal of these matrices determines the character of the Klauder wavelet left after processing, because its elements represent all possible auto-correlations which will eventually be stacked by the processing procedure of the complementary encoded Vibroseis system.

The quaternary correlation matrix (C.) has been subdivided into four submatrices. Submatrices I and III contain the same elements, in fact the  $2 \times 2$  matrices are identical. Submatrices II and IV contain different elements.

In the course of the research it became apparent that even a correlation matrix with four different submatrices, i.e. with two different elements in the main diagonal, can be applied to complementary series of certain lengths. Again, only series of length  $n=2^i$ , where  $i$  is an integer, make the use of the following matrix possible:

$$\begin{vmatrix} aa & ab & ac & ad \\ ba & bb & bc & bd \\ ca & cb & cc & cd \\ da & db & dc & dd \end{vmatrix} = \begin{vmatrix} k & -k & i & -i \\ -k & k & -i & i \\ j & -j & 1 & -1 \\ -j & j & -1 & 1 \end{vmatrix} \quad (D.)$$

Figures 34 and 35 show two examples of the complementary Vibroseis encoding technique employing the product table (D.). In Figure 34 the four code members used in the quaternary series of length  $n=8$  are:



c.) AFTER SUMMATION OF a.) AND b.)

FIG. 34 - VIBROSEIS ENCODING TECHNIQUE IV

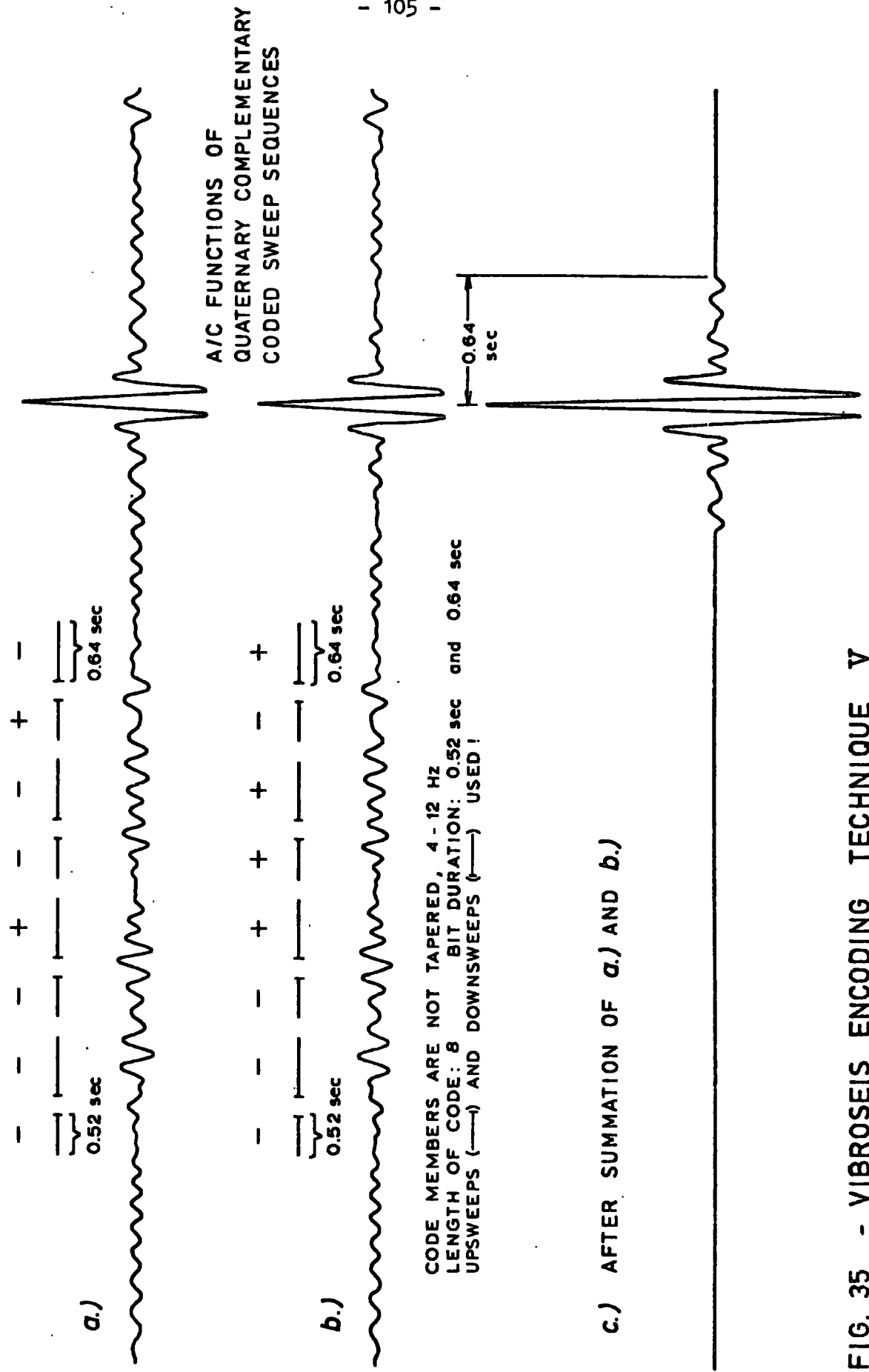


FIG. 35 - VIBROSEIS ENCODING TECHNIQUE V

a = upsweep; 4 Hz - 12 Hz; 0.52 sec.

b = phase inverted upsweep; 4 Hz - 12 Hz; 0.52 sec.

c = upsweep; 4 Hz - 12 Hz; 0.64 sec.

d = phase inverted upsweep; 4 Hz - 12 Hz; 0.64 sec.

For the same series (i.e. a c a d b d a d and a c a d a c b c) the quaternary code members in Figure 35 are replaced by

a = upsweep; 4 Hz - 12 Hz; 0.52 sec.

b = phase inverted upsweep; 4 Hz - 12 Hz; 0.52 sec.

c = downsweep; 12 Hz - 4 Hz; 0.64 sec.

d = phase inverted downsweep; 12 Hz - 4 Hz; 0.64 sec.

The result of adding the autocorrelation functions is the same in both Figures. It can clearly be seen that the complementary property has been preserved. However, the Klauder wavelet left is no longer the stack of 16 identical sweep autocorrelation functions. As indicated by the principle diagonal of the product matrix used, the detected signal is a 16 fold stack of the two different autocorrelation functions possible from the two signal pairs of 0.52 sec. and 0.64 sec. duration, respectively. It is obvious that the longer signal pair determines the sidelobe cut-off time, which in our case is 0.64 sec.

The correlation matrix (D.) is also satisfied if the code members were chosen as:

a = upsweep; 4 Hz - 12 Hz; 0.52 sec.

b = phase inverted upsweep; 4 Hz - 12 Hz; 0.52 sec.

c = upsweep; 20 Hz - 40 Hz, 0.52 sec.

d = phase inverted upsweep; 20 Hz - 40 Hz; 0.52 sec.

emphasizing the fact that a great number of signal suites can be found obeying either matrix (C.) or (D.). In the last example the sweeps are of equal duration but have different frequency ranges. By means of this code member choice it is possible to combat troublesome ambient noise like the  $16\frac{2}{3}$  Hz interference from the railway power supply lines.

## CHAPTER 7

### A CONTINUOUS TRANSMISSION SYSTEM

#### 7.1. Introduction

In 1972/73, a team of university seismologists and the Continental Oil Company (CONOCO) took part in an experiment, recording deep crustal reflections using the Vibroseis method (FOWLER and WATERS (1975)). Due to the complexity of the geological structure investigated, reflection events could not be identified with certainty. It was, however, demonstrated that a swept frequency method can produce records for receiver - transmitter separations of up to 66 km. The signal-to-noise ratio for refractions and for what appeared to be reflections, was reasonably good.

In the experiment six vibrators were used, one high power, low frequency research vibrator and five vibrators from one of CONOCO's Vibroseis field crews. A total of 240 downsweeps with a duration of 30 sec. were transmitted in each location. The listening period per sweep was maximal 64 sec. All recordings from one location had to be composited in order to improve the S/N-ratio and 4 to 7 hours was the time generally needed to complete a full acquisition cycle.

Likewise, using the Vibroseis system for normal exploration purposes, a considerable number of records has to be stacked, in order to achieve a reasonable signal to ambient noise ratio (ERLINGHAGEN). This means, that in routine work too, a relatively long recording time is necessary, during which, it is forbidden to release a new signal.

From the above, it becomes clear immediately, that it would

be of great advantage for low input power systems, like Vibroseis, to be able to transmit energy whilst listening to reflection or refraction events returning from the subsurface.

In theory, such a system can be designed by means of Welty's quaternary codes, the E-code and its mate, which have already been introduced in chapter 5. The E-code and its mate represent "Pulse Codes", i.e. their autocorrelation functions consist of a single pulse only, and both codes are also mutually exclusive or orthogonal, i.e. the crosscorrelation of an E-code with its mate is identically zero. However, Welty's codes only show the properties described above, if the correlation matrix (B.) is applied.

Correlation matrix (B.):

$$\begin{vmatrix} aa & ab & ac & ad \\ ba & bb & bc & bd \\ ca & cb & cc & cd \\ da & db & dc & dd \end{vmatrix} = \begin{vmatrix} 1 & -1 & 0 & 0 \\ -1 & 1 & 0 & 0 \\ 0 & 0 & 1 & -1 \\ 0 & 0 & -1 & 1 \end{vmatrix}$$

Assuming that four physically realizable signals can be found, which fulfil the matrix (B.), an E-coded signal and its mate could be transmitted alternately for any length of time. The method for recovering separate information about the subsurface reflectors is provided by the orthogonality of both waveforms under consideration. Two cross-correlation processes have to be performed on the received signal, correlating it firstly with the known E-coded signal and secondly with the mate. All crosscorrelation functions which might generate correlation noise in this processing method are zero by definition and do not interfere. Therefore, in one correlation function only the reflections of the E-coded waveform will be visible and the other

record only contains reflections due to the transmission of the mate. An appropriate stacking process has to be devised to composite the two sequences of consecutive seismograms. Finally, a further vertical stack can be performed on the two conventional seismograms resulting from the preceding data processing steps.

Unfortunately, it has not been possible to find a suite of signals obeying Welty's correlation matrix. The design of four such practical signals seems to be an impossible task, because according to Welty's product table all waveforms used must have an identical autocorrelation function and it is also required, that most of the possible crosscorrelations are identically zero.

Nevertheless, a continuous Vibroseis transmission system has been designed. The suggested system uses certain sets of mutually orthogonal complementary sequences, whose code members can be replaced by the practical quaternary and binary Vibroseis signals introduced in chapter 6.

## 7.2. The Complementary Continuous Transmission Code

It becomes evident through the study of Welty's codes, that any code useful for a continuous transmission system has to possess the property of orthogonality, i.e. two or more coded sequences have to crosscorrelate to zero, or their crosscorrelation functions have to compensate on addition. For binary sequences it is clearly not possible to achieve this orthogonality with just one pair of sequences.

In Chapter 5 the concept of mutually orthogonal complementary sets of sequences was introduced and a few examples were presented. Orthogonality between the given sets of binary codes was accomplished by adding the crosscorrelation functions of corresponding sequences. Each set also possessed a complementary property, that is to say, all autocorrelation functions of each set add up to zero except for the centre shift position, which gives the sets of mutually orthogonal complementary sequences the character of "Pulse Codes", as defined in connection with the E-codes.

It was this similarity between Welty's quaternary codes and the non-interactive sets of complementary binary codes, that convinced the author of a possible application of the latter in a continuous transmission system. A search for a suitable code was particularly inviting, because the suite of practical signals which could replace the binary bits was already known and tested on Golay's complementary series.

Basically, two binary sequences, each consisting of a set of complementary series, are needed for the complementary continuous transmission system (forthwith abbreviated as C.C.T.-system) presented

in this thesis. Figure 36 shows the building unit of the continuous code, the so-called "Block", and a second binary sequence which has been named the "Compensator Sequence". On comparison with Figure 20 it can be seen, that both codes are identical with column 1 and column 2 of the  $4 \times 4$  M.O.C.-matrix presented, but all four codes making up a set of complementary sequences, are now written one after another.

The basic principle of the suggested C.C.T.-system, as envisaged by the author, is illustrated in Figure 37. The block is transmitted without interruption over and over again for any length of time. It can easily be imagined that at the geophones a perfectly uninterpretable record is received, which needs decoding. The C.C.T.-data is recorded onto magnetic tape and processing normally takes place in the 'Processing Centre' because of the increased volume of information. Here, the long, continuous records are crosscorrelated with the block, which also acts as the pilot signal. The result is a slightly less confusing record, which, in our example, consists of a string of three high amplitude peaks (...autocorrelation of block), each associated with two smaller spikes (...crosscorrelation noise) to both sides. These spikes represent system induced noise, very similar to the noise encountered in the normal complementary coding technique. (See Figure 37 A.)).

In order to eliminate this disturbing noise the received data has to undergo a second crosscorrelation with the compensator sequence. This code is specially designed to show, on correlation, complementary property to the crosscorrelation noise of the output

**THE BLOCK** - building unit of a complementary continuous code.

+ - - - + - - - + - - - + - - -

COMPARE BOTH SEQUENCES WITH COLUMN 1 AND 2 OF THE 4 x 4 M.O.C - MATRIX IN FIG. 20.



- - + - + - + - - - + - - -

**THE COMPENSATOR SEQUENCE** - vital for correlation noise compensation.

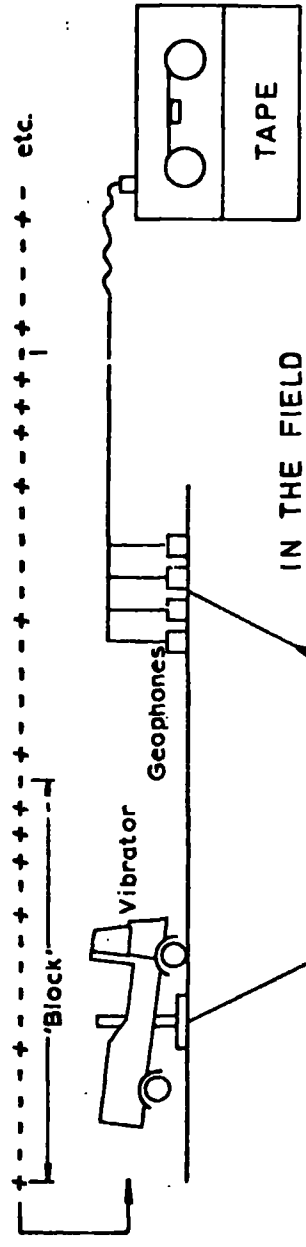
NOTE: The two code sequences can be interchanged!

FIG. 36 - BLOCK AND COMPENSATOR SEQUENCE

CONTINUOUS TRANSMISSION CODE

+ - - - -    - - + -  
 - + - - -    + + + -  
 - - + - -    + - - -  
 + + + - -    - + - -

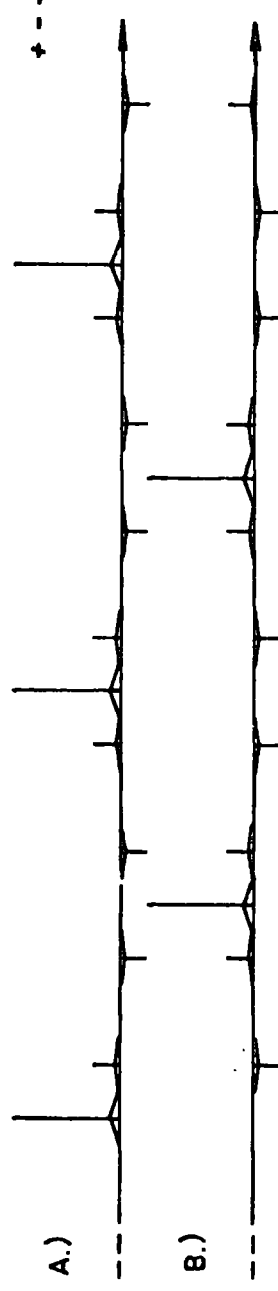
A MUTUALLY ORTHOGONAL  
COMPLEMENTARY SET OF  
SEQUENCES



PROCESSING

1.) CORRELATION WITH 'Block'

+ - - - - + - - - - + - - - -



2.) CORRELATION WITH COMPENSATOR SEQUENCE

- - - - - + + + - - - - -

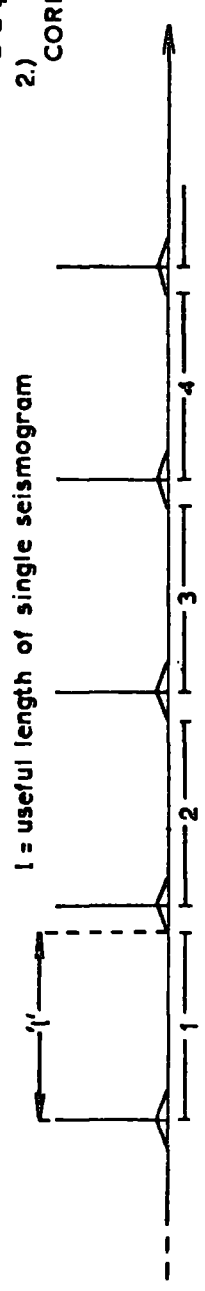


FIG.37 - THE PRINCIPLE OF CONTINUOUS VIBROSEIS TRANSMISSION

function resulting from the first processing step. (See Figure 37 B.)). It can be seen that the compensator sequence also autocorrelates with some regions of the continuous transmission code producing the two high amplitude peaks in the given example. Therefore, parts of the continuous code are identical with the compensator sequence.

The result of stacking both crosscorrelation functions is shown in Figure 37 C.). Only the high amplitude events remain, which in fact represent the zero- or break time of the consecutive individual seismograms 1 to 4. The duration of each seismogram, now having the appearance of any conventional seismic trace, is clearly defined by the separation of these time breaks. Should pulse compression signals replace the binary bits, sidelobes must be associated with each spike and therefore the useful length of a single seismogram might be restricted to the length '1', as can be seen in Figure 37 C.), where sidelobes are already indicated. Finally, the continuous string of seismograms has to be divided into its individual components, which are consequently stacked.

To conclude:

The introduced complementary continuous transmission code permits the emission of energy whilst listening to returning signals. Separate information about the investigated subsurface, i.e. seismograms, can be recovered by performing the following two processing steps:

- a) The received continuous code data is crosscorrelated with the block and the compensator sequence.

- b) The crosscorrelation functions are added together and the special properties of the binary codes (code length  $n=4$ ) become effective, making possible a total compensation of system induced noise between the high amplitude autocorrelation spikes, which represent the time breaks of the individual, successive seismograms.

Before the presentation of some computer calculations using Vibroseis signals as bits for the continuous code, let us investigate the performance of the block and compensator sequence in more detail. Figure 38 shows, for some representative shift positions, how the continuous transmission system works. The C.C.T.-code can be seen at the top of the graph, with the individual complementary binary codes ( $n=4$ ) of the mutually orthogonal complementary sets of sequences separated for illustrative purposes only.

It is readily appreciated, that for what has been defined as the 'Zero'-shift position, the two crosscorrelation functions using the block and the compensator sequence as correlator, will yield the stack of four single autocorrelation functions (i.e.  $16 \times \wedge$ ) and no output (i.e.  $8 \times \wedge$  plus  $8 \times \vee$ ), respectively. The crosscorrelation between the compensator sequence and the continuous transmission code is zero, because the complementary series of length  $n=4$  involved in this process are orthogonal.

For all other shift positions the situation is rather more complex except for the so-called 'A/C-Shift Positions' of the block and the compensator sequence, where autocorrelation of



one or the other with the continuous code takes place. In fact, the zero-shift position is also the first of the block's A/C-shift positions. In our example autocorrelations of the block will be found for all

$i \cdot k = 0, 16, 32, \dots$  etc. shift positions, where  $i =$  length of block and  $k = 0, 1, 2, 3, \dots$  etc. The compensator will autocorrelate for the following shift positions:

$j/2 + (j \cdot k) = 8, 24, 40, \dots$  etc, where  $i=j=$  length of compensator sequence.

For the 2nd shift position only parts of the two main crosscorrelation functions are considered at a time, mainly to give special prominence to the three properties the sets of sequences have to have in order to be useful in the design of a C.C.T.-system.

The sequences used in the example automatically possess the necessary complementary and orthogonality property, because they constitute a pair of non-interactive sets of complementary series. The areas where these properties are of interest in Figure 38 are marked 'C.P.' and 'O.P.', respectively.

However, there are still eight parts of the main cross-correlations left where the above mentioned properties would not be sufficient to ensure zero output between the high amplitude peaks, i.e. between two successive A/C-shift positions. Actually, the two sets involved must have a third property: The crosscorrelation-orthogonality property marked 'C.O.' in Figure 38.

- All possible different crosscorrelations between neighboring sequences in both sets add up to zero, i.e. are orthogonal. -

There are eight such crosscorrelations in our example and they are all listed in Figure 39.

It was found, that two sets of mutually orthogonal complementary sequences of length  $n=4$ , also possessing the crosscorrelation-orthogonality property, can be constructed by means of a simple algorithm.

- Given one set of complementary series of length  $n=4$  (and order 4, i.e. four sequences), a second set suitable for application in a C.C.T.-system can be constructed by placing the first sequence into the third position, the second into the fourth, the third into the first and the fourth sequence into the second position of the new set, which will constitute the compensator sequence. -

Therefore, both sets of complementary series contain the same four binary sequences, but in a different succession. This then explains why the compensator sequence can autocorrelate with the continuous code in certain shift positions. It should also be mentioned, that the sequences in the block and compensator can be interchanged without affecting the result. A few examples of complementary continuous transmission codes are given in Figure 40.

LET THE SET OF 4 BINARY SEQUENCES

|   |   |   |   |      |
|---|---|---|---|------|
| + | - | - | - |      |
| - | + | - | - | (A.) |
| - | - | + | - |      |
| + | + | + | - |      |

BE THE "BLOCK" OF A CONTINUOUS CODE AND LET THE SET OF SEQUENCES

|   |   |   |   |      |
|---|---|---|---|------|
| - | - | + | - |      |
| + | + | + | - | (B.) |
| + | - | - | - |      |
| - | + | - | - |      |

CONSTITUTE THE "COMPENSATOR"-SEQUENCE.

THEN THE TWO SETS HAVE THE FOLLOWING TWO PROPERTIES:

- 1.) THE SETS (A.) AND (B.) ARE MUTUALLY ORTHOGONAL COMPLEMENTARY SETS OF SEQUENCES.
- 2.) CROSSCORRELATION-ORTHOGONALITY PROPERTY: ALL POSSIBLE DIFFERENT CROSSCORRELATIONS BETWEEN NEIGHBORING SEQUENCES ADD UP TO ZERO, I.E. ARE ORTHOGONAL. IN THE ABOVE EXAMPLE THE FOLLOWING EIGHT CROSS-CORRELATIONS ARE ORTHOGONAL

|   |   |   |   |   |   |   |   |   |   |   |   |   |   |   |   |   |   |   |   |
|---|---|---|---|---|---|---|---|---|---|---|---|---|---|---|---|---|---|---|---|
| + | - | - | - | / | - | + | - | - | , | - | + | - | - | / | - | - | + | - | , |
| + | - | - | - | / | + | + | + | - | , | - | + | - | - | / | + | - | - | - | , |
| - | - | + | - | / | + | + | + | - | , | + | + | + | - | / | + | - | - | - | , |
| - | - | + | - | / | - | + | - | - | , | + | + | + | - | / | - | - | + | - | . |

FIG. 39

|     |   |   |   |   |
|-----|---|---|---|---|
| a.) | + | + | + | + |
|     | + | + | - | - |
|     | - | + | - | + |
|     | - | + | + | - |
|     | - | + | - | + |
|     | - | + | + | - |
|     | - | + | + | + |
|     | + | + | - | - |
| b.) | - | - | + | + |
|     | - | - | - | - |
|     | + | - | - | + |
|     | + | - | + | - |
|     | + | - | - | + |
|     | + | - | + | - |
|     | + | - | - | + |
|     | - | - | - | - |
| c.) | - | - | + | - |
|     | + | + | + | - |
|     | - | + | + | + |
|     | + | - | + | + |
|     | - | + | + | + |
|     | + | + | + | + |
|     | + | - | + | + |
|     | - | - | + | - |
|     | + | + | + | - |

FIG. 40 - MUTUALLY ORTHOGONAL  
COMPLEMENTARY SETS  
SUITABLE FOR CONTINUOUS  
CODING.

### 7.3. Example of a Complementary Coded Continuous Vibroseis System

As in the previous techniques the binary + and - signs have to be replaced by Vibroseis signals, i.e. by sweeps and phase inverted sweeps, respectively.

In Figure 41 abnormally short sweeps of 0.25 sec. duration and a frequency range of 5 Hz to 20 Hz have been selected for bit replacement purely to save computer time. The continuous code used in this test is shown in Figure 36. The block is repeated once and therefore only two individual seismogram regions can be expected in the processed record.

Similar to the complementary encoding technique described in the preceding chapter, a quaternary equivalent to the binary continuous codes can be found and a quaternary implementation using up- and downsweeps and their phase inverted versions as code members has also been tested on the computer.

Both test results are combined in Figure 41, which was possible, because the centre parts of the crosscorrelation functions are identical. To both sides of the useful region correlation noise of relatively high amplitude is present. The noise forerunners and tails of both crosscorrelations and stacks are different for the binary and quaternary implementation and are drawn separately. The duration of the noise is determined by the duration of the block used. Because the block is only repeated once in the given example, the noise will occupy a substantial part of the processed continuous record.

After summation of the two crosscorrelation functions,



there are basically three sweep autocorrelation functions left, two of which are representing the time breaks of the individual seismograms. The third wavelet just signals the end of the useful region in the processed continuous record. The time break autocorrelations are exactly the shape of a code member autocorrelation but 16 times amplified as the length of the block is  $n=16$ .

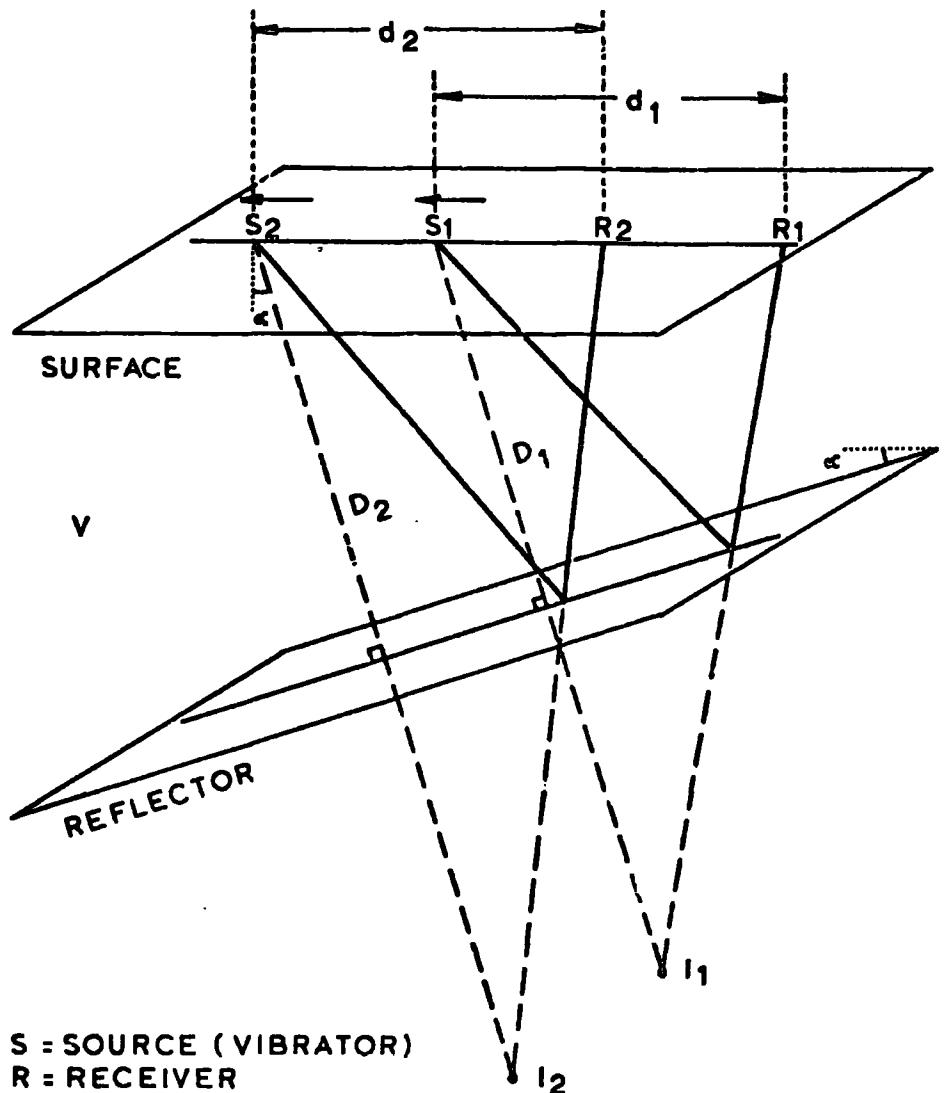
Each single seismogram lasts for half the duration of the block, in our example for 2 sec. The useful range of a seismogram is a little shorter, because one has to exclude the sidelobes to the left of the subsequent autocorrelation peak. It becomes clear, that the length of the seismogram or listening period for a given C.C.T.-code can be entirely determined by the choice of the code members. In the above example with 0.25 sec. long code members, the seismogram length is only 2 sec. The use of 1 sec. long sweeps allows an extension of the seismogram to 8 sec. and if even longer listening periods are required, the code members can be chosen to be of appropriate duration.

Finally, both seismograms have to be separated and stacked, lined up on their time break autocorrelation peaks, which in practice will account for another improvement of the signal-to-noise ratio. It should not be forgotten, however, that we have already taken advantage of the complementary property of the sequences used and that the processing of a continuous transmission record amounts to the stacking of  $n$  code member autocorrelation functions, where  $n$  equals the length of the block.

Besides its possible application in Vibroseis investigations of the earth crust or maybe in normal onshore exploration activities, a complementary coded continuous Vibroseis signal might also be applicable to geophysical offshore work. In principle, marine transducers continuously transmit a sequence of sweeps, phase encoded according to the chosen binary or quaternary block. The reflections from the subsurface are detected by a streamer towed by the vessel from which the vibrators are suspended. Generally, an offset of several hundred feet to the first trace is used. Throughout the whole data acquisition the boat will move along the profile with a constant velocity between 3 knots to 6 knots per hour.

Unfortunately, the fact that the ship is moving with respect to the subsurface can be responsible for the introduction of noise.

Let us consider the simple situation of a strongly dipping seabed, which shall also represent the principle reflector. In Figure 42 the source (e.g. a vibrator) and the receiver (a hydrophone) are shown in two different positions with respect to the dipping reflector. It is obvious from Figure 42 that the ray path  $\overline{S_2\text{-Reflector-R}_2}$  is longer than the ray path  $\overline{S_1\text{-Reflector-R}_1}$  and therefore under the assumption of a constant velocity of sound in water, the later parts of the block suffer a delay. There exists a relative motion between the source and the receiver and a "Doppler Shift" has to be expected. The time delay together with a shift in the frequency of the continuous signal at the hydrophones introduce Doppler shift distortions in the processed C.C.T.-seismograms (see Figure 43), because the Doppler shift has not affected the



S = SOURCE (VIBRATOR)  
 R = RECEIVER  
 V = SEISMIC VELOCITY  
 D = DEPTH TO REFLECTOR  
 $\alpha$  = ANGLE OF DIP  
 I = IMAGE  
 T = TRAVELTIME

$$d_1 = d_2 = d$$

$$\overline{I_1 R_1} < \overline{I_2 R_2}$$

$$T = \frac{(4D^2 + d^2 - 4Dd \sin \alpha)^{1/2}}{V}$$

FIG.42 - SIMPLE MODEL FOR  
 DOPPLER NOISE EVALUATION

Velocity of Source = 6 Knots

D = 500 m

d = 300 m

3.5° DIP

S/DN = -42 db

7.5° DIP

S/DN = -36 db

15.0° DIP

S/DN = -30 db

TWO CONSECUTIVE SEISMOGRAMS SHOW  
PARTIAL INVERSION OF DOPPLER NOISE.

S/DN = Signal to Doppler Noise ratio.

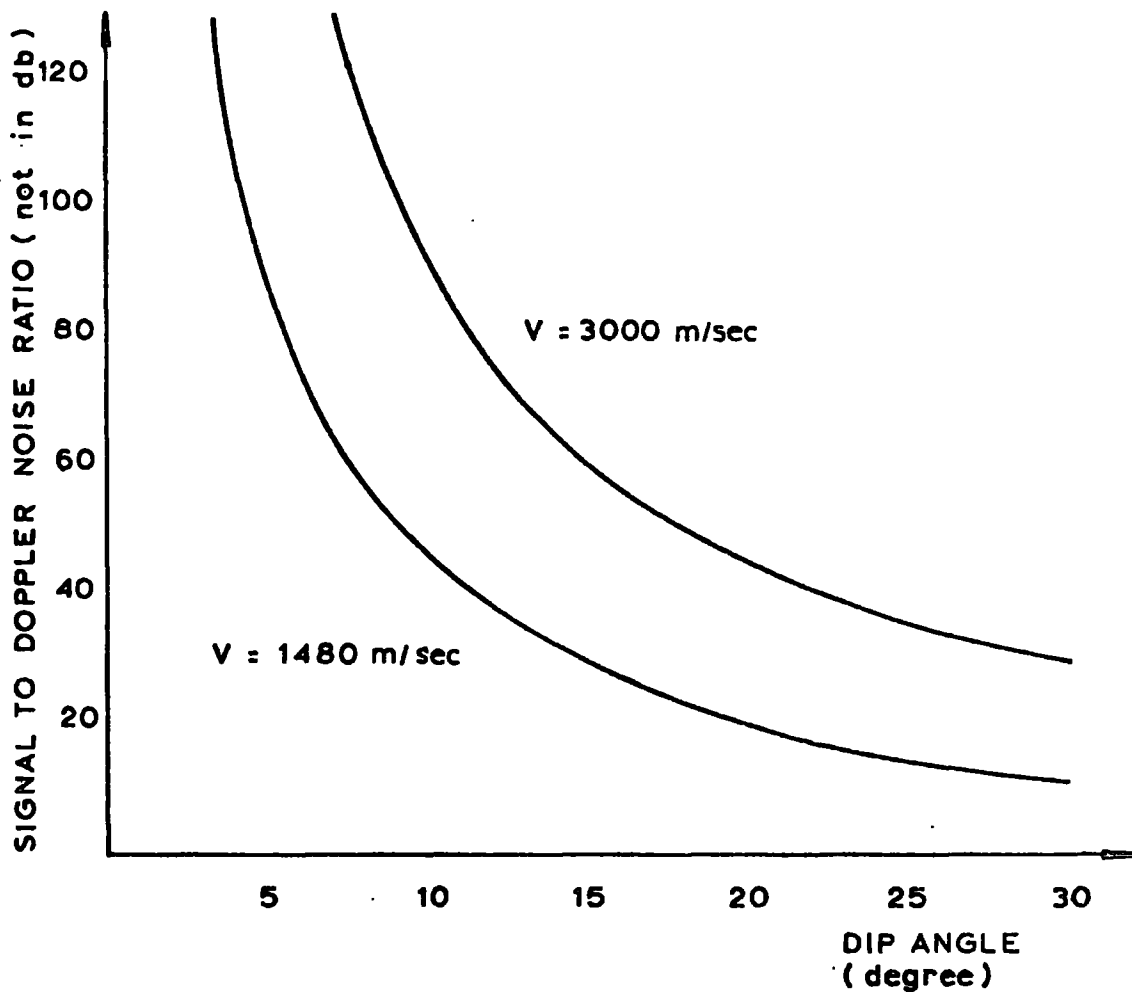
FIG. 43 - DOPPLER SHIFT DISTORTIONS

two sequences with which the received data has to be correlated, i.e. the reference signals. Imperfect compensation of wavelets in the crosscorrelation process as well as on stacking is the result.

In order to estimate the severity of Doppler noise in marine continuous transmission seismograms, examples were calculated for various dip angles  $\alpha$  using the simple model shown in Figure 42. For dips of  $3.5^\circ$ ,  $7.5^\circ$  and  $15.0^\circ$ , a ship speed of 6 knots (3m/sec.) and a depth of 500m to the horizon, the processed and stacked seismogram sections can be seen in Figure 43. The dependency between Doppler noise amplitude and dip angle is clearly indicated. The noise is getting stronger when the angle of dip is increased. Figure 44 is a graphical presentation of the whole Doppler noise evaluation, emphasizing the degenerate effects strong dips can have on the processed seismograms. For increased seismic velocities the noise level will be reduced.

On closer inspection of Doppler noise in two consecutive seismograms it was found that some noise wavelets will compensate when a stack of these seismograms is performed. Unfortunately, this is only true for every second noise wavelet, as can be seen from Figure 43.

The time delay has a worse effect on the continuous code than the shift in frequency. Due to the delay the stacking processes performed within the two crosscorrelations are no longer perfect, basically because the individual Klauder wavelets to be stacked are shifted with respect to each other. This becomes particularly apparent where the crosscorrelation functions used



$d$  = Source - Receiver Distance = 300 m

$D$  = 500 m

THE SOURCE IS MOVING WITH CONSTANT SPEED OF 3 m/sec (6 Knots) AS INDICATED IN FIGURE 42

FIG. 44 - DOPPLER NOISE

to be zero in the no-dip case, as now compensation is no longer total and noise wavelets remain which have different characteristics in the functions to be added.

Computer tests showed that the choice of code members also has an influence on the shape and amplitude of the Doppler noise wavelets. Code members of high  $f_2/f_1$  ratio and a good time-bandwidth-product will produce good, spiky autocorrelation functions. In the C.C.T.-system the use of such sweeps will result in comparatively stronger and more spike-like Doppler noise.

There is, however, a method of avoiding Doppler noise by adjusting the block and compensator sequence, so that both have experienced the same time and frequency distortions as the actually transmitted signal. These Doppler distortions could be implemented interactively on a computer, inspecting the processed output by eye after each adjustment. This method might even be used for a rough estimation of the dips involved if certain subsurface information and survey specifications are already known.

Although the continuous code has not yet been tested in the field further difficulties besides the Doppler noise generation in marine work can be foreseen. A continuous transmission also demands a facility for continuous recording over long periods. The use of an automatic gain control is meaningless, because the received signal will generally not change substantially over the recording period. One has therefore to rely on the dynamic range of the recording system to

detect the low amplitude arrivals superimposed on the intense direct wave transmission. Data processing will be more complex than for the conventional Vibroseis system, because long sequences will have to be correlated. The separation of individual records is also a new process and has to be performed with utmost care. Without doubt the transmission of long sequences of phase encoded sweeps will provide additional problems, some of which will be discussed in the next chapter about the practical implementation of the complementary coding technique.

#### 7.4. Summary

A complementary continuous transmission Vibroseis system has been suggested which allows to transmit energy continuously for any length of time. Separate information about the subsurface in form of individual seismograms can be obtained by means of the following processing steps:

- 1) Crosscorrelation of received data with the block, which is also the building unit of the continuous code.
- 2) Crosscorrelation of received data with a compensator sequence, which essentially eliminates system induced noise.
- 3) Stacking of the two crosscorrelation functions and separation of individual seismograms.

Besides the benefit of an increased volume of data the designed system also takes advantage of the complementary property of the sequences used in the construction of the continuous code. This means, in theory, perfect sidelobe compensation a predetermined distance away from the central detection peak.

The C.C.T.-Vibroseis system might find application in Vibroseis investigations of the crust of the earth and any other Vibroseis project where for reason of high ambient noise, for example, a great number of individual seismograms has to be stacked in order to improve the signal-to-noise ratio. The system's theoretical advantages are:

- a) Increased volume of data.
- b) Increased input power per given time.
- c) Exploitation of the complementary property, i.e. sidelobe compensation.

The anticipated disadvantages of a continuous transmission system are:

- a) The generation of Doppler noise in offshore operations over dipping horizons.
- b) The radical increase in the data volume and the introduction of at least two additional processing steps might prove uneconomical.
- c) A continuous transmission system has to rely on a recording system of very high performance, because an automatic gain control cannot be applied.

## CHAPTER 8

### FIELD TESTS OF THE ENCODED VIBROSEIS SYSTEM

#### 8.1. Introduction

So far the Vibroseis encoding technique has only been proved to work in theory, but the merit of a theoretically successful new method should be judged mainly on the benefits that can be drawn from its practical implementation.

In early 1976 the Prakla-Seismos GmbH, Hannover, West Germany, expressed their willingness to put the earlier outlined theoretical ideas to the ultimate practical test. The author is greatly indebted to the Company for the implementation of these tests and their kind cooperation during the latter part of this research.

As expected there are a great number of difficulties that have to be overcome, when one attempts to make such a theoretical model work in practice. This chapter will report on the problems encountered in the field tests of the Vibroseis encoding technique. Modifications to the ideal complementary coded waveforms were necessary to solve some of the problems involved, particularly in the transmission of the relatively sophisticated signals. These changes to code members are also described. Finally, some practical results are presented.

## 8.2. The Use of Computerized Recording Instruments in the Vibroseis

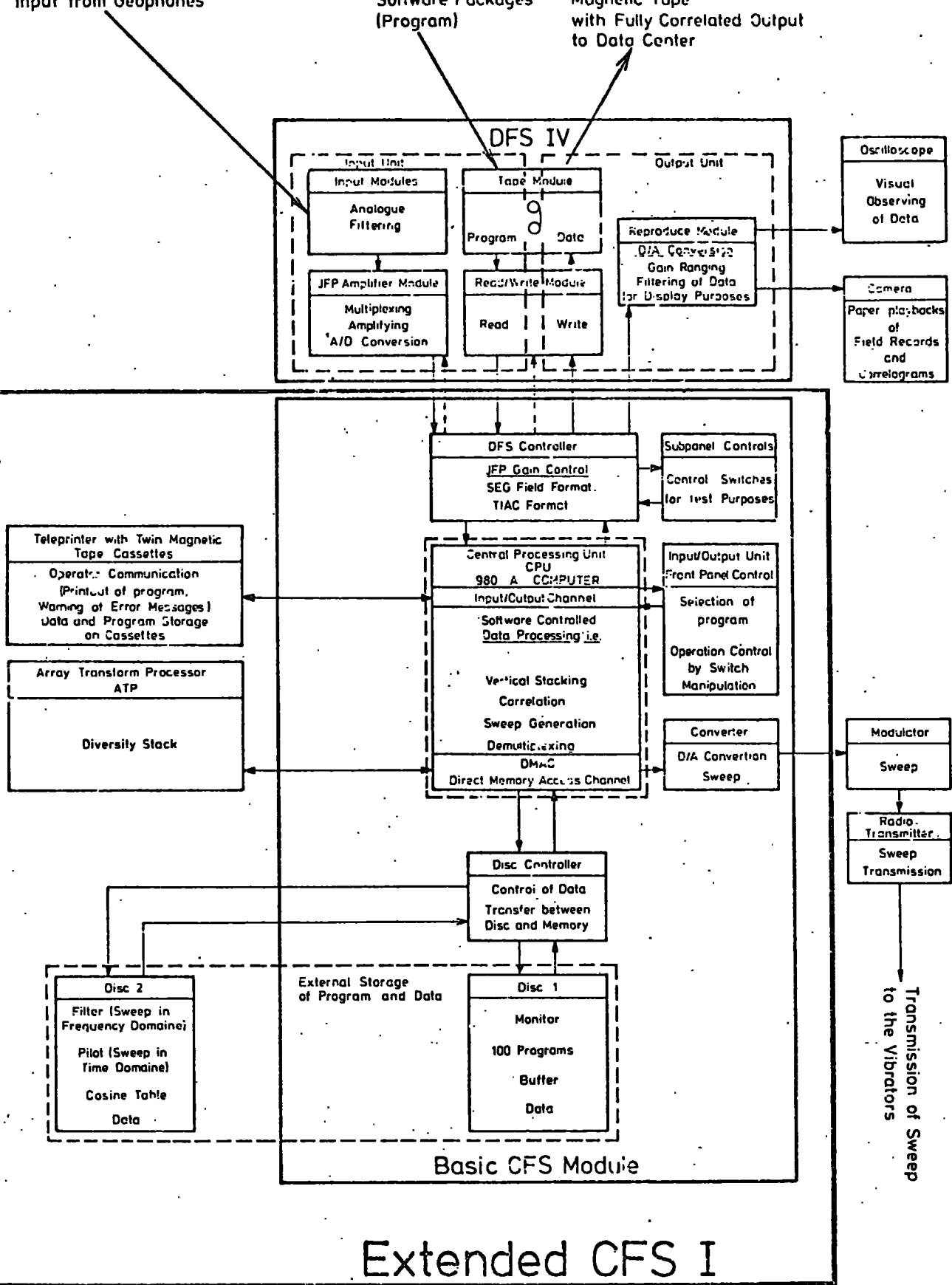
### Encoding Technique

Ideally one requires two separate transmission channels for any practical implementation of the complementary series. Each sequence is transmitted through its own channel and is received at its matched filter. The algebraic summation of the filter outputs cancels out sidelobes and will enhance the centre peak.

The earth obviously does not provide us with two channels which have no cross-coupling. The only way to implement complementary Vibroseis encoding is therefore by means of sequential transmission of the two coded sweep sequences. One also needs a memory device (e.g. a magnetic tape), storing the information which has been received as a result of the transmission of the first sequence, until the remainder of the data is available for further processing.

A Vibroseis crew using an "Extended CFS1" - recording equipment which appeared to have all necessary facilities, was selected by Prakla-Seismos to perform the first field tests in 1977. The abbreviation CFS1 stands for 'Computerized Field System 1'\*\* and such a system was only just recently introduced to the Vibroseis technique in January 1975 (WERNER et al (1975)). The CFS1 combines all the separate modules common to the conventional Vibroseis recording systems to a single unit and all operations take place under the command of a suitable field computer which is software controlled. Figure 45 shows some details of the "Extended CFS1".

\*\* Trademarks of Texas Instruments Inc.



Courtesy of PRAKLA-SEISMOS, W. GERMANY

FIG. 45

The possible operations of the system include, among others, the calculation of any sweep, vertical stacking, weighted vertical stacking, recording of stack seismograms and/or correlograms in multiplexed and/or demultiplexed format, and also provides automatic system diagnostics. The maximum acquisition period (... or recording loop) of this computerized system is 32 sec. long.

A schematic representation of the field implementation of the Vibroseis encoding technique is given in Figure 46 beneath a time scale chosen according to the maximum recording loop of the CFS1. Between the two coded sweep sequences A and B and after B a listening period of appropriate length has to be introduced. In our specific example the code members of a quaternary complementary code of length  $n=8$  are 1.5 sec. long (i.e. total signal duration =  $2 \times 8 \times 1.5$  sec. = 24 sec.). Each listening period lasts for 4 sec., making use of all the 32 sec. of recording loop available.

Figure 46 also shows a symbolized field record trace consisting of the recorded data A' and B'. On correlation the coded sweep sequences A and B are considered to be basically one signal and both sequences are shifted synchronously along A' and B' during the matched filter detection procedure. Two shift positions are indicated in Figure 46. It can be seen that the final output already represents the fully processed seismogram originating from two sequential transmissions of complementary sweep sequences.

The coded sweep sequences used in the field evaluations

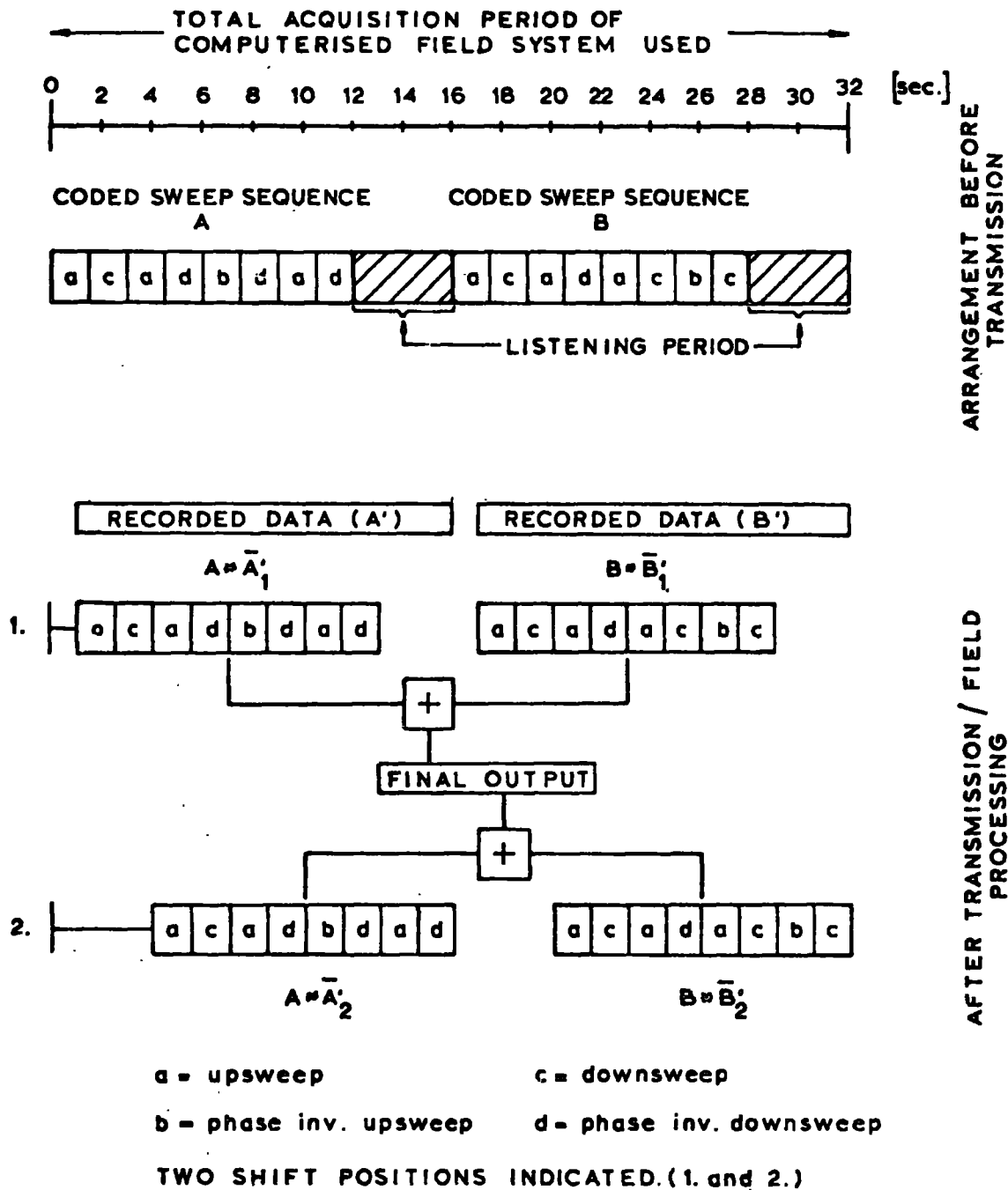


FIG.46 - FIELD IMPLEMENTATION OF VIBROSEIS ENCODING TECHNIQUE

were calculated by the author on the IBM 370/360 computer to the specifications of Prakla-Seismos, and consequently written onto magnetic tape. These 9 track tapes were sent to the Data Centre in Hannover to be converted into a suitable SEG (Society of Exploration Geophysicists) or TIAC (Texas Instruments Automatic Computer) format, which can be read by the field computer. In the CFS1 the signal data are finally transcribed from tape to disc (... disc 2 in Figure 45).

In order to examine the vibrators' response to the complicated pilot signals that the coded sweep sequences represent, the outgoing signal was recorded at the vibrators' base plates and also at a near field geophone. To facilitate a comparison with the actual pilot signal the two recorded traces were plotted next to the reference signal, as can be seen in Figures 47 and 48.

possible in Figs. 47 and 48.

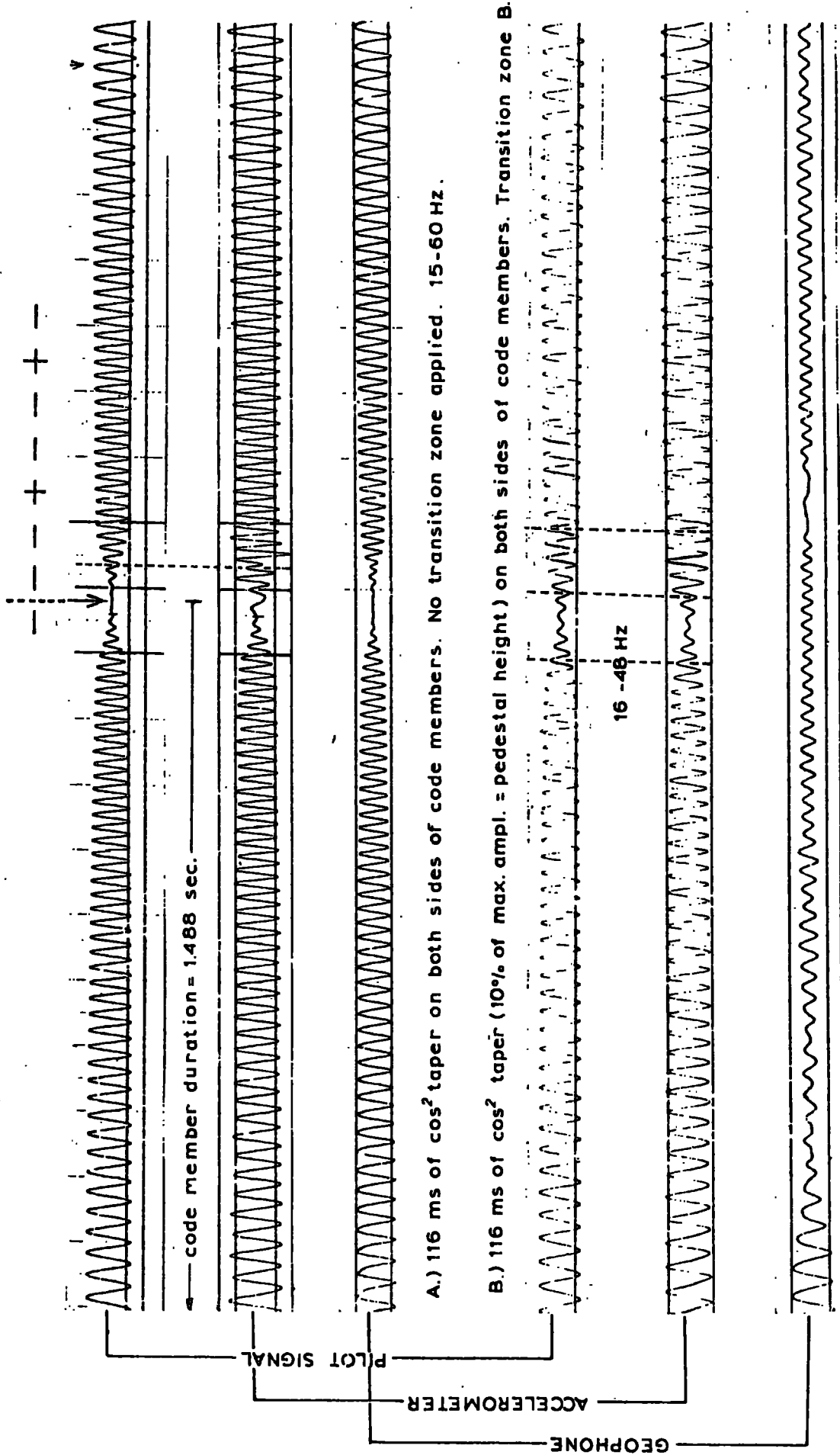


FIG. 47 - TRANSMISSION DISTORTIONS

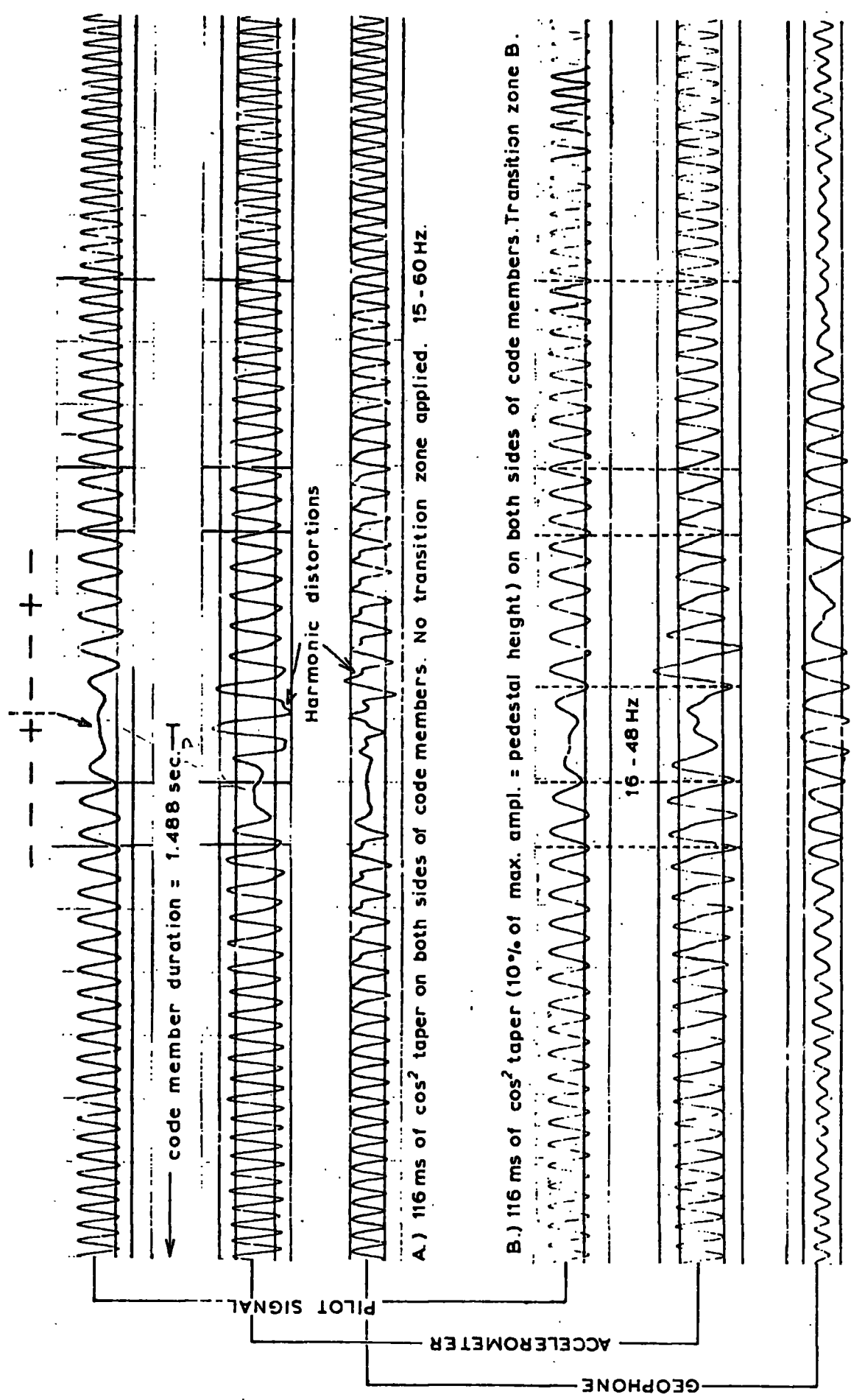


FIG. 48

### 8.3. Problems of the Practical Coded Signal Transmission and their Solution

On comparison with the binary Golay code, a quaternary complementary code with upsweep, downsweep and their phase inverted versions as the four different Vibroseis signals replacing the original quaternary code members, shows additional features which makes this code more attractive for the practical implementation. In the quaternary complementary coded sweep sequences, phase encoded sweeps increasing in frequency and decreasing in frequency alternate throughout the transmitted signal. Therefore, the vibrators do not have to transmit, for example, a high frequency sinusoid now and a sinusoid of considerably lower frequency only a moment later. Further advantage of quaternary codes can be taken at the processing stage. Any imperfections in the transmission of complementary coded Vibroseis signals, which violate the rule of bit equivalence, can lead to residual sidelobes on addition of the two correlation functions, in otherwise entirely correlation noise-free regions. The quaternary coded sweep sequences show lower sidelobes before stacking and consequently mismatch will not have such a pronounced effect.

However, one significant difficulty remains that even the application of quaternary codes does not overcome, -the so-called 'Discontinuous Bit Change-Overs'. In a few regions of the sequence of sweeps there is no smooth change-over in amplitude between two consecutive bits. Such (low frequency) transition zones are shown in Figures 49a and 51a. Obviously, these bit change-overs present a first order discontinuity to the Vibroseis vibrator, to which it

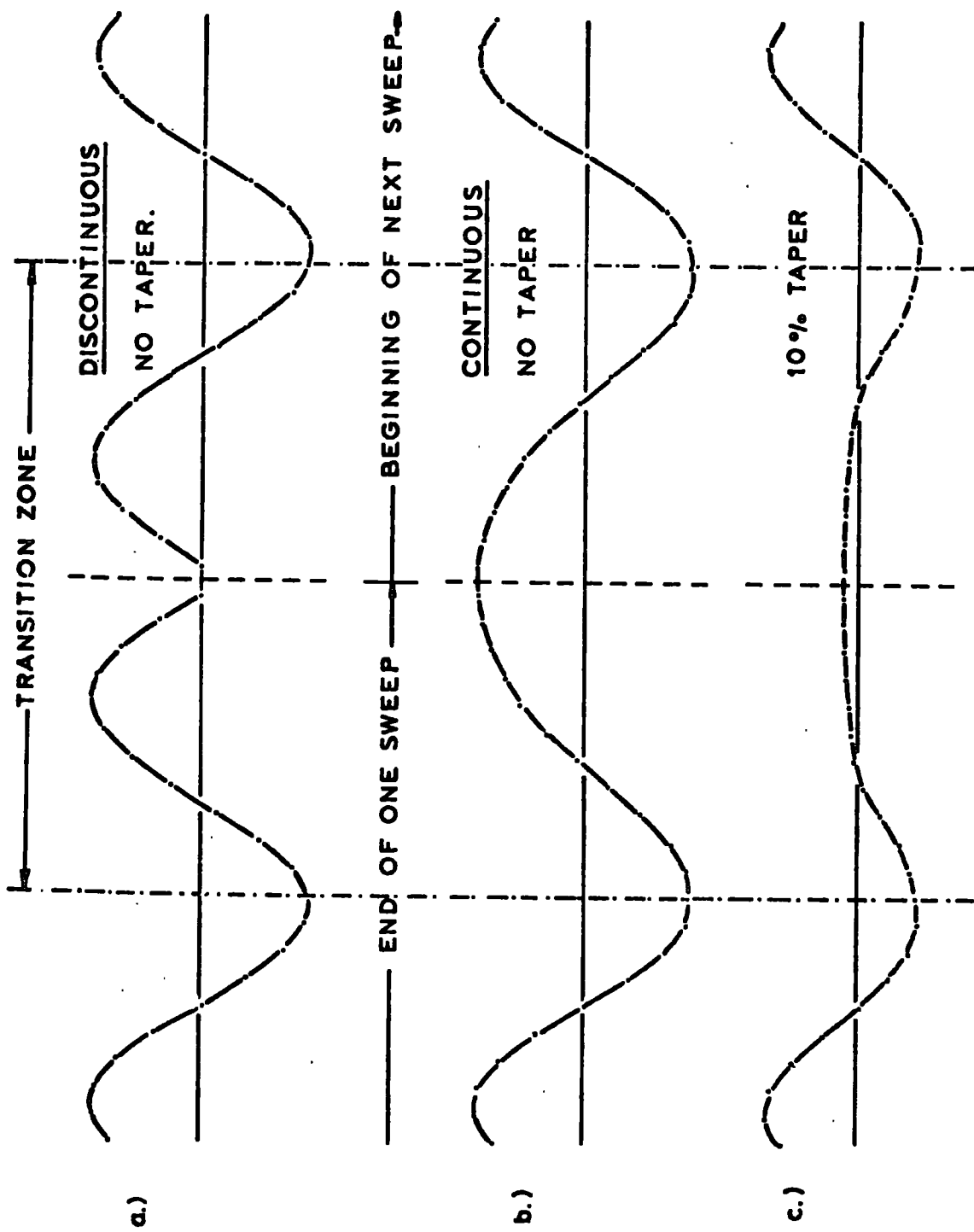
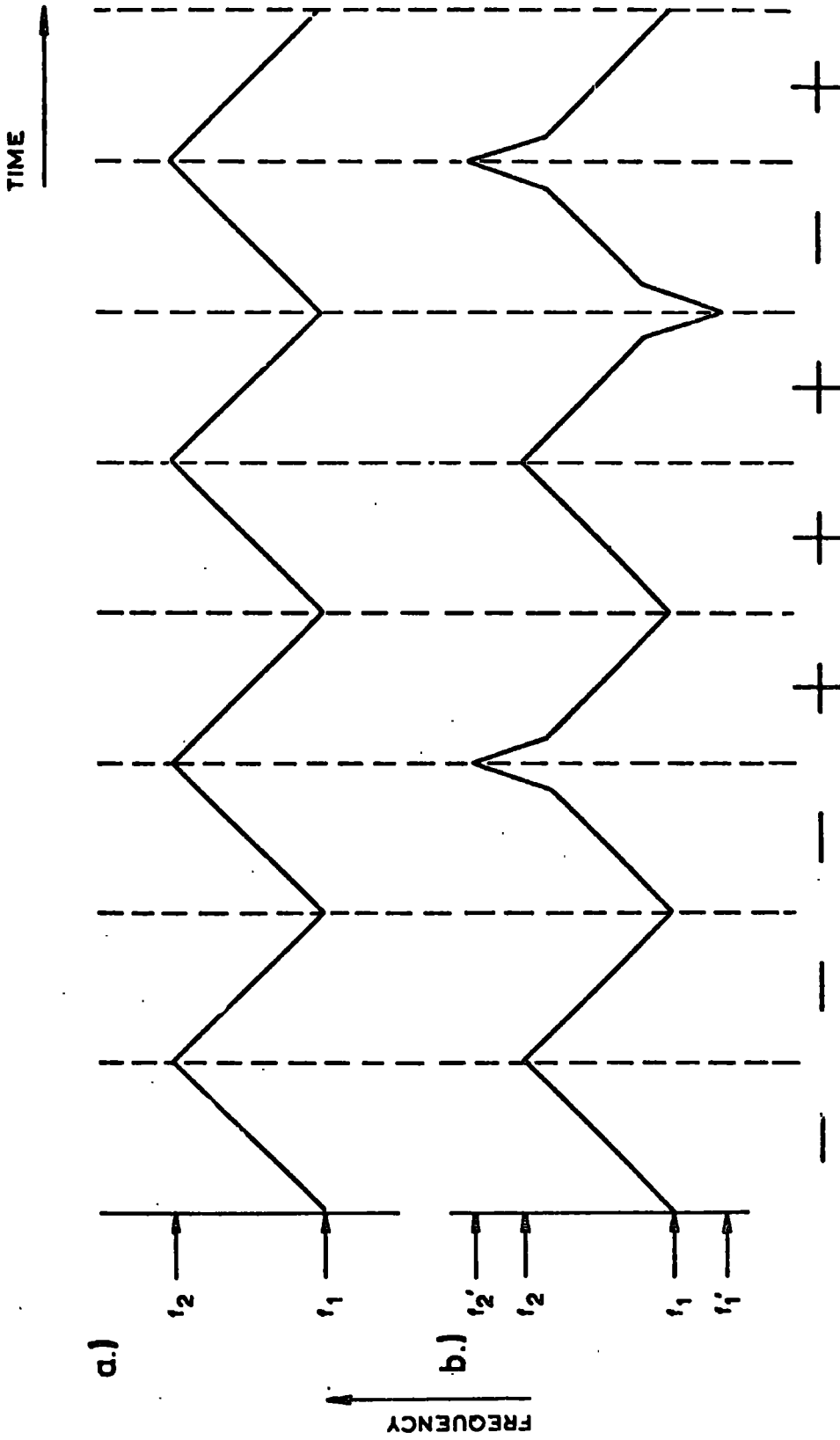


FIG.49 - TRANSITION ZONE A.



**FIG. 50 - FREQUENCY MODULATION OF COMPLEMENTARY CODED SWEEP SEQUENCE a.) WITHOUT AND b.) WITH TRANSITION ZONE A.**

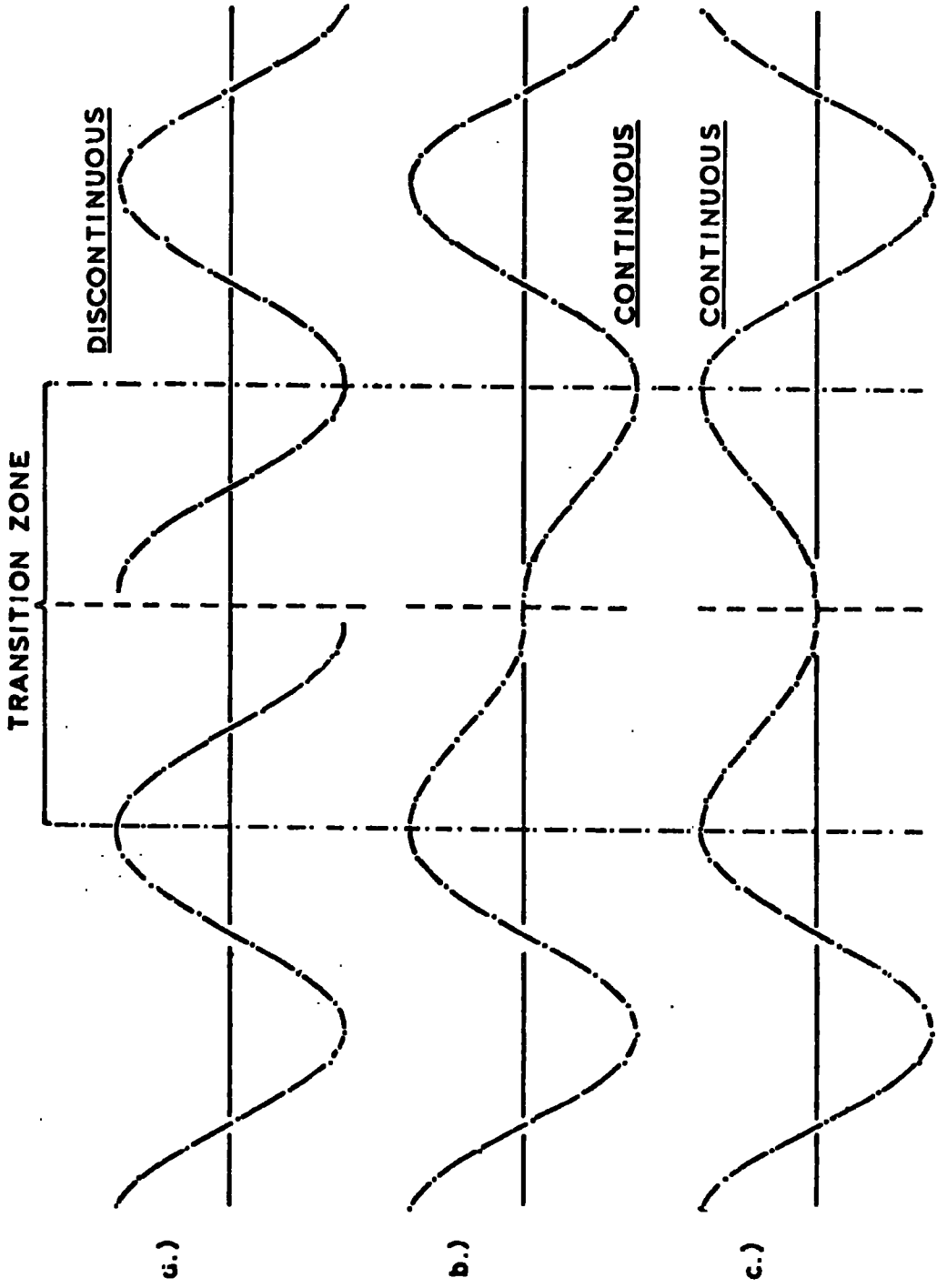


FIG. 51 - TRANSITION ZONE B.

cannot respond. This results in a selective number of sweep code members being distorted. Figure 47 A.) illustrates such a distortion as measured at the base plate of a vibrator. The bit equivalence rule is no longer fulfilled and the performance of the technique will be degraded.

Discontinuous bit change-over seems to affect mainly the complicated electronic "Phase Compensator" associated with each vibrator. The nominal values and actual values of the sweeps as fed back from an accelerometer on the base plate (see Figure 52), are compared and automatic adjustment is activated by the vibrator's electronic unit in order to eliminate phase shifts between the transmitted signal and the pilot signal received from the recording truck (WERNER et al (1975)). At the beginning of the sweep sequence the vibrators 'lock' onto the right phase after a very short time indeed and this deviation from the reference signal can be neglected. However, passing through a discontinuous transition zone it takes a relatively long time until the vibrators are back in phase with the pilot signal, generating an undefined waveform for the time the phase control is lost.

In Figures 47 A.) and 48 A.) the reference signal and the transmitted signal can be compared at two different positions in the coded sweep sequence. The trace of a near field geophone is also presented. Figures 47 A.) and 48 A.) show the vibrator response to a coded signal with a short cosine squared (pedestal height = 0.0) taper applied to both sides of its code members. It can be seen that the vibrators lose phase control and take a long time to lock onto the correct phase again. This is due firstly

(Redrawn from WERNER and TALKE (1975), PRAKLA-SEISMOS)

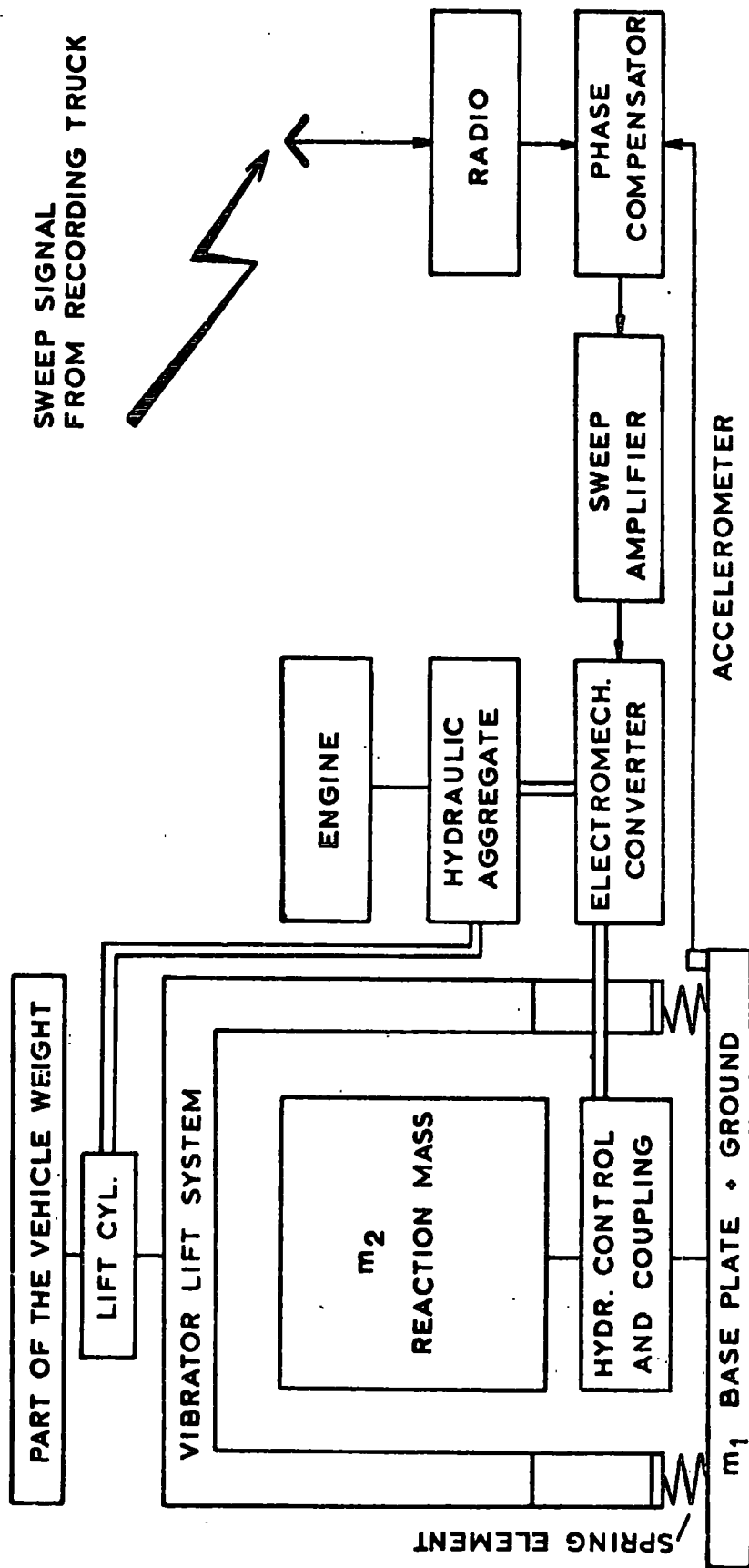


FIG. 52 - VIBRATOR PRINCIPLE

to discontinuous transition zones (as in Figure 47 A.) and secondly to the low amplitude of the pilot signal near the actual change-over point (as in Figure 48 A.), to which the vibrators are unable to respond.

It was concluded that the vibrators had to be provided with a continuous signal for the whole time of the transmission in order to avoid waveform distortions which would certainly introduce undesirable correlation noise at the processing stage.

In Figures 47 B.) and 48 B.) the coded signal has no longer any first order discontinuities due to the application of a so-called transition zone 'B', which will be discussed in more detail at a later stage. The vibrator shows a better response to this sweep sequence, partly because the taper applied has now a pedestal height of 10% of the maximum signal amplitude and allows the vibrator to pass through the change-over zone without losing much phase control.

Figures 49 and 51 show the two continuous transition zone solutions investigated. In Figure 50 one can see the frequency modulation function for one complementary coded sweep sequence without (Fig. 50a) and with (Fig. 50b) transition zone 'A' applied. Up- and downsweeps change from code member to code member starting with an up-sweep. In order to achieve a smooth continuous transition between the code members the beginning and/or the end of some sweeps had to be driven into lower or higher frequencies, respectively.

For example: The basic frequency range of a coded signal examined in the field tests was from  $f_1 = 16$  Hz to  $f_2 = 48$  Hz.

A number of code members was forced to sweep from 47.57 Hz to 65.0 Hz at the high frequency end and from 17.03 Hz down to 5.0 Hz at the low frequency side. Figure 49 shows the application of such a 'Frequency-Burst-Method' to the low frequency ends of two consecutive sweeps in the above mentioned test signal. This change of the sweep rate was only performed on  $3/4$  of the corresponding first and/or last full cycle of the code members concerned, in order to keep the distorted parts of the coded signal to a minimum.

It is easy to see from Figure 50 that the transition zone 'A' will only be applied to the discontinuous change-over positions, where the deviations from the reference signal are heaviest on transmission. In Figure 50 it is assumed that a + - or - + transition is discontinuous.

The use of solution 'A' produces a perfectly continuous coded Vibroseis input signal, but unfortunately the bit equivalence rule is not fulfilled. The error sidelobes for the particular code employed can be predicted to appear just 3 sec. away from the central detection peak, to give way to total sidelobe compensation after another 1.5 sec. The computer evaluation of the same complementary coded signals ( $n=8$ ) with transition zone 'A' confirms this fact, as can be seen in Figures 53 and 54. (Compare with Figures 32 and 33).

By means of code member tapering the degenerate effect of transition zone 'A' can be reduced. For a technical reason it was not possible to have long zero amplitude segments between the code members, because the vibrator could not respond to a

CODE USED: GOLAY SERIES n = 8 (Quaternary equivalent of

-- + + + + + -- + + + + + -- + + + + + -- + + + + + is used)

TRANSITION ZONE A.) AND NO TAPER APPLIED

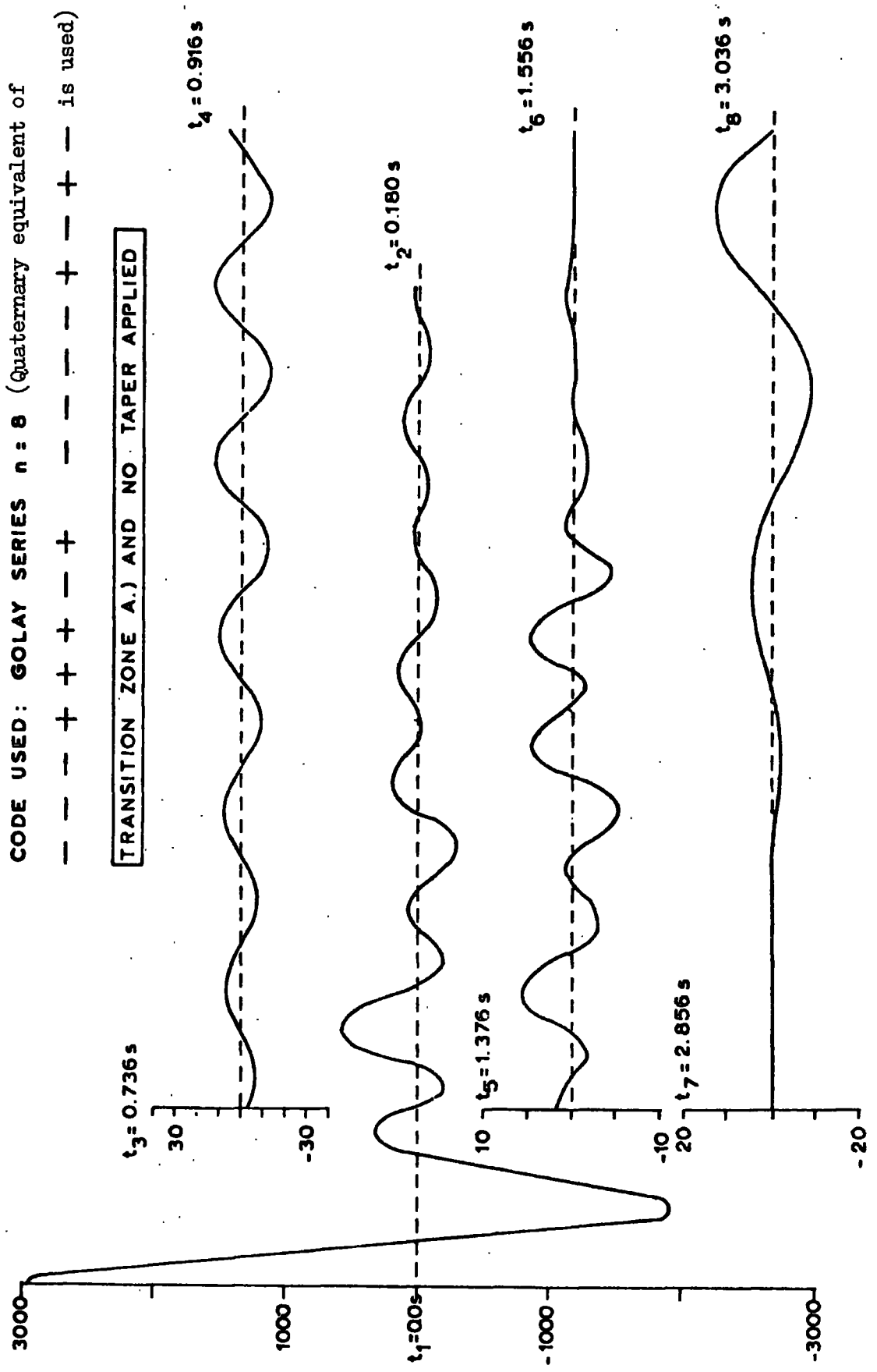


FIG. 53 - OUTPUT FUNCTION OF COMPLEMENTARY CODED VIBROSEIS SIGNALS  
(BASIC FREQUENCY RANGE: 16 - 48 Hz, SIGNAL DURATION 2 x 11.904 sec.)

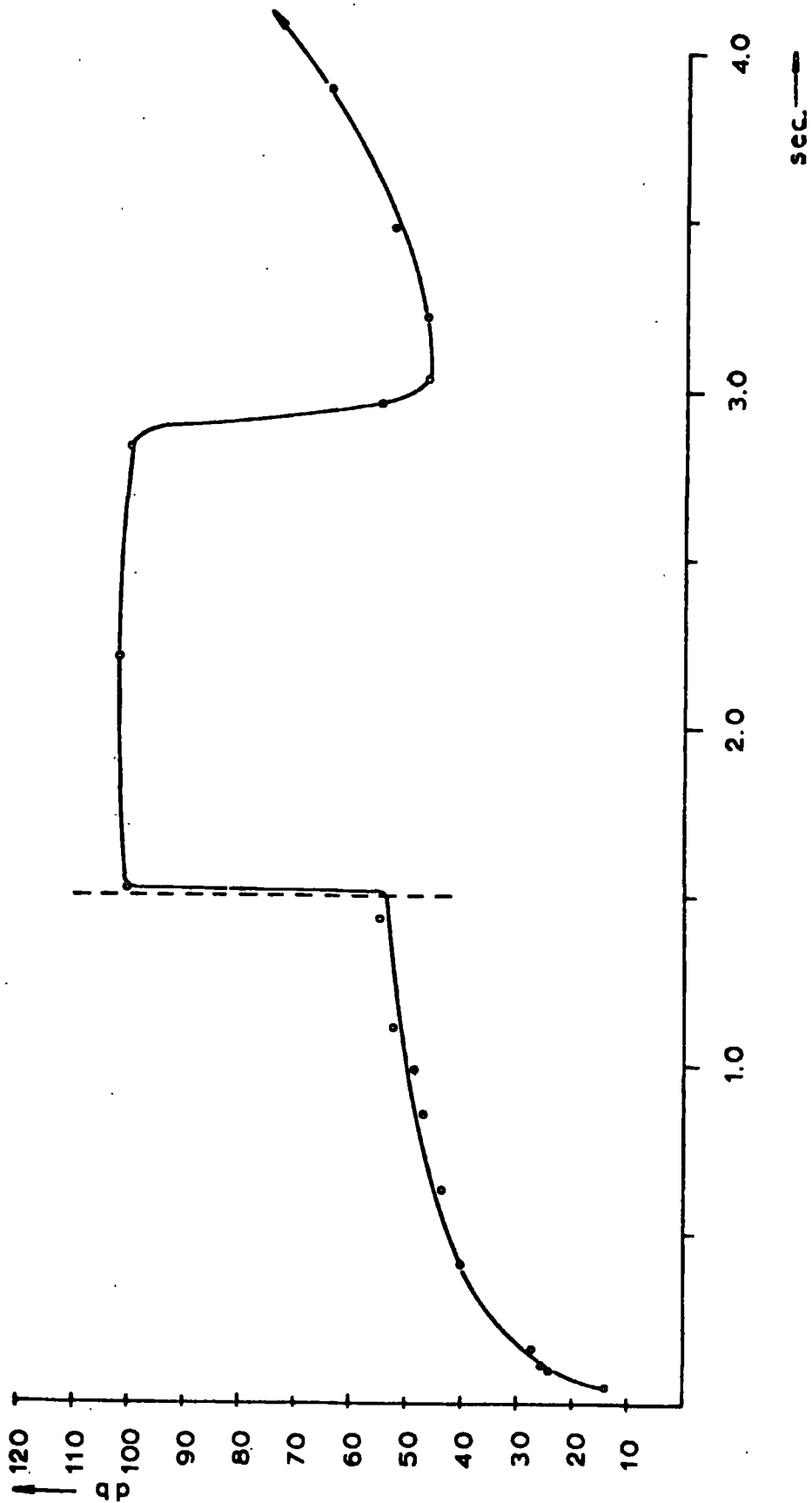


FIG.54 - "SIDELOBE SUPPRESSION versus TIME" - GRAPH  
( ... for output function shown in Figure 53 )

pilot signal which remained below a certain threshold amplitude for some time. Therefore, a taper with zero pedestal height had to be avoided. It was agreed to test the vibrator response to short duration tapers (116 ms) on both sides of all code members with different pedestal heights of 80%, 40%, 20% and 10% of the maximum signal amplitude. At the low frequency sides the taper lasted not much longer than the part of the sweeps affected by the transition zone. On comparison of Figures 55 and 56 with Figures 53 and 54 the reduction of the noise due to the introduction of the transition zone 'A' can clearly be seen. Naturally, the sidelobes to both sides of the centre peak are also reduced in amplitude.

It should be noted that the remaining sidelobes of the detected untapered coded sweep sequence with transition zone 'A' is also lower than the sidelobes in the output function of the complementary coded Vibroseis signal without any transition solution applied, as shown in Figures 32 and 33. The introduction of frequency bursts actually improves the signal-to-noise ratio in the detection window. The author will comment on this phenomenon in chapter 9.

Figure 51 (page 144) shows the transition zone 'B' applied again to the low frequency end of two 16 Hz - 48 Hz code members. Here a minor modification over only  $\frac{1}{2}$  a cycle of the leading and trailing edges of all alphabet members permits a smooth bit change-over. Basically, this transition represents an amplitude modulation of both ends of the sweeps used in the coded Vibroseis signal. The frequency range is

CODE USED : GOLAY SERIES n=8 (The quaternary equivalent of

-- + + + + + + -- -- -- + + + -- is used.)

TRANSITION ZONE A.) AND 10% TAPER APPLIED

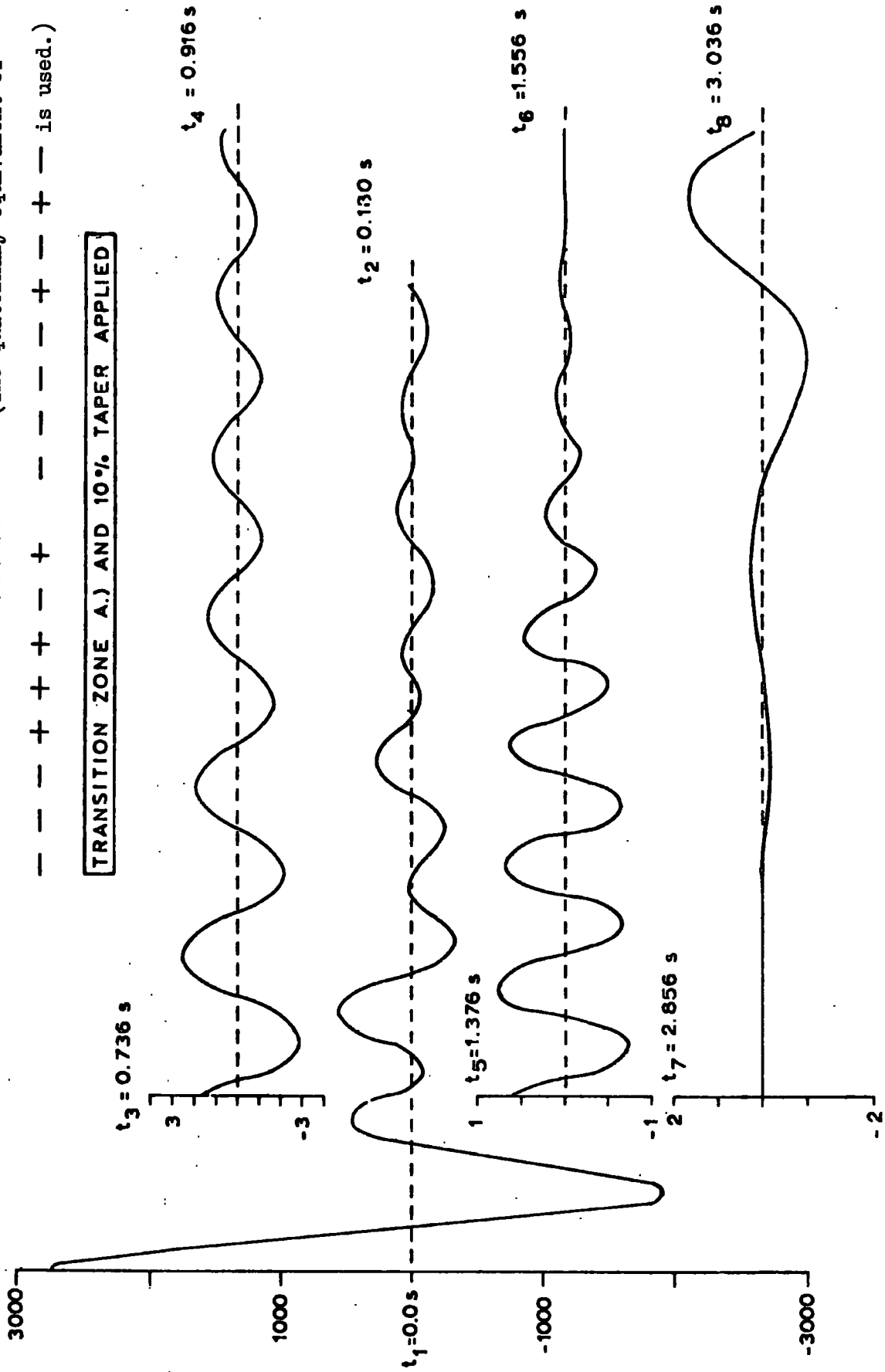


FIG. 55 - OUTPUT FUNCTION OF COMPLEMENTARY CODED VIBROSEIS SIGNALS  
(BASIC FREQUENCY RANGE: 16-48 Hz, SIGNAL DURATION: 2 x 11.904 sec.)

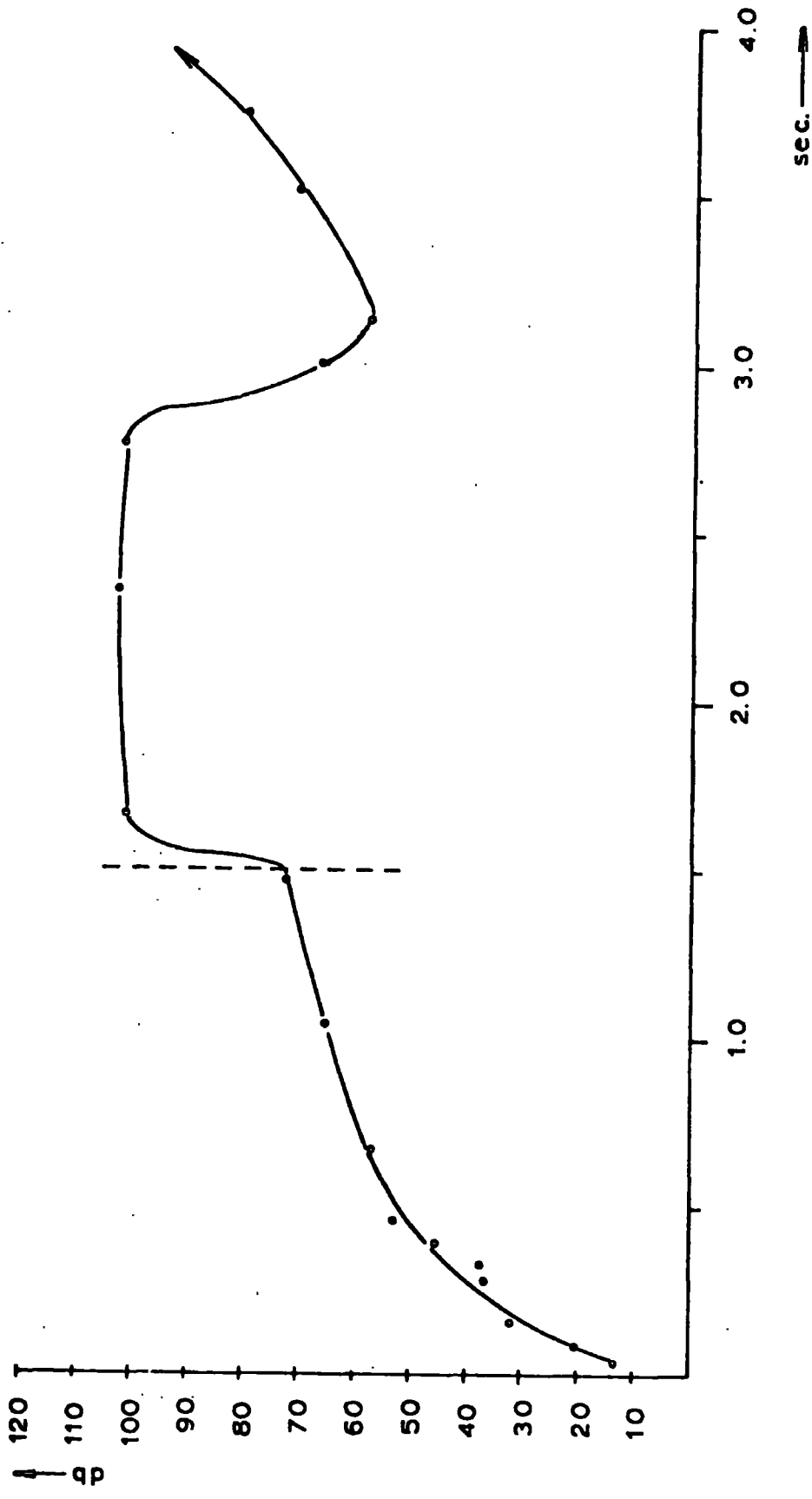


FIG. 56 - "SIDELOBE SUPPRESSION versus TIME"- GRAPH  
(... for the output function shown in Figure 55 )

unchanged. Initially, the sweeps have to be designed to start and end with the full amplitude (Figure 51a). As shown in Figure 51 for a low frequency transition zone, an amplitude modulation is applied only over  $\frac{1}{2}$  a cycle, slowing down the signal to a near zero amplitude. When performed on all code members this method will produce a continuous pilot signal. Two different continuous transition zones of type 'B' are shown in Figure 51 b and c.

The application of transition zone 'B' is in accordance with the bit equivalence rule, because this process is not selective within the coded signal duration. Therefore, there are no sidelobes outside the detection peak window as defined by the length of the code members and this can be seen in Figures 57 and 58.

However, even the minor amplitude modulation employed in solution 'B' has a negative affect on the autocorrelation functions of the sweep code members. This is reflected in the relatively high sidelobes which are hardly decreasing in amplitude throughout the detection window.

Figure 59 shows the spectra of a sweep code member without and with transition zone 'B' applied. The distortion due to the introduction of 'B' can clearly be seen, particularly towards the low frequency part of the spectrum. It is therefore not surprising to find an autocorrelation wavelet with a high sidelobe level.

Again, tapers with pedestal heights of 80%, 40%, 20% and 10% of the full signal amplitude were applied to all code

CODE USED: GOLAY SERIES  $n=8$  (The quaternary equivalent of  
- - + + + - - + - - - - + - - + - - is used.)

TRANSITION ZONE B.) AND NO TAPER APPLIED

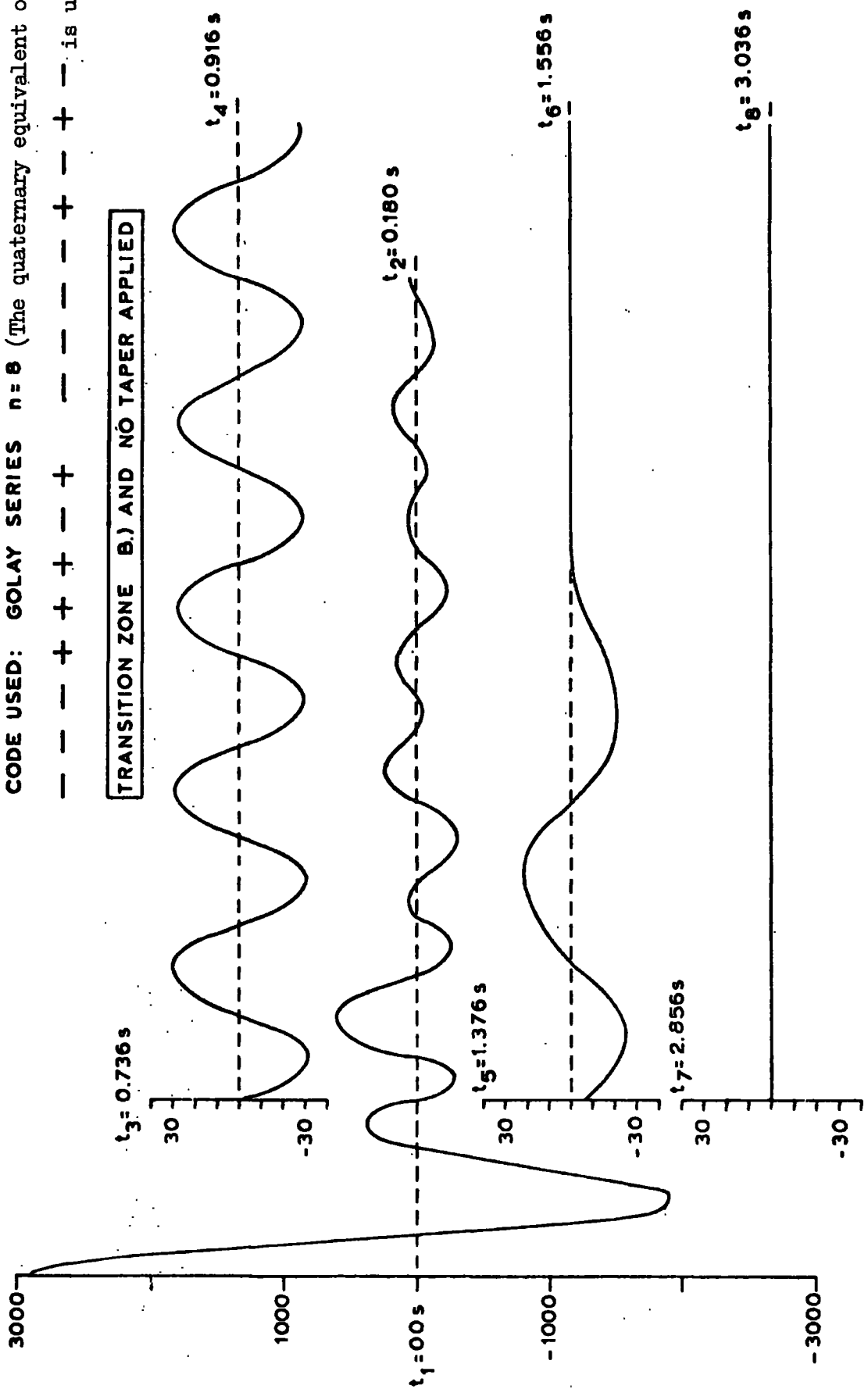


FIG. 57 - OUTPUT FUNCTION OF COMPLEMENTARY CODED VIBROSEIS SIGNALS  
(FREQUENCY RANGE: 16 - 48 Hz, SIGNAL DURATION: 2 x 11.904 sec.)

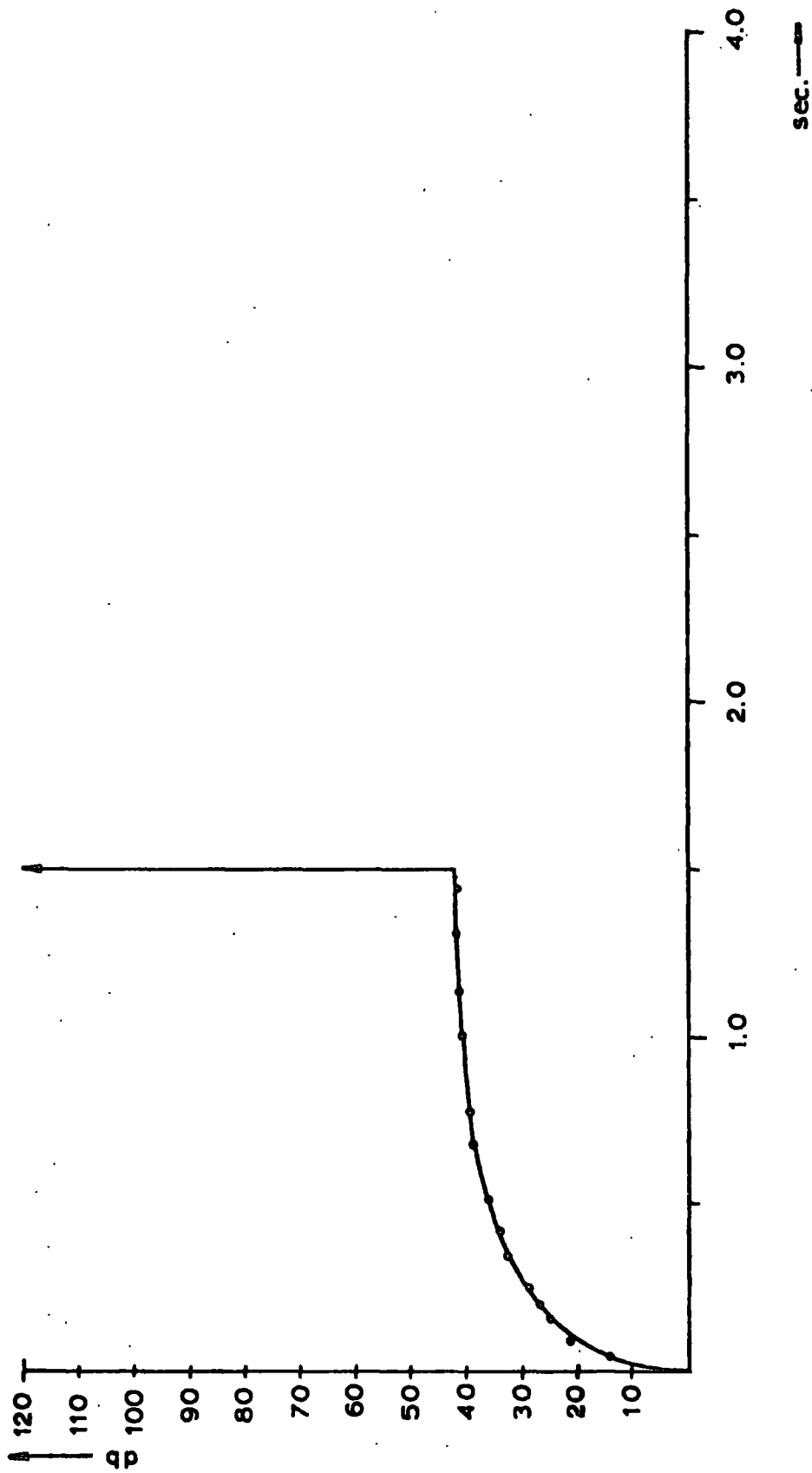


FIG. 58 - "SIDELOBE SUPPRESSION versus TIME" - GRAPH  
(...for the output function shown in Figure 57 )

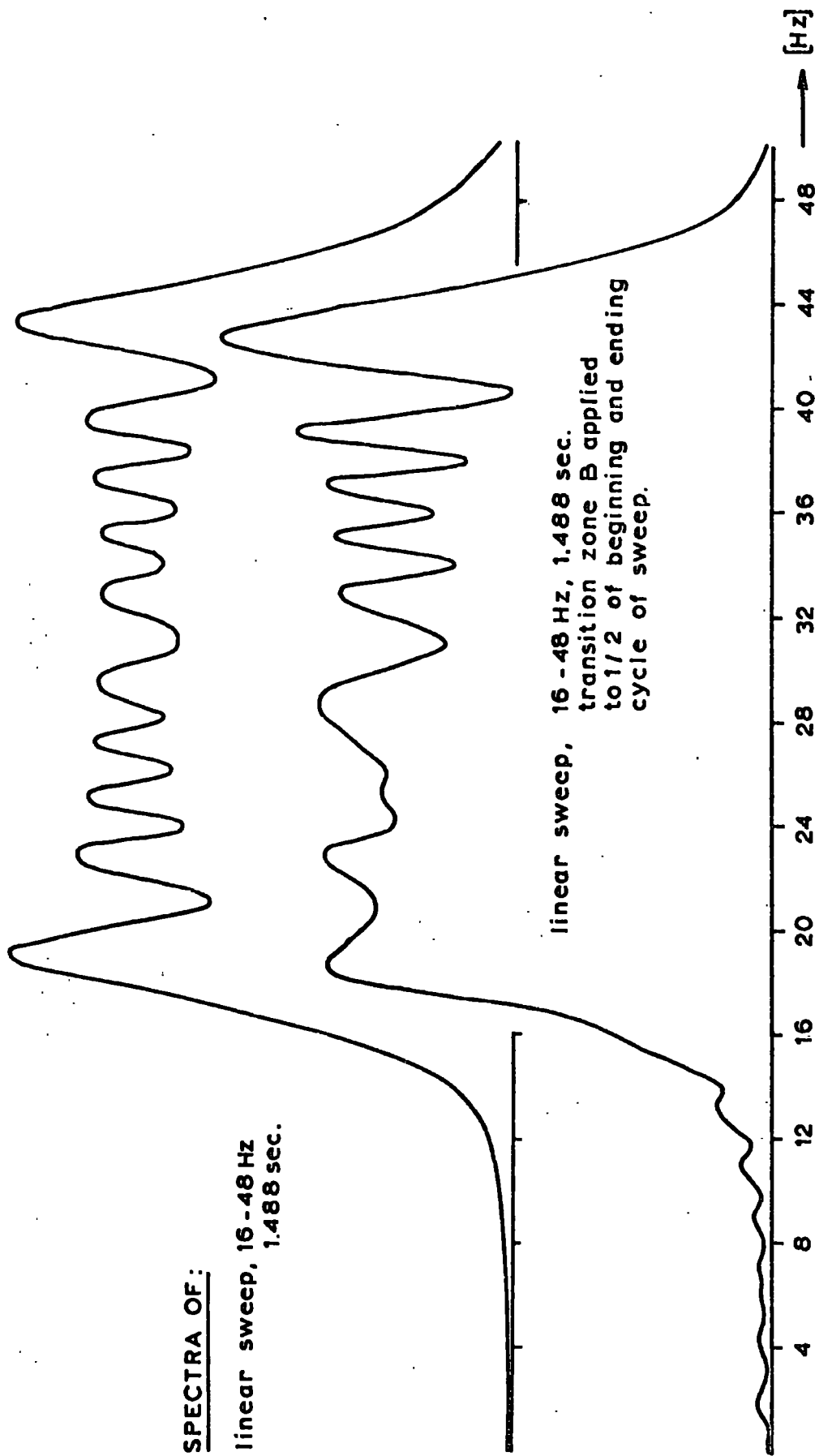


FIG. 59 SPECTRUM DISTORTION — TRANSITION ZONE B

members. The computer evaluations for a taper of 10% pedestal height is presented in Figures 60 and 61, clearly indicating the improvement achieved.

The vibrator's response to both transition zones and the different tapers has been investigated in a field test. Figures 62 and 63 show the fully processed one-sided crosscorrelation functions of the pilot signals with the corresponding outgoing signals as measured by the accelerometer on the base plate. The application of transition zone 'A' results, as forecasted, in disturbing noise about 3 sec. away from the centre peak (Fig. 63). Tapering yields an improvement. The detection peak window (about 1.5 sec. of the one-sided correlation function) is indicated in both Figures and shows clearly higher side-lobe levels when transition zone 'B' is employed (Fig. 62). However, the correlation noise is sharply reduced beyond 1.5 sec. for signals A, B and C in Figure 62, whilst the remaining sidelobes in the far-field of the results for signals D and E can be attributed to a different response of the vibrator to the two transitions possible when solution 'B' is applied (refer to Fig. 51b and c). Signal A in Figure 62 shows the best result with sidelobe reduction of approximately 70 db in the 3 sec. region. This is a better correlation noise attenuation than known from comparable conventional Vibroseis signals (EDELMAANN (1977/ Private Communication), KREY (1977)).

The described changes to the ideally coded Vibroseis waveform were necessary to adjust the signal to the specific characteristics of the vibrators used. Clearly, both transition zone solutions

CODE USED: GOLAY SERIES  $n = 8$  (The quaternary equivalent of

-- + + + + -- + + -- + + -- + + -- + + -- is used.)

TRANSITION ZONE B.) AND 10% TAPER APPLIED

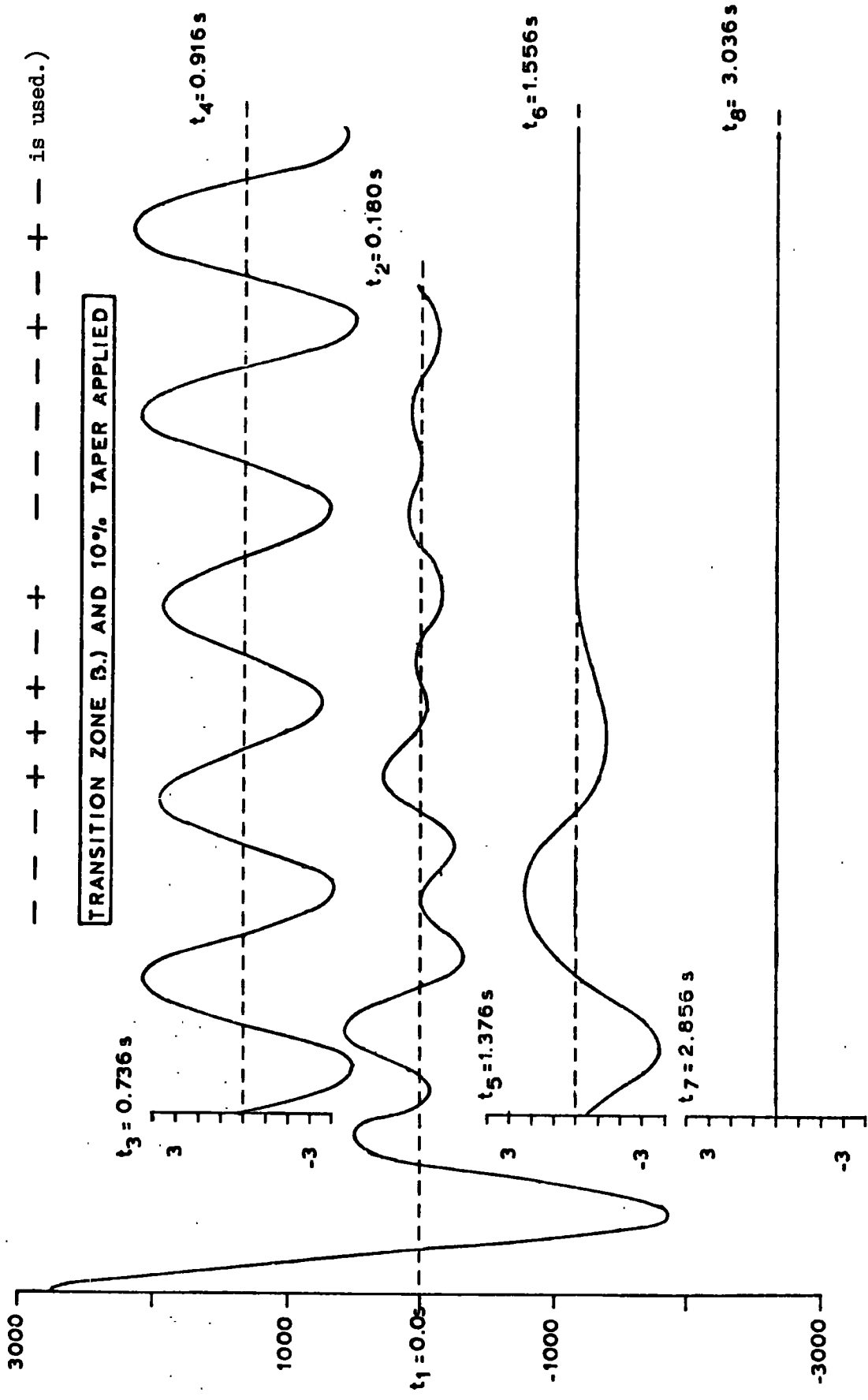


FIG. 60 - OUTPUT FUNCTION OF COMPLEMENTARY CODED VIBROSEIS SIGNALS  
(FREQUENCY RANGE: 16 - 48 Hz, SIGNAL DURATION: 2x11.904 sec.)

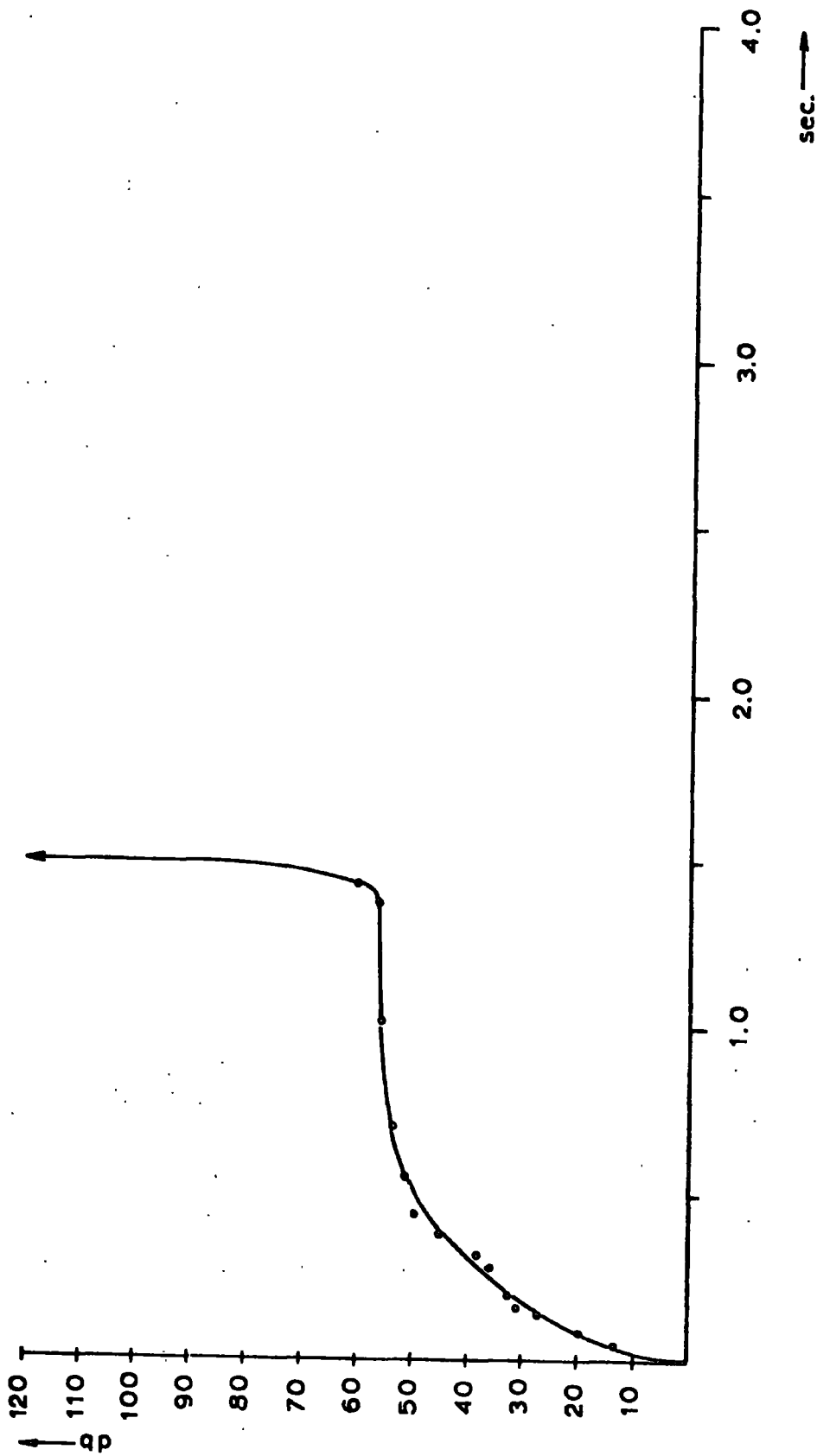


FIG.61 - "SIDELOBE SUPPRESSION versus TIME"- GRAPH  
( ...for the output function shown in Figure 60 )

Explanation and Key to Figures 62 and 63

The complementary signal pairs A to J (specified below) were used as pilot signals in field tests to evaluate the response of vibrators to the transition zones 'A' and 'B' with and without short time tapers of different pedestal height on all code members. The results of these tests are shown in Figs. 62 and 63.

The base plate accelerometer output was employed in the 'Complementary' processing as schematically indicated in Fig. 46. Figures 62 and 63 therefore show the fully processed one-sided cross-correlation functions of the ten reference signals A to J with their corresponding transmitted signals.

The quaternary equivalent to Golay's series n=8 (- - - + + + - +; - - - + - - + -) is used for the following coded Vibroseis signals.

The basic frequency range for all code members is 16 Hz to 48 Hz.

A - Transition zone 'B' applied; pedestal height of code member taper = 10% of max. input signal amplitude; code member duration = 1.488 sec.

B - as A, but 20% pedestal height,

C - as A, but 40% pedestal height,

D - as A, but 80% pedestal height,

E - as A, but no tapering.

F - Transition zone 'A' applied; other readings as for A,

G - as F, but 20% pedestal height,

H - as F, but 40% pedestal height,

I - as F, but 80% pedestal height,

J - as F, but no tapering.

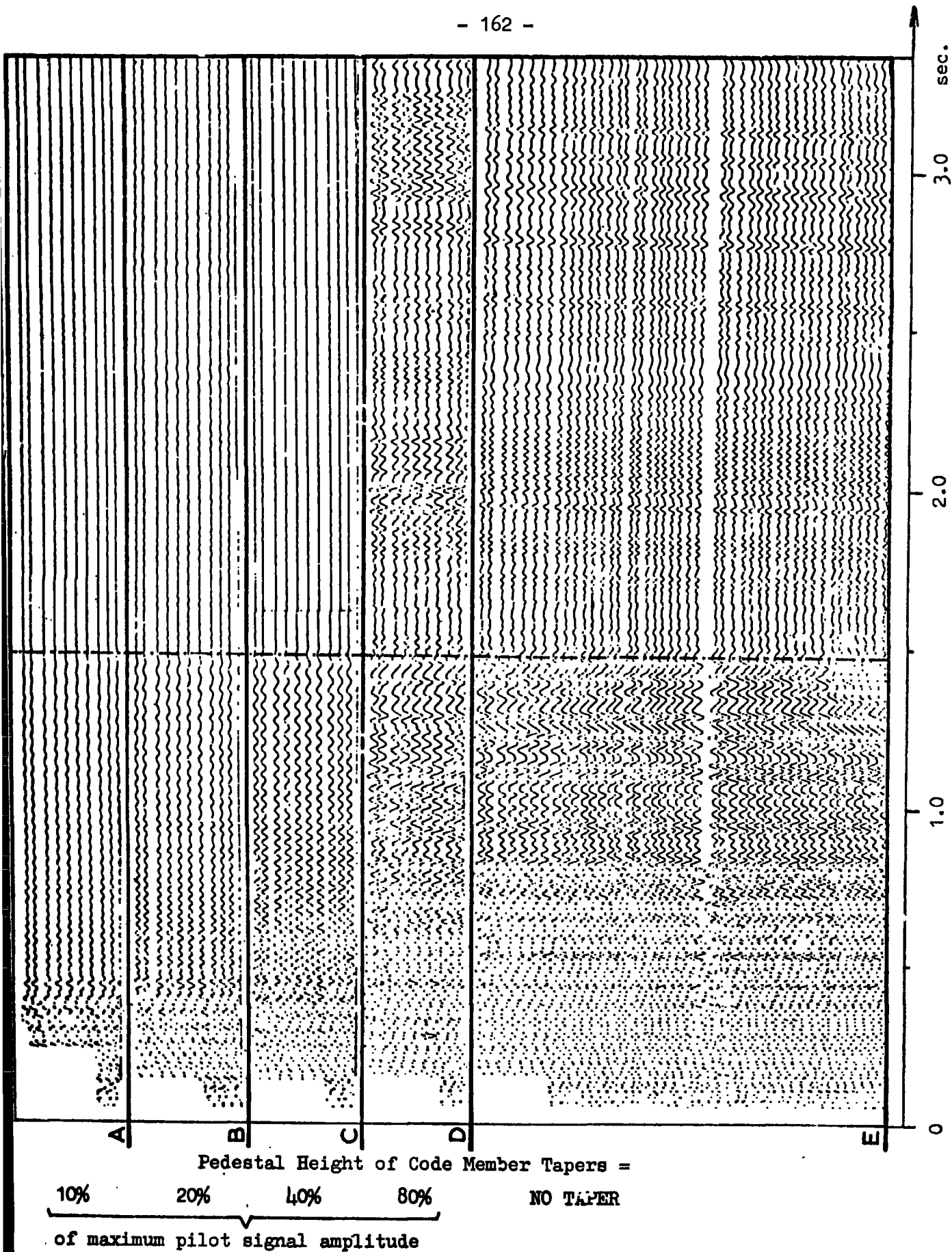


FIG. 62 - ONE-SIDED CROSSCORRELATION FUNCTIONS (PILOT SIGNAL/ACCELEROMETER OUTPUT)  
TRANSITION ZONE 'B' USED

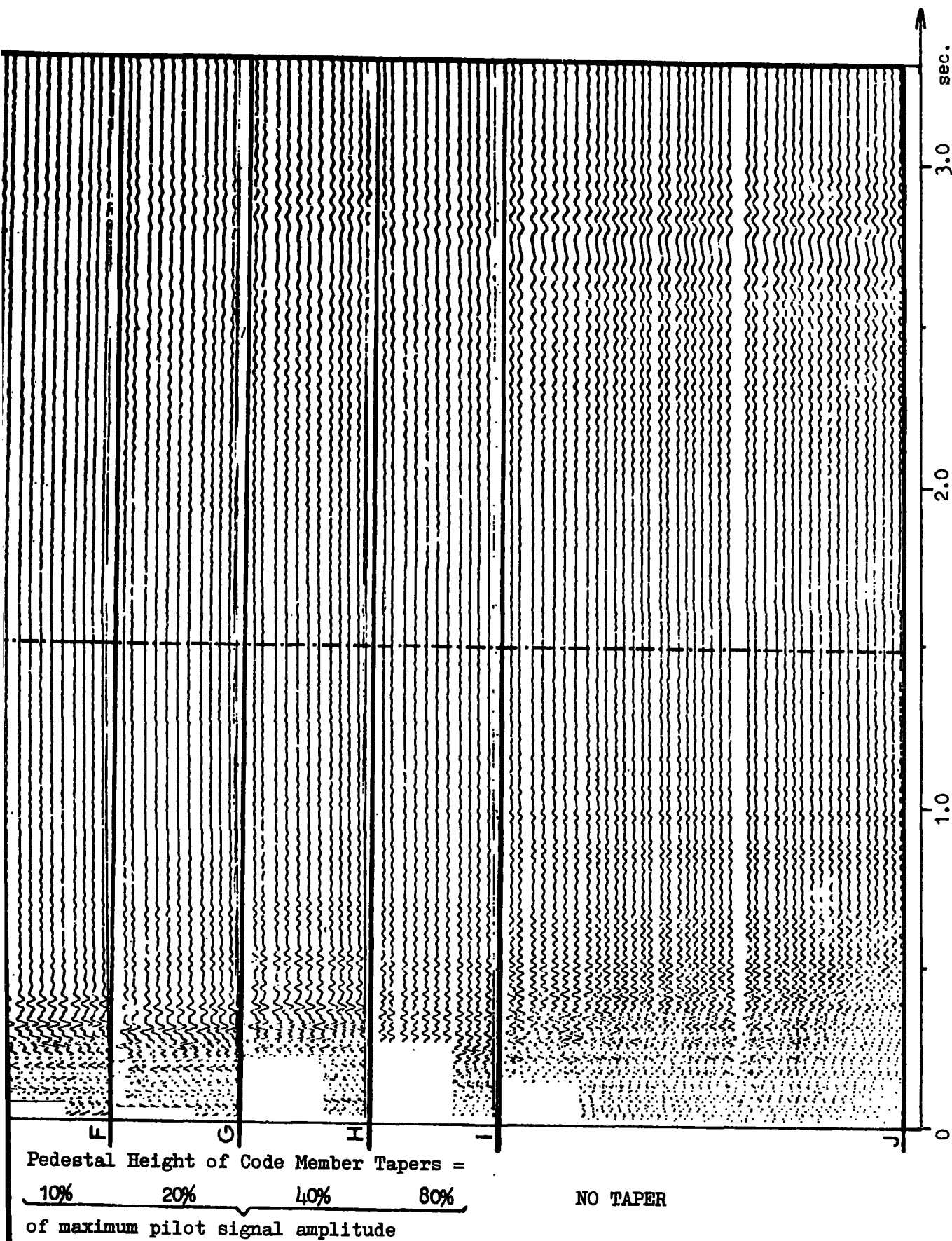


FIG. 63 - ONE-SIDED CROSSCORRELATION FUNCTIONS (PILOT SIGNAL/ACCELLEROMETER OUTPUT)  
TRANSITION ZONE 'A' USED

have a degenerate effect at the processing stage, either by creating correlation noise in the far-field of the correlogram or by increasing the sidelobes in the detection window.

The introduction of equally long pauses (or zero elements) between all code members in the pair of complementary coded sweep sequences does not affect the complementary property of the signals. In principle, it is best to transmit a number of time separated code members. After each sweep the vibrator comes to a standstill for a predetermined length of time before the start of the subsequent signal bit. It is expected that such a transmission mode permits an almost perfect sidelobe compensation, provided that the distortion effects, during the time the phase compensator tries to lock onto the correct phase of each sweep, are identical.

Unfortunately, the implementation of complementary coded Vibroseis signals with time separated code members is not possible without considerable alterations of the hardware and software of the used computerized vibrator system. E.g. it would be desirable to expand the recording loop of max. 32 sec., in order to avoid a further shortening of the code members (...or the listening period) due to the introduction of the inter-sweep pauses.

The time consuming and expensive hard- and software changes to the vibrator system could not be undertaken during the period of this study, because the Vibroseis crew employed for the coding tests was engaged in contract work for Prakla-Seismos for most of the time.

#### 8.4. Summary

The field tests of the Vibroseis encoding technique revealed that the coded sweep sequences contain a few changeovers between consecutive code members, which present the vibrator with first order discontinuities to which it cannot respond. The result is a distorted input signal, creating correlation noise where it should eliminate it.

Two continuous transition zones were suggested and tested. Zone 'A' employs frequency bursts at selected changeover positions, reducing the sidelobes in the detection peak window, but also generating noise in predeterminable regions of the correlogram.

Application of zone 'B' (...an amplitude modulation) on all code members preserves the complementary property. However, the sidelobe level after processing has increased due to the sweep distortions. Generally, tapering of all alphabet members improves the output waveform. A coded Vibroseis signal with transition zone 'B' and a short cosine-squared taper with 10% pedestal height, has been found to show better results than a comparable conventional sweep.

The coded sweep sequences with continuous transition zones became necessary because of the characteristics of the vibrators used. In principle, the easiest solution to discontinuous sweep sequences is to bring the vibrators to a standstill before commencing the transmission of the subsequent code member.

## CHAPTER 9

### PREDISTORTION AND ITS APPLICATION TO VIBROSEIS AND THE VIBROSEIS ENCODING TECHNIQUE

#### 9.1. Introduction

In the last chapter frequency bursts at one end or the other of the code members were used to overcome the problems associated with discontinuous transition zones in the coded sweep sequences. This method provided a perfectly continuous waveform for the whole of the transmission, but unfortunately, was responsible for the generation of disturbing noise a certain distance away from the centre Klauder wavelet, because the bit equivalence was destroyed. However, it was found that the introduction of frequency bursts also reduced the sidelobes near the main peak after processing and this can be seen quite clearly on comparison of Figure 32 and Figure 53.

This method of suddenly increasing or decreasing the frequency at the ends of a linear FM signal had already been investigated in its own right by COOK et al (1964) as a means of sidelobe reduction for the use in high power radar. Because the frequency modulation function of the sweeps is distorted before transmission the term 'Predistorted Sweeps' had been chosen for such FM signals.

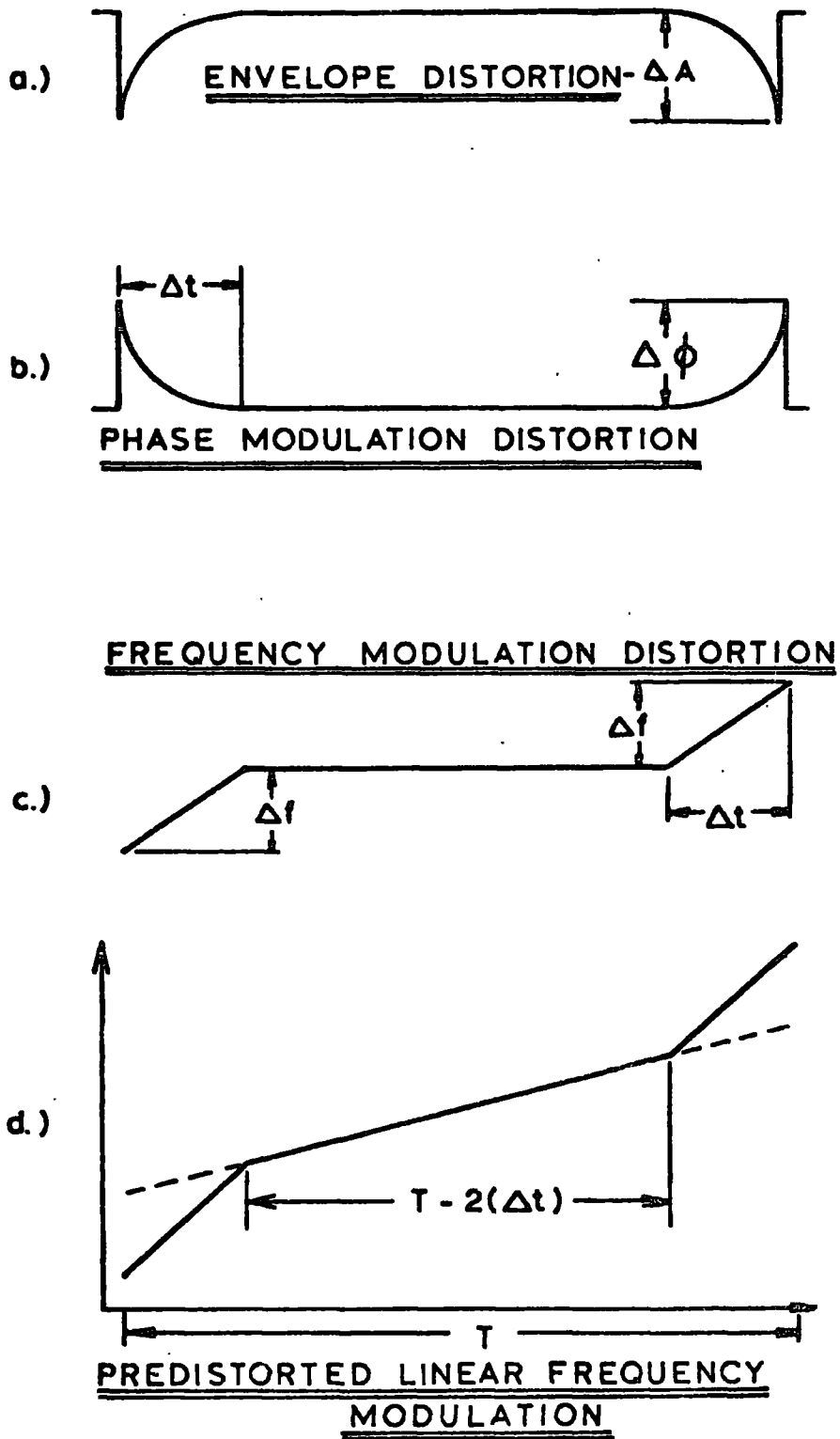
Evaluative studies on predistorted Vibroseis input signals confirmed Cook's findings and also revealed a new property, which could be of great use in an encoded Vibroseis system or in connection with a recently introduced Vibroseis method named 'Combi Sweeps' (KREY, WERNER (1977)).

First let us examine the basic principles of predistortion and the combi sweep method.

## 9.2. Predistortion

It was outlined previously that the deviation of the sweep's amplitude spectrum from the ideal rectangular shape introduces additional spectrum-associated sidelobes. An improvement of the signal-to-correlation noise ratio can be achieved if one succeeds in reducing the Fresnel ripples in the spectrum. Slowing down the fall and rise time of the signal envelope, i.e. tapering both ends of a sweep, has proved to be quite successful theoretically. In their paper Cook and Paolillo argue, that amplitude and phase distortions have functional similarity and produce similar effects on time waveforms provided that the distortions are small (COOK et al (1964)). Therefore, a phase modulation distortion as seen in Figure 64(b) should also reduce sidelobes, i.e. reduce the Fresnel ripples which are due to the sharp cut-off in amplitude of the sweep. Obviously, the frequency distortion modulation function is the derivative of the phase distortion modulation function (see Figure 64(c)). If this distortion function is used on a linear upsweep, for example, the predistorted linear frequency modulation function in Figure 64(d) results. This function is monotonic, because frequency modulations with slope reversals generally exhibit enhanced spectrum ripples.

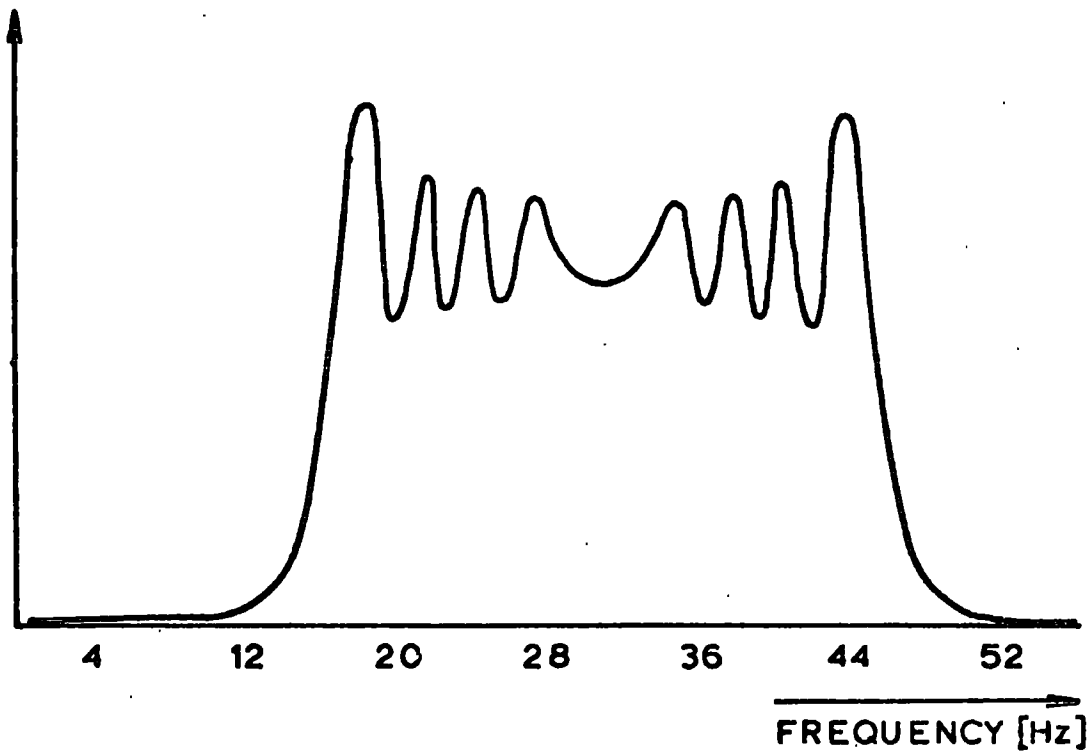
For the successful application of this sidelobe reduction method, the right choice of the predistortion parameters  $\Delta f$  and  $\Delta t$  is essential. An analytical determination of  $\Delta f$  and  $\Delta t$  is extremely complex. Even though a quantitative estimation of the parameters can be obtained from a paired-echo analysis, Cook et al preferred to present mainly experimental results using radar signals. For good



(AFTER COOK, PAOLILLO (1964))

FIG.64 PREDISTORTION

SPECTRUM OF LINEAR SWEEP, 2 sec.  
16 - 48 Hz



SPECTRUM OF PREDISTORTED SWEEP, 2 sec. ,  
5.728 - 17.728 - 46.272 - 58.272 Hz  
 $\Delta f = 12 \text{ Hz}$  ,  $\Delta t = 108 \text{ sec}$ .

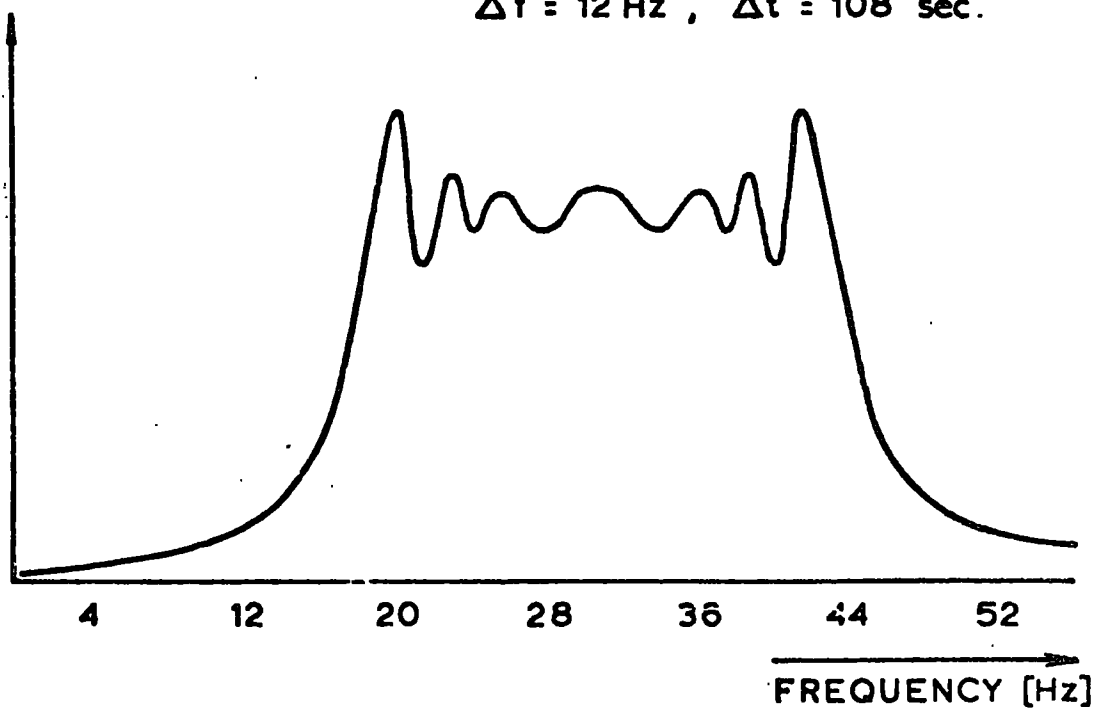


FIG. 65 -

SPECTRA

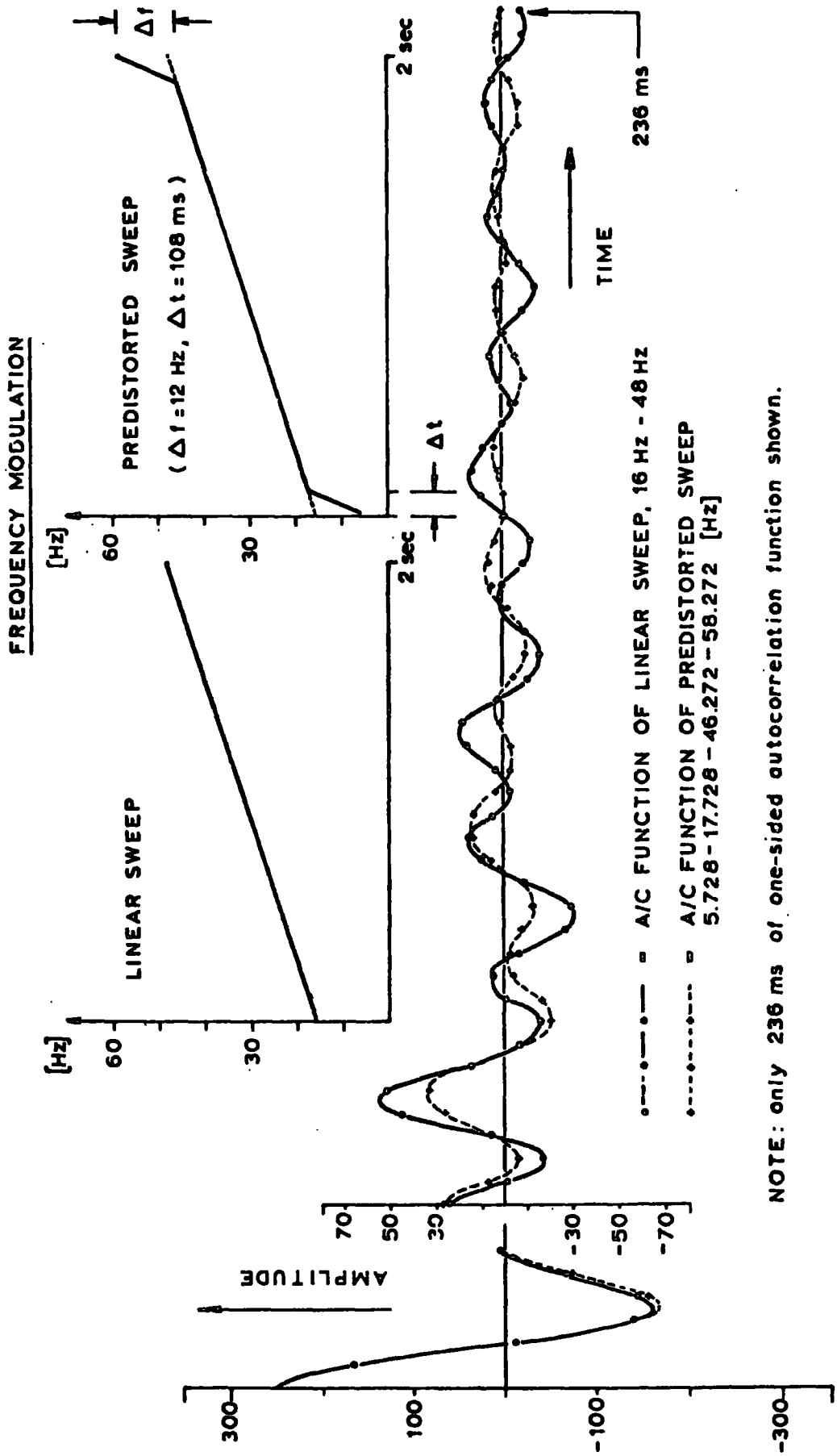


FIG. 66 - LINEAR SWEEP -- PREDISTORTED SWEEP

results the following ranges of parameters were suggested,

if  $D = 40 - 60$ .

$$\Delta f = 0.4 \cdot d \text{ to } 0.65 \cdot d$$

$$\Delta t = 0.8/d \text{ to } 1.20/d$$

where  $d = f_2 - f_1$ .

In Figure 65 the spectrum of a normal linear Vibroseis signal, 16 Hz - 48 Hz, 2 sec. duration and an equivalent predistorted sweep with parameters  $\Delta t = 108$  ms and  $\Delta f = 12$  Hz can be compared. The Fresnel ripples in the spectrum of the predistorted sweep are much smaller and also the rate of fall-off of the spectrum skirts has decreased. Figure 66 shows the associated frequency modulation functions and the one-sided autocorrelation functions in great detail. For reasons of space and clarity, the one-sided function is only plotted for 236 ms.

### 9.3. The Combi-Sweep Method

Combi sweeps are a new contribution to sweep techniques introduced by KREY and WERNER (1977) at the EAEG - Meeting in Zagreb. In this method advantage is taken of computerized recording instruments. A combi sweep consists of two or more conventional sweeps with a certain length of zero-elements, which represent the listening period or actual recording time, between each signal pair and after the last sweep. (This is similar to the complementary Vibroseis encoding implementation described in chapter 8). The length of the zero-elements has to be adjusted to the expected or desired reflection travel time and the maximum acquisition period of the complete computerized system has also to be taken into consideration in the combi sweep design.

On processing, the combi sweep is considered to be one signal and essentially correlation of the number of used conventional sweeps and stacking of the result takes place at the same time (...refer to Figure 46).

It is true, that the same result could be achieved by means of the conventional Vibroseis data acquisition method, but such a process of repeated signal transmission, recording and stacking would be very time consuming and not economical.

There are various applications for the combi sweep. For example, a combi sweep consisting of two or more sweeps, not comprising a 50 Hz component (e.g. 10 Hz - 25 Hz, 20 Hz - 48 Hz, 52 Hz - 70 Hz) can be successfully employed in areas with powerline interference, because the correlation process will combat this monofrequency noise.

An improvement of the sidelobe level can also be achieved by means of a combi sweep implementation as shown in Figure 67. The three sweeps used have a pyramid like ideal spectrum. The real spectrum is shown in the lower right hand corner of Figure 67 and indicates that this combi sweep arrangement essentially amounts to frequency weighting, which is reflected in the Klauder wavelet with its low sidelobes. Compared with the unweighted conventional Vibroseis system (see top of Figure 67) the penalty one has to pay is once more an increase in the sidelobes nearest to the centre.

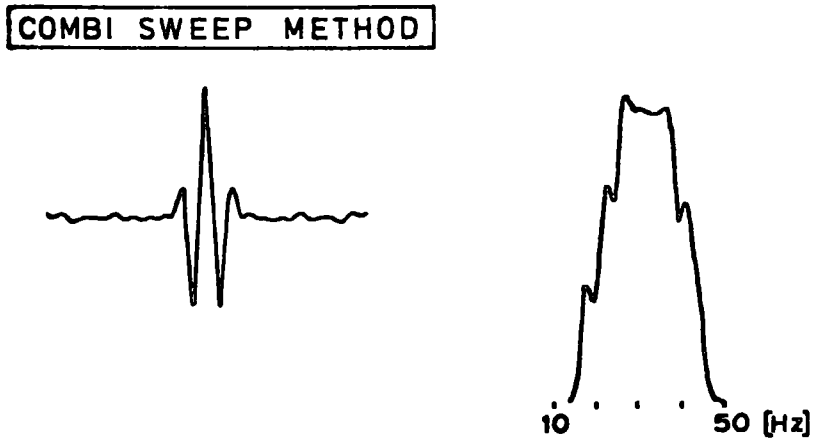
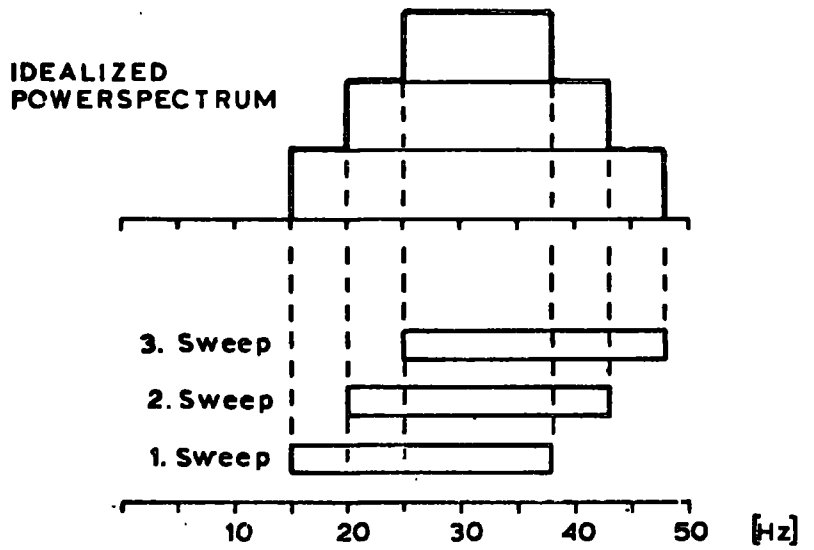
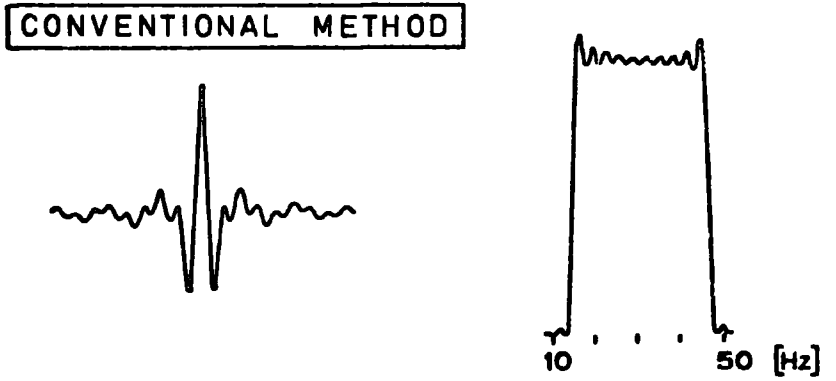
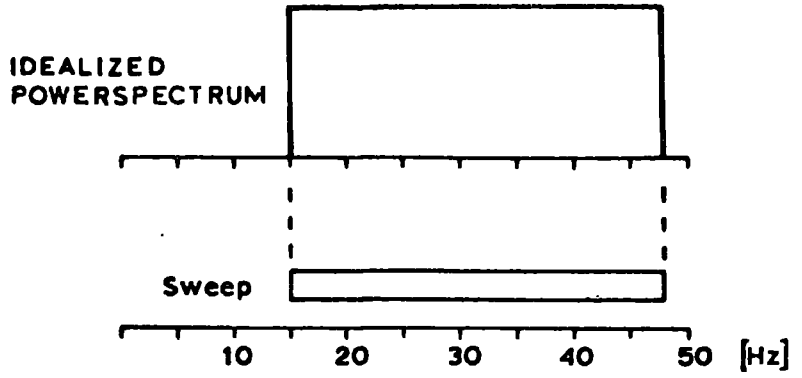


FIG. 67

#### 9.4. New 'Predistortion' - Analysis

During the studies of predistorted sweeps, a new property was discovered which makes these FM signals particularly interesting for the combi sweep method and what could be named a "Predistortion-Complementary Vibroseis Encoding Technique".

In Figure 68 four one-sided autocorrelation functions of one linear sweep (16 Hz - 48 Hz; 2 sec. long) and three different predistorted signals derived thereof, can be seen.  $\Delta f = 12$  Hz was found to be a reasonable predistortion parameter, ignoring the fact that  $\Delta f$  is not quite in the range of values given by Cook et al, but keeping a future practical application in mind.  $\Delta t$  has been varied from 80 ms to 200 ms. For  $\Delta f = 12$  Hz,  $\Delta t$  can be chosen from a much wider range than indicated by Cook et al, without considerably affecting the sidelobe reduction property. A  $\Delta t$  of only 37.5 ms ( $d = 32$  Hz;  $\Delta t = 1.2/32$  Hz = 37.5 ms) might render possible better sidelobe suppression results, but also yields too steep a gradient in the predistortion region of the frequency modulation function to be practically realizable with the relatively inert vibrators used.

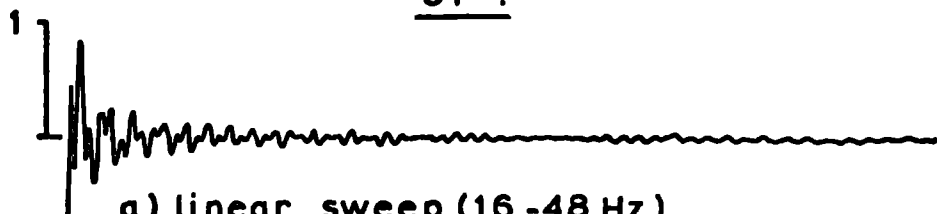
As expected, the autocorrelation function of the linear sweep shows the highest sidelobes throughout the function. All predistorted signals possess a better autocorrelation function, with the sidelobes for  $\Delta t = 200$  ms behaving best (... in a seismic sense!). Two stacks were performed (with adjusted amplitude scale) showing an interesting further improvement.

Figure 69 and Figure 70 show the corresponding spectra for all sweeps or autocorrelations involved. In both Figures it becomes clear that the used signals have spectra of complementary character

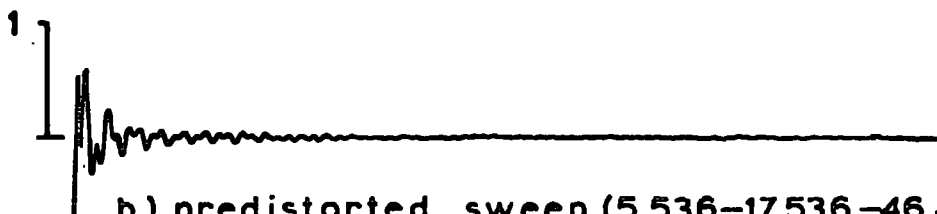
ONE-SIDED A/C FUNCTION (without centre peak)

OF :

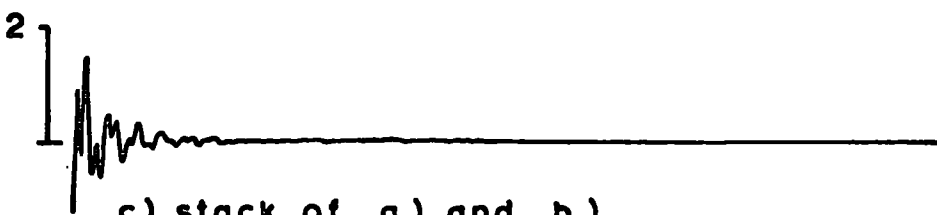
Related to spectra shown in Fig. 69



a.) linear sweep (16 -48 Hz)



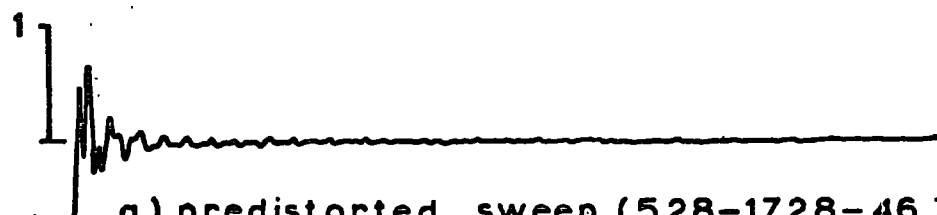
b.) predistorted sweep (5.536-17.536-46.464-58.464 Hz),  $\Delta f = 12$  Hz,  $\Delta t = 96$  ms



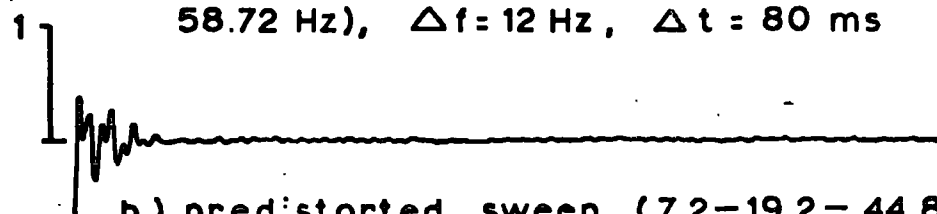
c.) stack of a.) and b.)

-----

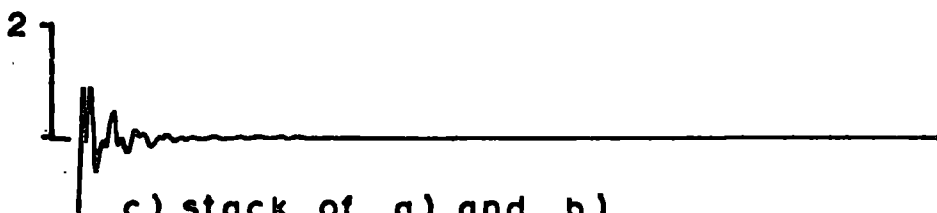
Related to spectra shown in Fig.70



a.) predistorted sweep (5.28-17.28-46.72-58.72 Hz),  $\Delta f = 12$  Hz,  $\Delta t = 80$  ms



b.) predistorted sweep (7.2-19.2-44.8-56.8 Hz),  $\Delta f = 12$  Hz,  $\Delta t = 200$  ms



c.) stack of a.) and b.)

FIG.68

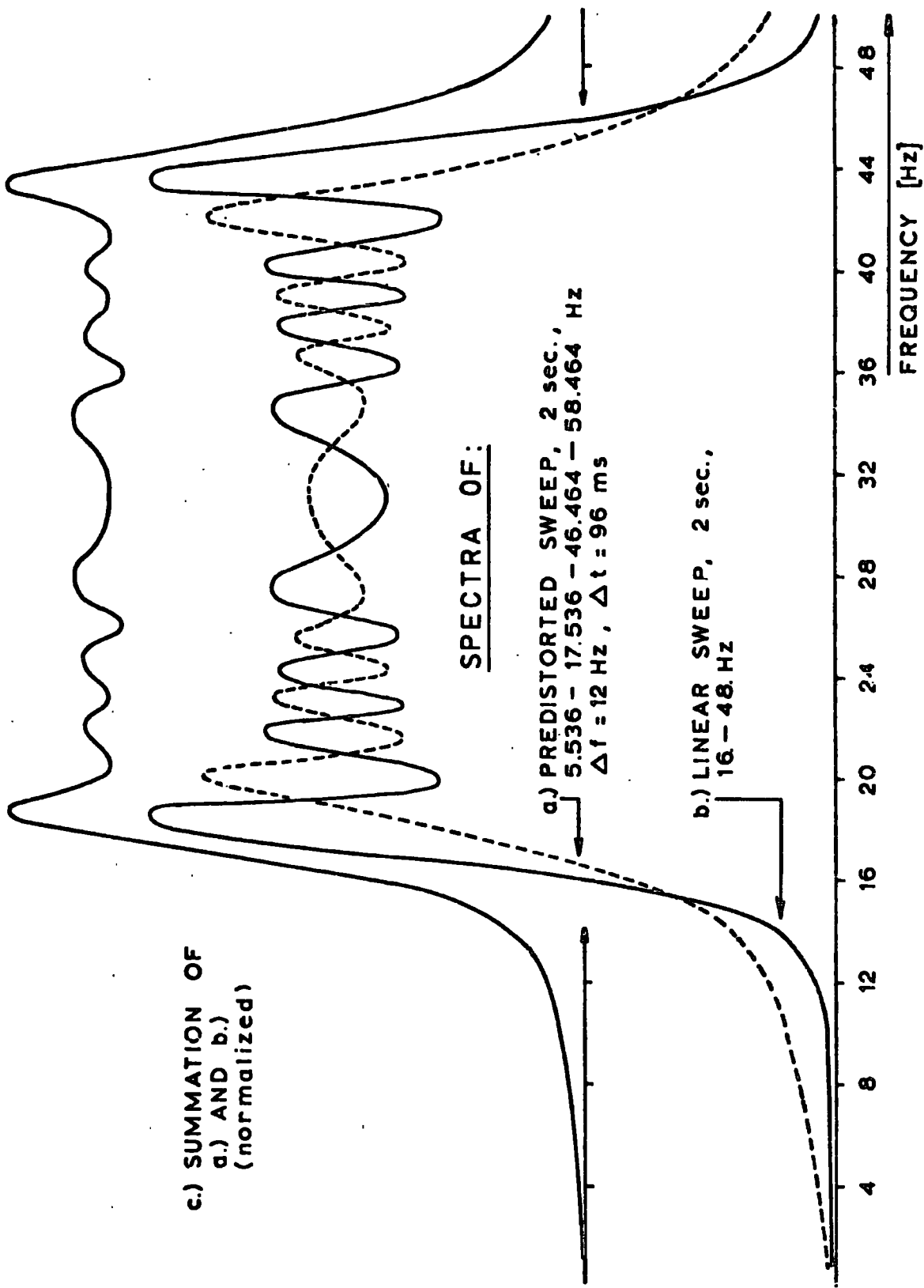


FIG. 69 - SPECTRUM WHITENING

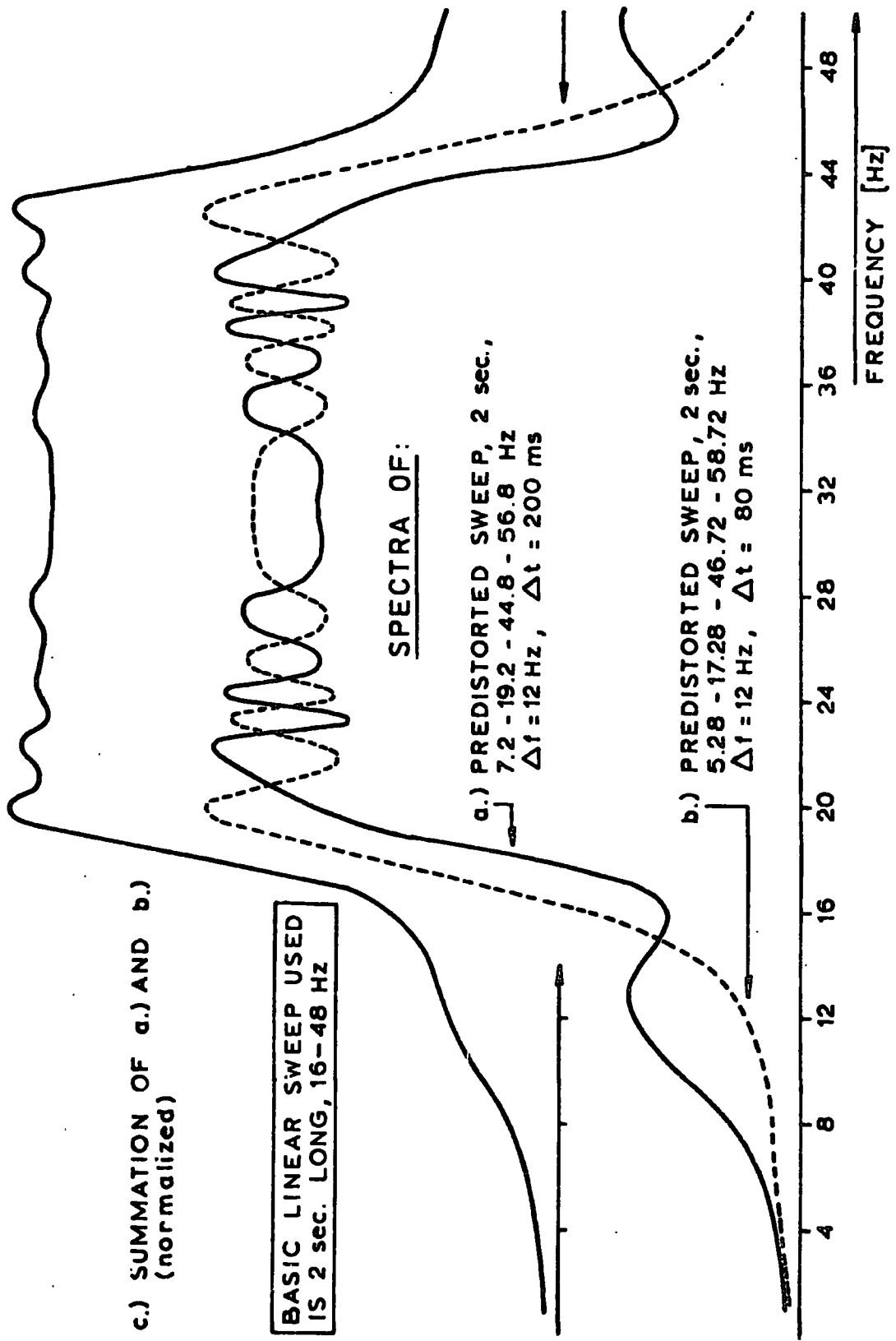


FIG. 70 — SPECTRUM WHITENING

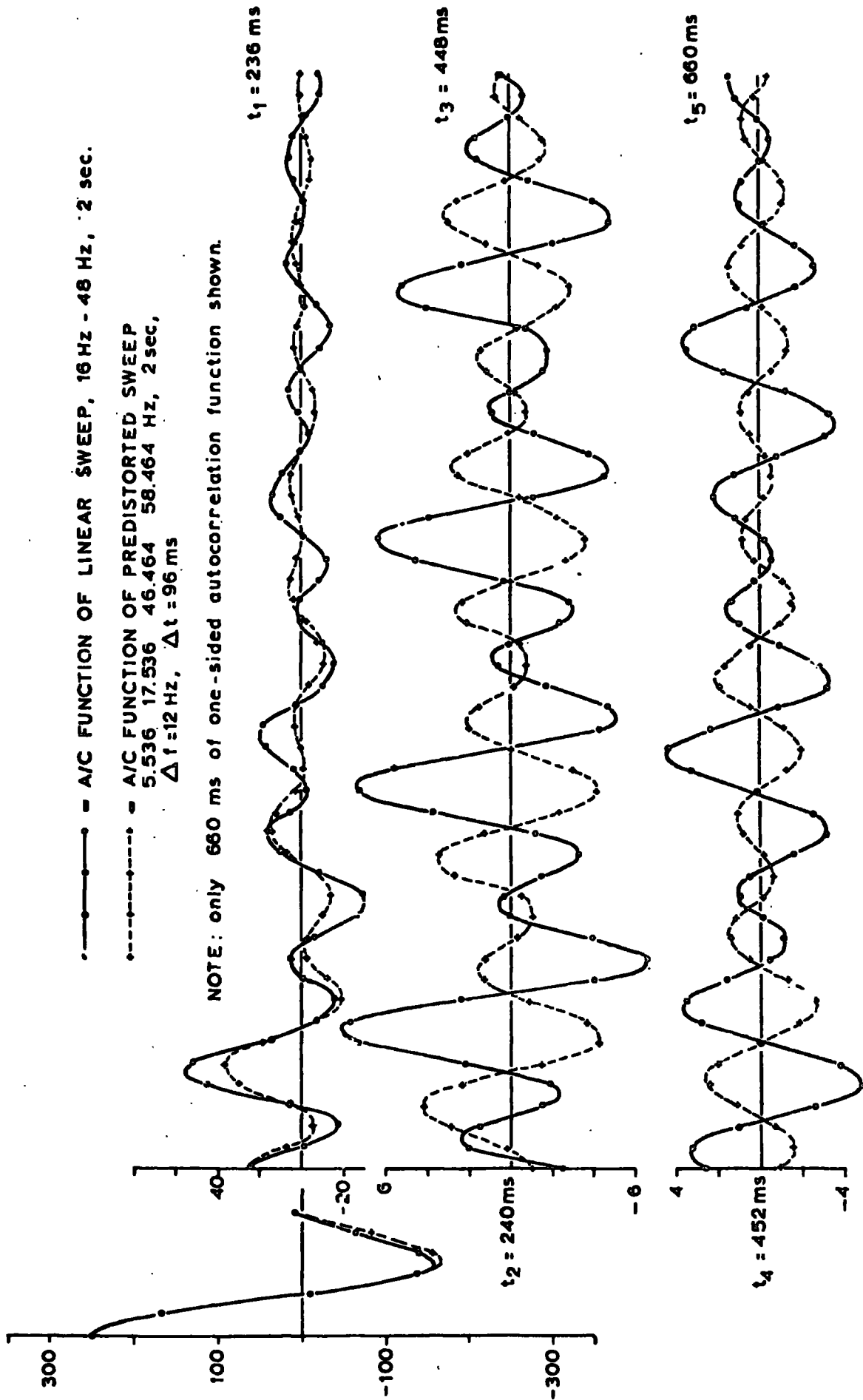


FIG. 71

as far as the Fresnel ripples are concerned. On addition, this will obviously result in a whitening of the spectra, making them more rectangular. This then must be reflected in the sidelobe level and indeed it does, as the stacks show in Figure 68. The two humps to both sides of the main feature of the spectrum for the predistorted sweep with  $\Delta t = 200$  ms, indicate that the predistortion parameters have been pushed very near to their limit. The humps are basically an attempt of the two frequency burst regions in the sweep to set up their own spectra, deforming the main spectrum. However, the Fresnel ripples are very low in amplitude and that explains why the autocorrelation of this signal shows such a low sidelobe level. On addition of the two spectra in Figure 70 we have almost eliminated the Fresnel ripples accounting for the very good stack shown at the bottom of Figure 68.

Let us have a closer look at the autocorrelation function of a linear sweep and a corresponding predistorted sweep with  $\Delta f = 12$  Hz and  $\Delta t = 96$  ms (top of Figure 68). A more detailed graph has been drawn of both functions in Figure 71. Only 660 ms of the correlogram is sufficient to see the almost perfect phase inversion between the two functions, which is starting not far away from the centre peak. This phase inversion is consistent throughout the correlogram except for the last 100 ms or so. This then accounts for the relatively reduced sidepeaks of the stacks in the examples given in Figure 68.

Keeping the useful  $\Delta f$  predistortion parameter constant the author found, that by increasing  $\Delta t$ , the phase of the predistortion autocorrelation function will shift through  $360^\circ$  in relation to the autocorrelation of the basic linear sweep. Once both functions are

back in phase again, i.e. after  $360^\circ$  phase shift, a further increase of  $\Delta t$  will cause the good signal-to-correlation noise ratio to deteriorate and in fact the sidelobes of the predistortion autocorrelation will eventually grow dramatically. The  $\Delta t = 200$  ms example represents such a  $360^\circ$ -shift case. For  $\Delta t$  greater than 200 ms nothing definite can be said about the phase relation to the autocorrelation of the basic linear sweep and sidelobe levels rise because the frequency bursts deform the spectrum more heavily.

Even though this chapter only reports about a side product of this research, the predistortion sweeps seem to have some useful properties which should be investigated more closely. Next, the particular advantage of such non-linear sweeps in the light of what has been said above is outlined and two possible applications will be discussed.

### 9.5. Predistortion in the Vibroseis Encoding Technique and the Combi Sweep Method.

As already mentioned, the most severe distortions to the sweep on its ray path is due to the earth filter with an approximate attenuation of -1 db per wavelength or more in the range of seismic frequencies. This suggests an attenuation of e.g. approximately -160 db for 80 Hz and -40 db for 20 Hz, if the traveltime is assumed to be 2 sec. Therefore, one has to expect a sweep amplitude ratio of about 120 db between the lowest and the highest frequencies (EDELMAANN (1977)). What is important to this aspect is that it is almost certain that amplitude tapering on transmission will not show a signal improvement.

Although the amplitude of a sweep might suffer immensely because of this differential attenuation, it seems that the phase characteristics are generally preserved. The phase encoded Vibroseis technique can thus profit by this fact.

In chapter 6 a quaternary product table (D.) having two different elements in its principle diagonal was introduced. If such a table was applied to a quaternary complementary code, the remaining wavelet of the processed signals was no longer the  $2n$ -fold (where  $n$  = code length) stack of identical autocorrelations, but essentially the stack of  $n$  autocorrelations of one description with  $n$  autocorrelations of a different description.

Let us recall that the correlation matrix (D.) permits a certain degree of wavelet design in the detection window. Together with predistortion this important property can be exploited.

The use of the following equally long sweeps as quaternary

code members, will result in a substantial improvement of the wavelet left after processing, if the predistortion parameters are chosen correctly: -

e.g. a = upsweep

b = phase inverted upsweep

c = predistorted upsweep

d = phase inverted predistorted upsweep

(c and d are based on the upsweep (a) with the predistortion parameters suitably chosen).

There should not only be a theoretical improvement of the wavelet but also a practical one, because we take considerable advantage of the fact that the phase characteristic of seismic signals is relatively undistorted on reception. This is done by using a phase encoded signal and also code members whose particular phase relation to each other, after autocorrelation, ensures a high quality output wavelet. An increase in resolution can therefore be expected. This is assuming that the technical problems associated with the transmission of such sophisticated signals can be solved in future.

Finally, one or more suitable predistortion sweep pairs could also help advancing the combi sweep method as far as its concern is sidelobe suppression. The same arguments hold as above.

## CHAPTER 10

### CONCLUSIONS

The design of complementary coded Vibroseis signals has proved, in theory, to rigorously suppress correlation noise, one code member duration away from the central detection peak. Binary and quaternary coded sweep sequences are equally well guaranteed to remove this system induced noise. In practice, however, a quaternary complementary coded signal is to be preferred because it will minimize the effects of an accidental receiver mismatch.

The transition zones, introduced to overcome the discontinuous bit change-overs, can only be considered as a temporary solution to the problem, which was imposed on us by the characteristics of the vibrator. In principle, it would be best to bring the vibrator to a standstill before commencing the next sweep code member transmission. This, however, means a manipulation of the existing hardware and software of the computerized Vibroseis systems.

The field tests implemented so far indicated the potential of complementary coded sweep sequences to reduce correlation noise a predetermined distance away from the centre peak. Unfortunately, transmission distortions mainly affecting the phase of the coded signal near the discontinuous change-overs, prevented better results than presented.

A wide range of signal design techniques became possible with the help of the four element correlation matrix (D.). In particular, the use of the predistortion signal design should lead to a high quality correlation wavelet in the detection window, further improving this high resolution technique.

The increase in data volume together with the exploitation of the complementary property, are the great advantages of the designed 'Continuous Transmission System'. The economics of the data processing and the dependancy of such a system on a recording device with very high dynamic range might cause problems in the onshore application. The additional Doppler noise effect in an offshore continuous transmission version can be extremely disturbing if the areas to be investigated have strongly dipping horizons. The success of an interactive compensation of Doppler noise by adjusting the reference signal to the frequency and time shift which the transmitted signal has experienced, is questionable.

The final decision about the usefulness of a continuous Vibroseis transmission system must depend upon some practical tests which will give the ultimate answers to the still open questions.

BIBLIOGRAPHY

- Anstey, N.A., 1963, "'VIBROSEIS' Gentle Massage Obtains Structural Data Safely, Economically", The Oil and Gas Journal, March 18, pages 110-118.
- Anstey, N.A., 1964, "'Correlation Techniques' - A Review", Geophysical Prospecting, Vol. 12, pages 355-382.
- Attewell, P.B. & Ramana, Y.V., 1966, "Wave Attenuation and Internal Friction as Functions of Frequency in Rocks", Geophysics, Vol. 31, pages 1049-1056.
- Barbier, M.G. & Viallix, J.R., 1973, "SOSIE: A New Tool for Marine Seismology", Geophysics, Vol. 38, pages 673-683.
- Barbier, M.G. & Viallix, J.R., 1974, "Pulse Coding in Seismic Prospecting: SOSIE and SEISCODE", Geophysical Prospecting, Vol. 22, pages 153-175.
- Barbier, M.G. & Bondon, P. & Mellinger, R. & Viallix, J.P., 1976, "Mini-SOSIE for Shallow Land Seismology", Geophysical Prospecting, Vol. 24, pages 518-527.
- Baumert, L. & Golomb, S.W. & Hall Jr., M., 1962, "Discovery of a Hadamard Matrix of Order 92", American Mathematical Society Bulletin, Vol. 68, pages 237-238.
- Bernfeld, M. & Paolillo, J. & Cook, C.E. & Palmieri, C.A., 1964/65, "Matched Filtering, Pulse Compression and Waveform Design", Microwave Journal, Vol. 7 & 8, No.10,11,12,1. (Parts I-IV, No.10: pages 57-64; No.11: pages 81-90; No.12: pages 70-76; No.1(1965): pages 73-81)
- Bernhardt, T., 1975, "Coding Techniques for the Vibroseis System", unpublished M.Sc. Thesis, University of Durham.

- Bernhardt, T. & Peacock, J.H., 1977, "Encoding Techniques for the Vibroseis System", Geophysical Prospecting, (in press).
- Boehmer, A.M., 1967, "Binary Pulse Compression Codes", IEEE Transactions on Information Theory, Vol. IT-13, No.2, pages 156-167.
- Broding, R.A. & Hess, J.M. & Wanous, R.E., 1971, "A High Power Computer Controlled Marine Vibroseis System", IEEE Transactions on Geoscience Electronics, Vol. GE-9, No.2, pages 90-95.
- Chin, J.E. & Cook, C.E., 1959, "The Mathematics of Pulse Compression", Sperry Engineering Report, Vol.12, No.3, pages 11-16.
- Cole, J.R., 1967, "Vibroseis Effective, Harmless Seismic Exploration Tool", The Oil and Gas Journal, October 30.
- Cook, C.E., 1958, "Modifications of Pulse Compression Waveforms", National Electronics Conference Proceedings, pages 1058-1067.
- Cook, C.E., 1960, "Pulse Compression - Key to More Efficient Radar Transmission", Proceedings of the IRE, Vol. 48, No.3, pages 310-316.
- Cook, C.E. & Paolillo, J., 1964, "A Pulse Compression Predistortion Function for Efficient Sidelobe Reduction in a High-Power Radar", Proceedings of the IEEE, Vol. 52, pages 377-389.
- Cook, C.E. & Bernfeld, M., 1967, "Radar Signals - An Introduction to Theory and Application", Academic Press, -Electrical Science Series of Monographs and Texts-, New York, London.
- Crawford, J.M. & Doty, W.E. & Lee, M.R., 1960, "Continuous Signal Seismograph", Geophysics, Vol. 25, pages 95-105, 9 Figs.

- Davitt, W.E., 1976, "Understanding the Vibroseis System", Paper presented at the 46th Annual International Meeting of the Society of Exploration Geophysicists in Houston, Texas, October 24-28.
- Delong Jr., D.F., 1959, "Three-Phase Codes", MIT, Lincoln Laboratory, Group Report 47.28, Contract No. AF19(604)-5200, unclassified version.
- Edelmann, H., 1966, "New Filtering Methods with Vibroseis", Geophysical Prospecting, Vol. 14, pages 455-469.
- Edelmann, H., 1977, Private communications.
- Elsplas, B., 1955, "A Matched Filter Radar Receiver Based on Statistical Estimation Theory", Stanford University, Applied Electronics Laboratory Technical Report, 361-1AD207896.
- Erlinghagen, L., 1975, "Vibroseis - New Results Under Different Geophysical Aspects", PRAKLA-SEISMOS Publication, -paper originally held at the Geophysical Symposium in Budapest/Szentende, 1975, pages 1-8.
- Erlinghagen, L., "Unterdrueckung von Noise waehrend der Feldregistrierung bei Anwendung des Vibroseis Verfahrens", PRAKLA-SEISMOS Publication.
- Fowler, J.C. & Waters, K.H., 1975, "Deep Crustal Reflection Recordings Using Vibroseis Methods - A Feasibility Study", Geophysics, Vol. 40, No.3, pages 399-410, 9 Figs.
- Frank, R.L., 1963, "Polyphase Codes With Good Non-periodic Correlation Properties", IEEE Transactions on Information Theory, Vol. IT-9, pages 43-45.
- Geyer, R.L., 1970, "Vibroseis Parameter Optimization", Oil and Gas Journal, Vol. 68, April 13 and 27.

- Golay, M.J.E., 1949, "Multislit Spectrometry", Journal of the Optical Society of America, Vol. 39, pages 437-444.
- Golay, M.J.E., 1951, "Static Multislit Spectrometry and its Application to the Panoramic Display of Infra-red Spectra", Journal of the Optical Society of America, Vol. 41, pages 468-472.
- Golay, M.J.E., 1961, "Complementary Series", IRE Transactions on Information Theory, Vol. IT-7, pages 82-87.
- Golay, M.J.E., 1962, "Note on Complementary Series", Proceedings of the IRE, page 84.
- Golomb, S.W. & Scholtz, R.A., 1965, "Generalized Barker Sequences", IEEE Transactions on Information Theory, Vol. IT-11, No.4, pages 533-537.
- Goupillaud, P.L. & Lee, M.R., 1963, "Some Theoretical Aspects of the Vibroseis System and their Practical Implications", paper presented at the Annual Meeting of the Society of Exploration Geophysicists, New Orleans.
- Goupillaud, P.L., 1976, "Signal Design in the Vibroseis Technique", Geophysics, Vol.41, No.6, pages 1291-1304, 16 Figs.
- Gurbuz, B.M., 1972, "Signal Enhancement of Vibratory Source Data in the Presence of Attenuation", Geophysical Prospecting, Vol. 20, pages 421-438.
- Huffman, D.A., 1962, "The Generation of Impulse-Equivalent Pulse Trains", IRE Transactions on Information Theory, Vol. IT-8, pages S10-S16.
- Jauregui, S., 1962, "Complementary Sequences of Length 26", IRE Transactions on Information Theory, Vol. IT-8, page 323.

- Klauder, J.R. & Price, A.C. & Darlington, S. & Albersheim, W.J., 1960, "The Theory and Design of Chirp Radars", The Bell System Technical Journal, Vol. 34, No.4, pages 745-808.
- Knopoff, L., 1956, "The Seismic Pulse in Materials Possessing Solid Friction, I: Plane Waves", Bulletin of the Seismological Society of America, Vol. 46, pages 175-183.
- Krey, Th., 1969, "Remarks on the Signal-to-Noise Ratio in the Vibroseis System", Geophysical Prospecting, Vol. 17, pages 206-218.
- Krey, Th., 1972, "VIBROSEIS", Prakla-Seismos Report 3/72, pages 3-9.
- Krey, Th. & Werner, H., 1977, "Combi-Sweeps - A Contribution to Sweep Techniques", Paper held at the EAEG Meeting in Zagreb 1977.
- Krustal, J.B., 1961, "Golay's Complementary Series", IRE Transactions on Information Theory, Vol. IT-7, pages 273-276.
- Laing, W.E., 1972, "Some Basics and Applications of the Vibroseis System of Exploration", American Institute of Mining, Metallurgical and Petroleum Engineers, Inc., Dallas, Texas, Paper Number: SPE 4157.
- Landrum, R.A., 1967, "Extraction of Signals from Random Noise by Cross-correlation", Paper read at the 37th Annual International Meeting of the Society of Exploration Geophysicists in Oklahoma City, Oklahoma, USA.
- Lee, M.R., 1968, "The Marine Vibroseis System", Preprint of a paper presented on April 11th, 1968 at the Symposium of 'Marine Non-Dynamite Energy Sources', Houston, Texas; Preprint received from Continental Oil Company, Ponca City, Oklahoma.
- Luenberger, D.G., 1963, "On Barker Codes of Even Length", Proceedings of the IEEE (Correspondence), Vol. 51, pages 230-231.

- North, D.O., 1943, "Analysis of Factors Which Determine Signal-to-Noise Discrimination in Radar", RCA Laboratories, Princeton, New Jersey, Rept. PTR-66
- Paley, R.E., 1933, "On Orthogonal Matrices", Journal of Mathematics and Physics, MIT, Vol. 12, pages 311-320.
- Ramp, H.O. & Wingrove, E.R., 1961, "Principles of Pulse Compression - Key to More Efficient Radar Transmission", Proceedings of the IRE, Vol. 48, No.3, pages 310-316.
- Ristow, D. & Jurczyk, D., 1975, "Vibroseis Deconvolution", Geophysical Prospecting, Vol. 23, No.2, pages 363-379.
- Robinson, E.A., "Statistical Communication and Detection with Special Reference to Digital Data Processing of Radar and Seismic Signals", Charles Griffin & Company Ltd.
- Rocheport, J.S., 1954, "Matched Filters for Detecting Pulsed Signals in Noise", IRE Convention Record, pt.4, pages 30-34.
- Schweitzer, B.P., 1971, "Generalized Complementary Code Sets", Ph.D Dissertation, University of California, Los Angeles.
- Shannon, C.E., 1948, "The Mathematical Theory of Communications", University of Illinois Press, Urbana.
- Sheriff, A.J. & Kim, W.H., 1970, "The Effect of Harmonic Distortion in the Use of Vibratory Surface Sources", Geophysics, Vol. 35, No.2, pages 234-246, 17 Figs.
- Spense, E., 1967, "A New Class of Hadamard Matrices", Glasgow Mathematical Journal, Vol. 8, pages 59-62.
- Taki, Y. & Miyakawa, H. & Hatori, M. & Namba, S., 1969, "Even-Shift-Orthogonal Sequences", IEEE Transactions on Information Theory, Vol. IT-15, No.2, pages 295-300.

- Tseng, C.C. & Liu, C.L., 1971, "Complementary Sets of Sequences", IBM Thomas J. Watson Research Centre, Yorktown Heights, N.Y., Report RC-3397.
- Tseng, C.C. & Liu, C.L., 1972, "Complementary Sets of Sequences", IEEE Transaction on Information Theory, Vol. IT-18, No.5, pages 644-651.
- Turin, G.L., 1960, "An Introduction to Matched Filters", IRE Transactions on Information Theory, pages 311-329.
- Turyn, R., 1960, "Optimum Codes Study", Final Report, Sylvania Electronic Systems, Contract AF19(604)-5473.
- WELTI, G.R., 1960, "Quaternary Codes for Pulsed Radar", IRE Transactions on Information Theory, Vol. IT-6, pages 400-408.
- Werner, H. & Braun, G., 1975, "Die rechnergestuetzte Aufnahmeapparatur CFS 1", Prakla-Seismos Report 1/75, pages 4-9.
- Werner, H. & Talke, H., 1975, "Das Prakla-Seismos Vibrator System VVCA", First part in Prakla-Seismos Report 2/75, pages 3-7, and part two in Prakla-Seismos Report 3/75, pages 11-14.
- Wiener, N., 1942, "Extrapolation, Interpolation and Smoothing of Stationary Time Series", MIT Press, Cambridge, Mass., and John Wiley, 1949, New York.
- Wheeler, H.A., 1939, "The Interpretation of Amplitude and Phase Distortion in Terms of Paired Echoes", Proceedings of the IRE, Vol. 27.

APPENDIX

PAIRED ECHO ANALYSIS IN PULSE COMPRESSION SYSTEMS

The "Paired Echo Analysis" was initially designed to study the effect of small amplitude and phase distortions in picture transmission systems, such as television (WHEELER (1939)). In the analysis it is assumed that the amplitude and phase distortions of a system can be expressed as a combination of simple sinusoidal components. If the paired echo distortion method is applied to network functions a composite network output waveform that contains delayed and advanced replicas of the input signal results, i.e. the output distortion is made up of a pattern of echoes ('Paired Echoes'), each echo corresponding to a small distortion in the spectrum.

Paired echo signals resulting from spectra distortions in pulse compression systems are very similar to the correlation noise generated by the matched filter detection, but they can not be reduced sufficiently by means of a weighting function. Therefore, in order to achieve low sidelobe levels it is important to keep these spectrum distortions as small as possible.

The amplitude spectrum of a linear sweep contains a number of disturbing amplitude ripples, the so-called 'Fresnel Ripples', which can be approximated as a combination of simple cosine functions (see Figure 1.). The spectrum can be described as being rectangular with an associated error function superimposed, i.e.

$$|F(w)| = [1 + (a_1 \cdot \cos(C_1 w))(1 + a_2 \cdot \cos(C_2 w))] \quad (1)$$

$$w_1 \ll w \ll w_2$$

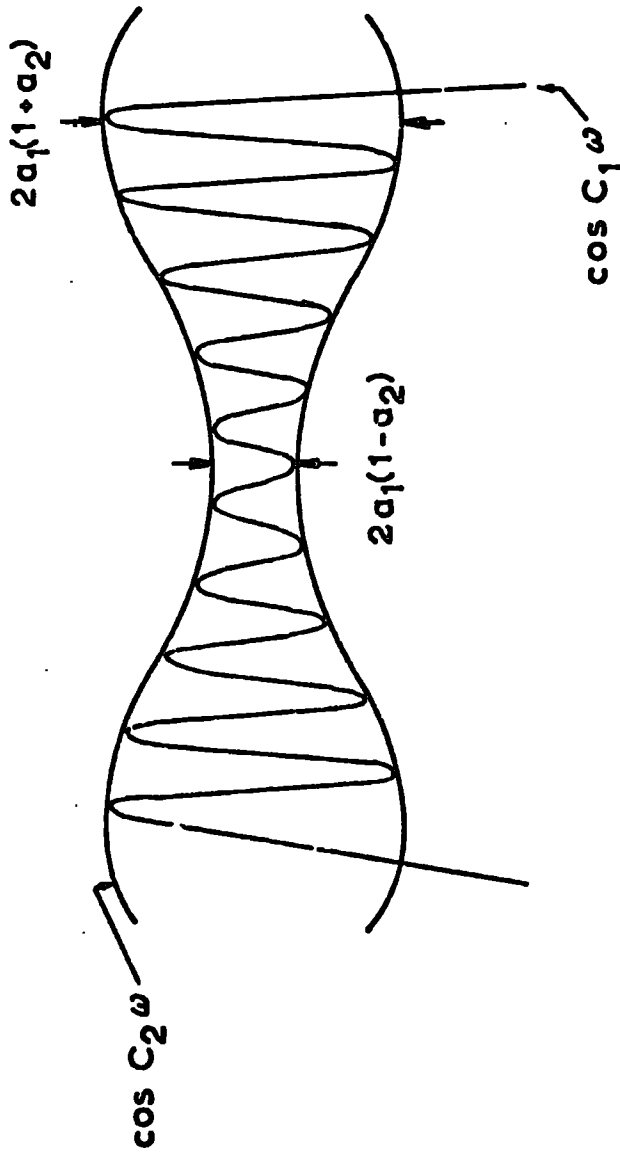


FIG. 1 - FRESNEL RIPPLE APPROXIMATION FOR PAIRED ECHO ANALYSIS

In general, pulse compression output signals can be described by:

$$g(t) = \frac{1}{2\pi} \int_{w_1}^{w_2} |F(w)| \cdot H(w) \cdot \exp(iwt) \, dw \quad (2)$$

where  $H(w)$  = frequency response function.

With (2) the weighted compressed time function  $g(t)$  becomes:

$$g(t) = \frac{1}{2\pi} \int_{w_1}^{w_2} [1 + (a_1 \cdot \cos(C_1 w)) (1 + a_2 \cdot \cos(C_2 w))] \cdot H(w) \cdot \exp(iwt) \, dw \quad (3)$$

After some rearrangements and algebraic steps one will arrive at the following unwieldy formula:

$$\begin{aligned} g(t) = & \frac{1}{2\pi} \left[ \int_{w_1}^{w_2} H(w) \cdot \exp(iwt) \, dw \right. \\ & + a_1/2 \left( \int_{w_1}^{w_2} H(w) \cdot \exp[i(t+C_1)w] \, dw \right. \\ & + \left. \int_{w_1}^{w_2} H(w) \cdot \exp[i(t-C_1)w] \, dw \right) \\ & + a_1 a_2/4 \left( \int_{w_1}^{w_2} H(w) \cdot \exp[i(t+C_1+C_2)w] \, dw \right. \\ & + \int_{w_1}^{w_2} H(w) \cdot \exp[i(t-C_1-C_2)w] \, dw \\ & + \int_{w_1}^{w_2} H(w) \cdot \exp[i(t+C_1-C_2)w] \, dw \\ & \left. + \int_{w_1}^{w_2} H(w) \cdot \exp[i(t-C_1+C_2)w] \, dw \right) \end{aligned} \quad (4)$$

(After COOK (1964))

The first term in (4) represents the idealized compressed waveform, assuming a rectangular amplitude spectrum. The remaining six terms are time displaced paired echo distortions.

